EVALUATION OF PARTITIONING ELECTRON DONORS FOR BIOREMEDIATION OF CHLORINATED SOLVENTS: MASS TRANSFER PROPERTIES AND CONTRIBUTION TO BIOENHANCED DISSOLUTION

A Thesis

Submitted by

Danielle Sylvia

in partial fulfillment of the requirements for the degree of

Master of Science

In

Civil and Environmental Engineering

TUFTS UNIVERSITY

February 2016

THESIS COMMITTEE:

Dr. Natalie Cápiro (*Tufts University*)
Dr. Kurt Pennell (*Tufts University*)
Paul Dombrowski, P.E. (*AECOM*)

Abstract

Bioremediation of chlorinated solvent source zones faces two major challenges: sustained release of electron donors at the appropriate (low) concentrations and delivery of electron donors to the intended target microbes. To address these issues, three candidate partitioning electron donors (PEDs), n-butyl acetate, 2-ethyl-1-hexanol, and isopropyl-propionate, were investigated as a long-term source of electron donor at the contaminant-water interface. A series of batch reactors and column experiments were used to determine the extent and rate of partitioning of the PEDs into the dense non-aqueous phase liquid (DNAPL), the lifetime of the PEDs in the DNAPL source zone, and the ability of the PEDs to be utilized by organohalide respiring bacteria to reduce tetrachloroethene to ethene and promote bioenhanced dissolution. Results suggest that PEDs have the potential to reduce the frequency of electron donor injections, while stimulating organohalide respiring bacteria to produce ethene in a similar timeframe to conventional electron donors.

Acknowledgements

I would like to thank my advisor Dr. Natalie Cápiro for all her guidance and support for the entirety of this project. I would also like to thank the rest of my thesis committee, Dr. Kurt Pennell and Paul Dombrowski for their valuable comments and advice. Thanks to the entire lab group, especially Rhiana Meade, Eimy Bonilla, Lucica Hiller, and Tiffany Duhl for helping setup, sample, and analyze data for various experiments. Funding for this research was provided by National Science Foundation (NSF) award number 1215837.

Table of Contents

Abstract ..... **ii**
Acknowledgements ..... **iii**
Chapter 1- Introduction and Objectives **1**
Chapter 2- Background Information and Literature Review **5**
2.1 The Chlorinated Solvent Problem 5
2.2 Relevant Chemical Properties and Behavior of Chlorinated Solvents 7
2.3 Overview of Existing Remediation Techniques 9
2.4 Microbial Organohalide Respiration of Chlorinated Ethenes 12
2.5 Commonly Used Electron Donors 15
2.6 Partitioning Electron Donors 17
Chapter 3: Evaluation of PED Mass Transfer Properties under Abiotic Conditions **21**
3.1 Introduction and Objectives 21
3.2 Candidate PEDs 23
3.3 Materials 26
3.4 Design and Setup of Abiotic Batch Reactors 27
3.4.1 Design and Setup of Abiotic Batch Reactors 27
3.4.2 Design and Setup of Abiotic Batch Reactors with Soil 29
3.5 Column Experiment Design and Setup 30
3.5.1 Abiotic Column Setup 30
3.5.2 Column Modeling 34
3.6 Analytical Methods 36
3.7 Experimental Results and Discussion 36
3.7.1 Abiotic Batch Reactor Results- Equilibrium Partitioning Coefficients 36
3.7.2 Abiotic Batch Reactors- Mass Transfer Parameters 41
3.7.3 Abiotic Batch Reactors with Hexadecane Results 44
3.7.4 Abiotic Batch Reactors- Soil Partitioning Coefficients 46
NM= Not Measured 48
3.8 Abiotic Column Results 48
3.8.1 Non-reactive Tracer Results 48
3.8.2 PED Breakthrough 49
3.8.3 Flow Interruptions 51
3.8.4 Column Modeling Results 51
3.9 Abiotic Batch Reactor and Column Experiment Conclusions 54
Chapter 4: PED Utilization by Organohalide Respiring Bacteria and Contribution to Bioenhanced Dissolution **57**
4.1 Introduction and Objectives 57

4.2 Materials 58
4.3 Medium Preparation and Inoculum 59
4.4 Design and Setup of Biotic Batch Reactors 60
4.5 Column Experiment Design and Setup 61
4.6 Analytical Methods 64
4.6.1 Aqueous Phase Chemical Analysis 64
4.6.2 Biological Analysis 65
4.7 Biotic Batch Reactor Results 67
4.8 Biotic Column Results 84
4.8.1 Negative Control Column Results 84
4.8.2 Microbial Elution Phase 88
4.8.3 NAPL Dissolution Phase 90
4.8.4 Electron Donor Concentrations 97
4.8.5 Comparative Cumulative Mass Recoveries and Mass Transfer Enhancement Factor 99
4.9 Column Experiment Conclusions 103
Chapter 5: Engineering Implications and Recommendations 106
5.1 PED Significance and Engineering Implications 106
5.2 Future Work 109
Appendix A: Biotic Batch Reactor Results 111
Appendix B: Column Results 120
References 121

List of Tables

Table 2.1 Relevant physical and chemical properties of chlorinated ethenes and ethene. 9
Table 2.2 Relative performance of alternative technologies for source remediation (McCarty 2010). 10
Table 2.3 Comparison of *in situ* technologies including percent mass reduction and medium costs. 11

Table 3.1 Summary of chemical properties and prices of the three candidate partitioning electron donors and lactate. 25
Table 3.2 Summary of experimental conditions for abiotic column experiments. 34
Table 3.3 Octanol-water partitioning (K_{OW}), soil organic content-water partitioning (K_{OC}), and NAPL-water partitioning coefficients (K_{NW}) in trichloroethene for each of the partitioning electron donors and n-hexanol. 40
Table 3.4 Summary of the average percent of PED adsorbed in the soil batch reactor experiments. 48
Table 3.5 Peclet numbers (PE), pore volumes (PV), and dispersivty (α) for each column. 49
Table 3.6 Pore Volumes of initial breakthrough and until washout of the PED in each of the column experiments. 50

Table 3.7 Percent drops and rise in PED concentration during a 12 hour flow interruption. 51
Table 3.8 Summary of retardation factors (R_F), NAPL-aqueous partitioning coefficients (K_{NW}), lumped mass transfer coefficients (k), fractions of sites at equilibrium (F), and the sum of squared residuals (SSQ). 54

Table 4.1 Summary of the electron donor properties and amounts added to each batch reactor. 60
Table 4.2 Summary of biotic batch reactors completed (Bonilla 2015). 61
Table 4.3 Summary of experimental conditions for control column experiments. 63
Table 4.4 A comparison of the time (days) of disappearance and appearance of each of the chlorinated ethenes in the biotic batch reactors containing tetrachloroethene. 81
Table 4.5 A comparison of the time (days) of disappearance and appearance of each of the chlorinated ethenes in the biotic batch reactors containing 0.25 mol tetrachloroethene: 0.75 mol hexadecane. 82
Table 4.6 Summary of the peclet numbers (PE), dispersivity (α), retardation factor (R_F), NAPL-aqueous partitioning coefficient (K_{NW}), lumped mass transfer coefficient (k), and fractions of sites at equilibrium (F). 88
Table 4.7 Cumulative chlorinated ethene recoveries and mass transfer enhancement factors for the lactate and n-butyl acetate columns at pore volume 60. 102
Table 4.8 Cumulative chlorinated ethene recoveries and mass transfer enhancement factors for the lactate column at pore volume 77. 103

Table B.1 Summary of PED maximum concentration, PED recovery, and NAPL recovery for each abiotic column experiment. 120

List of Figures

Figure 2.1 Description of DNAPL transport in the environment (Texas A&M University [TAMU] 2008). 8
Figure 2.2 Process schematic of biodegradation of PCE to Ethene (ITRC 2008). 13
Figure 2.3 The difference between a soluble electron donor and a partitioning electron donor (Cápiro 2012). 18

Figure 3.1 Hydrolysis of n-butyl-acetate to form acetic acid and butanol (eMolecules 2014). 24
Figure 3.2 Hydrolysis of isopropyl propionate to form propionic acid and isopropyl alcohol (eMolecules 2014). 25

Figure 3.3 Abiotic batch reactors containing a partitioning electron donor and non-aqueous phase liquid, on an oscillating shaker table. 28
Figure 3.4 Batch reactor containing Appling Soil, mixing on an oscillating shaker table. 30
Figure 3.5 Abiotic column containing residual tetrachloroethene dyed with 32
Figure 3.6 Schematic diagram of the column setup. 33
Figure 3.7 Equilibrium partitioning coefficients for n-butyl acetate in both tetrachloroethene and trichloroethene. 38
Figure 3.8 Equilibrium partitioning coefficients for isopropyl propionate in both tetrachloroethene and trichloroethene. 38
Figure 3.9 Equilibrium partitioning coefficients for 2-ethyl-1-hexanol in both tetrachloroethene and trichloroethene. 39
Figure 3.10 The relationship between ionic strength and equilibrium partitioning coefficient for n-butyl acetate and tetrachloroethene batch reactor experiments. 41
Figure 3.11 Effective mass transfer for n-butyl acetate in both tetrachloroethene and trichloroethene. 42
Figure 3.12 Effective mass transfer for isopropyl propionate in both tetrachloroethene and trichloroethene. 43
Figure 3.13 Effective mass transfer for 2-ethyl-1-hexanol in both tetrachloroethene and trichloroethene. 43
Figure 3.14 Equilibrium partitioning coefficients for n-butyl acetate in hexadecane, 0.75 mol hexadecane: 0.25 mol tetrachloroethene, and 0.95 mol hexadecane: 0.05 mol trichloroethene. 45
Figure 3.15 Equilibrium partitioning coefficients completed for each of the electron donors and 0.75 mol hexadecane: 0.25 mol tetrachloroethene at 90 mM ionic strength. 45
Figure 3.16 Soil partitioning coefficients for each of the partitioning electron donors in Appling Soil. 46
Figure 3.17 The relationship between the soil partitioning coefficient and the organic carbon content for n-butyl acetate and isopropyl propionate. 47
Figure 3.18 Trichloroethene column observed and modeled results for all three partitioning electron donors. 53
Figure 3.19 Tetrachloroethene column observed and modeled results for all three partitioning electron donors. 53

Figure 4.1 Schematic showing the system used to keep the influent anoxic and the glass sampling bulb. 64
Figure 4.2 The chlorinated ethene concentrations for the abiotic batch reactor Containing lactate and tetrachloroethene. 68
Figure 4.3 Chlorinated ethene concentrations for the biotic batch reactors containing 2-ethyl-1-hexanol and tetrachloroethene. 69
Figure 4.4 Electron donor concentrations for the biotic batch reactors containing 2-ethyl-1-hexanol and tetrachloroethene. 70

Figure 4.5 Chlorinated ethene concentrations for the biotic batch reactors containing lactate. Graph A shows the lactate and tetrachloroethene results. Graph B shows the lactate and 0.25 mol tetrachloroethene: 0.75 mol hexadecane results. 71
Figure 4.6 Electron donor concentrations in the biotic batch reactor containing lactate and tetrachloroethene. 72
Figure 4.7 Chlorinated ethene concentrations for the biotic batch reactors containing n-butyl acetate. Graph A shows the n-butyl acetate and tetrachloroethene results. Graph B shows the n-butyl acetate and 0.25 mol tetrachloroethene: 0.75 mol hexadecane results. 73
Figure 4.8 Electron donor concentrations in the abiotic batch reactor containing n-butyl acetate and tetrachloroethene. 74
Figure 4.9 Electron donor concentrations in the biotic batch reactors containing n-butyl acetate. Graph A shows the n-butyl acetate and tetrachloroethene results. Graph B shows the n-butyl acetate and 0.25 mol tetrachloroethene: 0.75 mol hexadecane results. 76
Figure 4.10 Chlorinated ethene concentrations for the biotic batch reactors containing isopropyl propionate. Graph A shows the isopropyl propionate and tetrachloroethene results. Graph B shows the isopropyl propionate and 0.25 mol tetrachloroethene: 0.75 mol hexadecane results. 78
Figure 4.11 Electron donor concentrations in the biotic batch reactors containing isopropyl propionate. Graph A shows the isopropyl propionate and tetrachloroethene results. Graph B shows the isopropyl propionate and 0.25 mol tetrachloroethene: 0.75 mol hexadecane results. 80
Figure 4.12 pH levels in the batch reactors. 83
Figure 4.13 Hydrogen concentrations in the biotic batch reactors. 84
Figure 4.14 Column results for the abiotic column with lactate and 0.25 mol tetrachloroethene: 0.75 mol hexadecane showing the observed lactate relative concentrations, bromide tracer, equilibrium modeling results, and non-equilibrium modeling results. 86
Figure 4.15 The total number of moles recovered of n-butyl acetate, as n-butyl acetate and as butanol, between each sample. 87
Figure 4.16 Column results for the abiotic column with n-butyl acetate and 0.25 mol tetrachloroethene: 0.75 mol hexadecane showing the observed n-butyl acetate relative concentrations, bromide tracer, equilibrium modeling results, and non-equilibrium modeling results. 88
Figure 4.17 *Dehalococcoides mccartyi (Dhc)* and *Geobacter Lovleyi (G. lovleyi)* cells in lactate column effluent samples prior to NAPL addition. 89
Figure 4.18 *Dehalococcoides mccartyi (Dhc)* and *Geobacter lovleyi (G. lovleyi)* cells in n-butyl acetate column effluent samples prior to NAPL addition. 90

Figure 4.19 Chlorinated ethene concentrations, flow interruptions, and flow reductions for the column containing lactate. 92
Figure 4.20 *Dehalococcoides mccartyi (Dhc)* and *Geobacter lovleyi (G. lovleyi)* cell concentrations in the effluent of the lactate column. 93
Figure 4.21 Chlorinated ethene concentrations, flow interruptions, flow reductions, and n-butyl acetate additions for the column containing n-butyl acetate. 95
Figure 4.22 *Dehalococcoides mccartyi (Dhc)* and *Geobacter lovleyi (G. lovleyi)* concentrations in the effluent of the n-butyl acetate column. 96
Figure 4.23 pH in the lactate and n-butyl acetate columns. 97
Figure 4.25 Concentrations of lactate, acetate, and propionate in milli-reducing equivalents/L for the lactate column. 98
Figure 4.26 Concentrations of n-butyl acetate, acetate, and butanol in milli-reducing equivalents/L in the n-butyl acetate column. 99
Figure 4.27 Cumulative mass recovery of tetrachloroethene in the lactate column. 100
Figure 4.28 Cumulative mass recovery of tetrachloroethene in the n-butyl acetate column. 101

Figure A.1 Chlorinated ethene concentrations in the abiotic batch reactor containing lactate and 0.25 mol tetrachloroethene:0.75 mol hexadecane. 111
Figure A.2 Chlorinated ethene concentrations in the abiotic batch reactor containing 2-ethyl-1-hexanol and tetrachloroethene. 111
Figure A.3 Chlorinated ethene concentrations in the abiotic batch reactor containing 2-ethyl-1-hexanol and 0.25 mol tetrachloroethene: 0.75 mol hexadecane. 112
Figure A.4 Chlorinated ethene concentrations in the abiotic batch reactor containing n-butyl acetate and tetrachloroethene. 112
Figure A.5 Chlorinated ethene concentrations in the abiotic batch reactor containing n-butyl acetate and 0.25 mol tetrachloroethene: 0.75 mol hexadecane. 113
Figure A.6 Chlorinated ethene concentrations in the abiotic batch reactor containing isopropyl propionate and tetrachloroethene. 113
Figure A.7 Chlorinated ethene concentrations in the abiotic batch reactor containing isopropyl propionate and 0.25 mol tetrachloroethene: 0.75 mol hexadecane. 114
Figure A.8 Chlorinated ethene concentrations in the biotic batch reactor containing 2-ethyl-1-hexanol and 0.25 mol tetrachloroethene: 0.75 mol hexadecane. 114
Figure A.9 Lactate concentrations in the abiotic batch reactor containing lactate and tetrachloroethene. 115
Figure A.10 Lactate concentrations in the abiotic batch reactor containing lactate and 0.25 mol tetrachloroethene: 0.75 mol hexadecane. 115

Figure A.11 2-ethyl-1-hexanol concentrations in the abiotic batch reactor containing 2-ethyl-1-hexanol and tetrachloroethene. 116
Figure A.12 2-ethyl-1-hexanol concentrations in the abiotic batch reactor containing 2-ethyl-1-hexanol and 0.25 mol tetrachloroethene: 0.75 mol hexadecane. 116
Figure A.13 n-butyl acetate, butanol, and acetate concentrations in the abiotic batch reactor containing n-butyl acetate and 0.25 mol tetrachloroethene: 0.75 mol hexadecane. 117
Figure A.14 Isopropyl propionate concentrations in the abiotic batch reactor containing isopropyl propionate and tetrachloroethene. 117
Figure A.15 Isopropyl propionate concentration in the abiotic batch reactors containing isopropyl propionate and 0.25 mol tetrachloroethene: 0.75 mol hexadecane. 118
Figure A.16 Lactate, acetate, and propionate concentrations in the biotic batch reactor containing lactate and 0.25 mol tetrachloroethene: 0.75 mol hexadecane. 118
Figure A.17 2E1H, acetate, and propionate concentrations in the biotic batch reactor containing 2-ethyl-1-hexanol and 0.25 mol tetrachloroethene: 0.75 mol hexadecane. 119

EVALUATION OF PARTITIONING ELECTRON DONORS FOR BIOREMEDIATION OF CHLORINATED SOLVENTS: MASS TRANSFER PROPERTIES AND CONTRIBUTION TO BIOENHANCED DISSOLUTION

Chapter 1- Introduction and Objectives

Chlorinated solvents such as tetrachloroethene (PCE) and trichloroethene (TCE) are among the most widespread and persistent groundwater contaminants in the United States (Agency for Toxic Substances and Disease Registry [ATSDR] 2013). These contaminants are difficult to remediate especially when present as dense non-aqueous phase liquids (DNAPLs) that act as long term sources due to their low aqueous-phase solubility and rate-limited dissolution (Isalou et al. 1998, Kavanaugh and Rao 2003). Commonly employed physical-chemical remediation technologies including pump and treat, vapor stripping, solvent extraction, thermal technologies, and chemical oxidation, can remove up to 90% of contaminant mass (Lyon and Vogel 2013, National Research Council [NRC] 2013). However, the residual mass remains a source of groundwater contamination emanating concentrations exceeding regulatory limits (United States Environmental Protection Agency [USEPA] 1993). Bioremediation, the use of microorganisms to degrade contaminants in the soil and groundwater, has become a commonly applied technique for chlorinated solvent treatment and has been applied to hundreds of sites to date (NRC 2013). Bioremediation has the potential to be both less expensive and more effective than other technologies when treating chlorinated solvent source zones (InterstateTechnology and Regulatory Council [ITRC] 2008).

Bioremediation has been shown to be effective in treating down-gradient plumes, but only recently has been used to treat source zones (ITRC 2008). Previously, the high concentrations present at source zones were believed to be toxic for organohalide

respiring microorganisms. However, studies completed in the late 1990s and early 2000s found that microorganisms were capable of organohalide respiration close to DNAPLs (Isalou et al. 1998, Harkness et al. 1999, Adamson et al. 2003). Bioremediation of source zones can shorten the source lifetime by enhancing DNAPL dissolution over abiotic conditions alone (Yang and McCarty 2000, Yang and McCarty 2002, Amos et al. 2008). Bioenhanced dissolution has the potential to reduce source zone longevity by accelerating depletion of the source zone contaminant mass and, consequently, reducing remediation time and cost. However, it is limited by delivery of sufficient electron donor to the contaminant source (Yang and McCarty 2000), inconsistent supply of reducing equivalents (Yang and McCarty 2002, Chu et al. 2004), and insufficient residence times (Da Silva et al. 2006).

Organohalide respiration reduces PCE to innocuous ethene, and requires certain bacteria within the genus *Dehalococcoides mccartyi (Dhc)* and hydrogen as the electron donor (Löffler et al. 2013a). Electron donors generally fall under two categories: water soluble and separate phase electron donors. The use of water soluble electron donors for remediation of chlorinated solvents is often costly because they are consumed by competitor microorganisms; this limits the efficiency and leads to repeated electron donor additions (ITRC 2008). Separate phase or insoluble electron donors require fewer injections, but drawbacks include difficult injection, reduction in hydraulic conductivity, and impacts on water flow paths (ITRC 2008). Soluble and insoluble electron donors have been shown to enhance DNAPL dissolution two to three times, but insoluble electron donors are used by organohalide respiring bacteria at a higher efficiency (Yang and McCarty 2002).

The goal of the present work is to investigate candidate esters, organic alcohols, and fatty acids to serve as partitioning electron donors (PEDs) that provide a sustained source of electron donor for bioremediation of chlorinated solvents. This research focuses on three candidate PEDs: n-butyl acetate (nBA), isopropyl propionate (IPP), and 2-ethyl-1-hexanol (2E1H). PEDs incorporate the desirable attributes of both soluble and insoluble electron donors, because PEDs are water soluble compounds that are easy to inject and do not impact water flow paths, but favorably partition into the DNAPL which would reduce to the need for frequent injections (Cápiro et al. 2011). Recent abiotic studies have shown that the PED and TCE-DNAPL simultaneously dissolve into the aqueous phase resulting in sustained concentrations of dissolved PED at the DNAPL:water interface (Cápiro et al. 2011). The dissolved PED could provide an electron donor source for the organohalide respiring bacteria, because the compounds that are being considered as PEDs have been shown to hydrolyze or ferment to yield electron donors or products that further breakdown to form electron donors (He et al. 2002, Roberts 2008). Many commonly used electron donors, such as lactate, undergo fermentation rapidly and supply large amounts of hydrogen, which is consequently consumed by competitor microorganisms (ITRC 2008). On the other hand, fatty acid fermentation is thermodynamically constrained, which means that if the PEDs do undergo hydrolysis or fermentation to form electron donors, their breakdown products, such as propionate or butyrate, will ferment slowly resulting in a sustained low level of hydrogen (Schink 2002). This can reduce the loss of electron donor to competitor microorganisms because other microbial groups, such as methanogens, are sensitive to high chlorinated solvent concentrations and organohalide respiring bacteria, such as *Dhc*, can outcompete the methanogens at low hydrogen partial pressures (Ballapragada et al. 1997, Löffler et al. 2000).

Implementing bioremediation with PEDs has the potential to be less expensive than with conventional electron donors because they can be injected in the aqueous phase but require fewer injections, have reduced consumption by competitor microorganisms, and can enhance DNAPL dissolution. Despite this potential, only limited data is available regarding PED mass transfer parameters in TCE and PCE, and this approach has not been evaluated under conditions that allow for comparisons with conventional electron donors. This work focuses on expanding upon the previous work performed with n-hexanol and nBA in the presence of TCE (Cápiro et al. 2011) by performing an in-depth screening of additional potential PEDs in the presense of both TCE and PCE and comparing the potential PEDs to the conventional soluble electron donor, lactate, under biologically active conditions. The specific objectives of this study include:

1) Measure the mass transfer parameters for each of the candidate PEDs in both PCE and TCE.
2) Compare the lifetime of candidate PEDs in DNAPL source zones to other commonly used electron donors.
3) Determine the ability of the candidate PEDs to be utilized by organohalide respiring bacteria to reduce PCE to ethene.
4) Evaluate bioenhanced dissolution, or an increased rate of DNAPL dissolution in the aqueous phase due to microorganisms over abiotic dissolution alone, when candidate PEDs provide the electron donor source.

Chapter 2- Background Information and Literature Review

2.1 The Chlorinated Solvent Problem

Chlorinated solvents are among the most prevalent contaminants in the United States as a result of their extensive use beginning in the 1900s (Agency for Toxic Substances and Disease Registry [ATSDR] 2013). For example, in 2011 the estimated commercial production of trichloroethene (TCE) in the United States was 270 million pounds (ATSDR 2013). Chlorinated solvents are used in paints, paint strippers, adhesives, dry cleaning, and degreasing operations for metal parts and textiles (ATSDR 2013), and have been detected at a variety of sites including dry cleaning sites, landfills, aircraft maintenance facilities, metal facilities, solvent production facilities, military facilities, and electronics manufacturing facilities (McGuire et al. 2004). In 2011, environmental releases of TCE reported under the Environmental Protection Agency (EPA) Toxic Release Inventory were greater than 2.6 million pounds in air emissions, 452 pounds in surface water discharges, 18,364 pounds in releases to soil, and 9,578 pounds in releases via underground injection (ATSDR 2013). The maximum contaminant level goals (MCLGs) in groundwater for both tetrachloroethene (PCE) and TCE are 0 mg/L and the maximum contaminant levels (MCLs) for both PCE and TCE are 0.005 mg/L (USEPA 1993). The vapor intrusion acceleration action level for TCE is 6 $\mu g/m^3$; the EPA requires immediate relocation of residences if indoor air levels exceed this concentration (ATSDR 2013). Concentration of TCE or PCE above 0.0005 mg/kg/day orally consumed or inhaled can cause headaches, drowsiness, eye irritation, and nose or skin irritation. Long term exposure can cause damage to kidneys, liver, nervous system, and immune system (ATSDR 2013). The EPA has determined that there is convincing evidence for an association between TCE and kidney and liver cancer, non-Hodgkin's lymphoma, and neurodegenerative diseases (ATSDR 2013).

Due to improper storage and disposal and the physical-chemical properties of chlorinated solvents (e.g., low aqueous solubility and density greater than water), groundwater contamination is widespread. For instance, TCE has been detected in as many as 55% of public water supply wells in California (ATSDR 2013). Nationwide, it is estimated that between 60-65% of drinking water supply wells have detectable levels of volatile organic compounds (VOCs) and 1% of all drinking water supply wells have VOCs, most commonly PCE and TCE, at concentrations above MCLs (National Resource Council [NRC] 2013). As of 2007, PCE and TCE were present at 924 and 1,022, respectively, of the 1,689 sites on the EPA National Priority List (NPL), a list of U.S. sites with known releases or threatened releases of hazardous substances, pollutants, or contaminants (McCarty 2010). In 2010, it was estimated that 75% of the 36,000 active dry cleaning facilities have chlorinated solvent contamination (State Coalition for Remediation of Drycleaners [SCRD] 2010). The EPA estimates that there are between 9,000 and 90,000 inactive dry cleaning sites that could have chlorinated solvent contamination (NRC 2013). Only 3,817 dry cleaning sites, including 693 closed facilities, have had at least an initial contamination assessment completed. The EPA estimates that billions of dollars will have to be spent to remove contaminants from chlorinated solvent sites (NRC 2013).

Production of chlorinated solvents decreased in the 1970s as the federal government began to realize the importance of reducing pollution. As a result, laws were introduced to both reduce the use of polluting contaminants, and to mandate the proper handling and disposal of hazardous waste (NRC 2013). Regulation began with the Federal Clean Air Act of 1970 that set air emission standards to limit the use of TCE throughout the United States (NRC 2013). The Resource Conservation and Recovery Act (RCRA) was first created in 1976, which regulated handling and disposal of hazardous waste to reduce

spills; however, the extent of groundwater contamination was not realized until the 1980s when requirements for groundwater monitoring were expanded (NRC 2013). In 1980, the Comprehensive Environmental Response, Compensation and Liability Act (CERCLA) was created to give the federal government authority to respond directly to releases of hazardous materials. This act also enabled taxes to be imposed on chemical and petroleum industries, which were used to fund the cleanup of contaminated sites. CERCLA was amended in 1986 with the Superfund Amendments and Reauthorization Act (SARA), which stressed the importance of permanent and innovative solutions to combat contamination and increased state involvement in site remediation (NRC 2013). According to a survey of 191 chlorinated solvent sites performed by McGuire et al. (2004), 60% of these surveyed sites were contaminated before 1970 and only 15% of the surveyed sites had been contaminated after 1980.

2.2 Relevant Chemical Properties and Behavior of Chlorinated Solvents

Chlorinated solvents are difficult to remediate because of their chemical properties. Many chlorinated solvents exist as dense non-aqueous phase liquids (DNAPLs), which have a higher density than water, and have a low solubility in water (Isalou et al. 1998). Due to their high densities, DNAPLs sink until they reach an impermeable layer, such as clay or bedrock as shown in Figure 2.1 (Kavanaugh and Rao 2003).

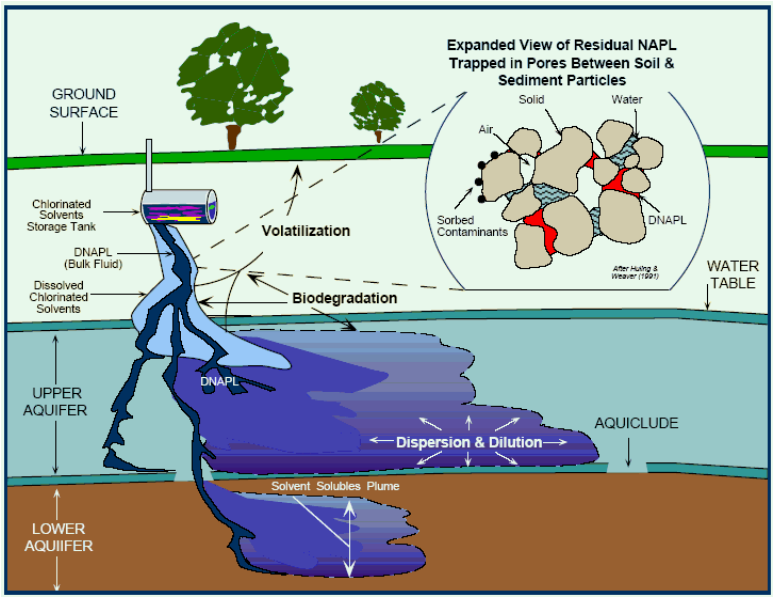

Figure 2.1 Description of DNAPL transport in the environment (Texas A&M University [TAMU] 2008).

Non-aqueous phase (i.e., free product) chlorinated solvents collect in pools at impermeable interfaces or exist as ganglia (i.e., droplets) trapped in the soil (Kavanaugh and Rao 2003). Small volumes of non-aqueous phase PCE or TCE can create large volumes of contaminated groundwater well above MCLs. The solubility of PCE and TCE is 200 and 1,100 mg/L, respectively, values which are considerably higher than the MCL of 0.005 mg/L. Additionally these chemicals, with the exception of PCE, do not have high partitioning coefficients into the organic phase of soil (K_{oc}) indicating that they are not strongly retarded, which can allow plumes to travel large distances. Chlorinated solvents can have plumes that are miles long and will continue to grow if not contained or remediated at the source (Russell et al. 1992). A summary of the relevant chemical and physical properties for various chlorinated volatile organic compounds can be found in Table 2.1.

Table 2.1 Relevant physical and chemical properties of chlorinated ethenes and ethene.

	Molecular Weight (g/mol)	Density (g/cm3)	Solubility in water at 25°C (mg/L)	Log Kow	Koc
PCE	165.8	1.63	200	2.88	665
TCE	131.4	1.46	1,100	2.29	160
cis-DCE	96.9	1.28	3,500	1.86	35
VC	62.5	0.91	2,700	1.38	8.2
Ethene	28.5	NA	131	NA	NA

Log K_{ow}=octanol-water partitioning coefficient, equal to the ratio of the compound's concentration in the octanol phase to its concentration in the aqueous phase in a two-phase octanol/water system. K_{oc}= organic carbon-water partitioning coefficient, equal to the solid-water distribution coefficient (K_D) divided by the fraction organic carbon content (f_{oc}) of the solid phase. Data obtained from ITRC (2008). NA= Not Applicable.

2.3 Overview of Existing Remediation Techniques

The first widely used remediation technique for chlorinated solvents was pump and treat, in which several pumping wells are used to physically remove the dissolved-phase contaminant mass. Although pump and treat is still used for plume containment, it is used less often for remediation because it has proven to be ineffective at reducing contaminant concentrations in DNAPL source zones even when applied for decades (McCarty 2010). Of the 77 sites reviewed by the NRC that began using pump and treat remediation in the 1980s, 69 had not yet met cleanup goals (NRC 1994). Several other technologies have been developed to treat sources, including fluid flushing, thermal treatment, chemical treatment, and microbial treatment (McCarty 2010).

Table 2.2 lists the relative performance of various remediation technologies. The median reduction in total chlorinated ethene concentrations in source zone groundwater ranges from 60-80% for injection-based technologies, including *in situ* bioremediation and *in situ* chemical oxidation (Stroo et al. 2012). Residual DNAPL is particularly challenging for injection based technologies because flow paths often bypass large amounts of the contamination (Stroo et al. 2012). These low recoveries encourage research into improving source remediation.

Table 2.2 Relative performance of alternative technologies for source remediation (McCarty 2010).

Technology	**Description**	**Residual Groundwater Concentration**	**Residual Sorbed Concentration**	**Cleanup Time**
Conventional Pump and Treat	Use of extraction wells to remove contaminated groundwater.	Low to Medium	Medium to High	Long
Vacuum Extraction and Bioventing	Extraction of air to stimulate present microbes to accelerate contaminant reduction.	NA	Low to Medium	Short
Air Sparging	Injection of air into saturation zone to increase volatilization with recovery via soil vapor extraction.	Low to Medium	Low to Medium	Short to Medium
***In situ* Bio-remediation**	Injection of electron donor or microbes to accelerate dissolution of DNAPL and contaminant reduction.	Low to Medium	Low to High	Medium to Long
Cosolvent or Surfactant Flushing	Stabilization or mobilization, recovery via extraction wells and a variety of surfactants, foams, or cosolvents.	Low to Medium	Low to Medium	Short to Medium
Stream Stripping	Steam injection into saturated zone, mobilization and volatilization, recovery via extraction wells.	Low to Medium	Low to Medium	Short
***In situ* Thermal Desorption**	Electrical heating of subsurface to increase mobilization and volatilization, recovery via extraction wells.	Low to Medium	Low to Medium	Short
***In situ* Chemical Oxidation**	Abiotic chemical oxidation by chemical injection into subsurface.	Low to High	Low to High	Short to Long
***In situ* Reactive Barrier**	Contaminant containment and reduction via chemical barrier.	Low to Medium	Low to High	Medium to Long

Bioremediation is a remediation technique that uses microorganisms to degrade contaminants in soil and groundwater. Similar amounts of mass are removed using bioremediation as other injection-based technologies, but bioremediation is significantly less expensive (McCarty 2010). Bioremediation is currently widely used due to its low capital costs, minimal infrastructure requirements, minimal exposure risk, and absence of effluent waste streams (NRC 2013). Cost and effectiveness of all *in situ* treatment technologies are compared in Table 2.3.

Table 2.3 Comparison of *in situ* technologies including percent mass reduction and medium costs.

Technology	Performance	Median Cost
Thermal	95-99+ percent mass reduction	$88/yd^3
Chemical Oxidation	55-90 percent mass reduction	$125/yd^3
Surfactant Flushing	65-90+ percent mass reduction	$385/yd^3
Cosolvent Flushing	65-85 percent mass reduction	$385/yd^3
Bioremediation	60-90 percent mass reduction	$29/yd^3

Performance data taken from Table 4-11 Source Zone Technology Summaries in NRC (2013). Medium cost data obtained from McDade, McGuire et al. (2005).

As shown in Table 2.3, bioremediation generally provides the lowest cost option of *in situ* treatment technologies with a median cost of $29/yd^3 (McDade et al. 2005). At chlorinated solvent sites treated with bioremediation, a median of 81% mass reduction has been reported (Stroo et al. 2012). Although thermal remediation is capable of removing much larger amounts of contaminant mass (>99%) in short time frames, the treatment could be more than twice as expensive, with a median cost of $88/yd (McDade et al. 2005). Previous research suggests that aggressive source zone mass removal technologies significantly shorten source longevity but may require a staged second step (i.e., polishing step) (Christ et al. 2005). Using bioremediation as a polishing step may reduce contaminant mass flux to a level that ensures plume containment and ultimately site closure (Ramsburg et al. 2004, Christ et al. 2005).

2.4 Microbial Organohalide Respiration of Chlorinated Ethenes

The goal of enhanced bioremediation is to accelerate microbial activity by adding nutrients and substrate and/or creating conditions conductive to biodegradation by changing geochemical properties such as pH and temperature (ITRC 2008). Nutrients such as nitrate, phosphate, and potassium are required to support microbial growth. Microorganisms also require a substrate, most often a carbon source, for growth or as a source of electrons for energy (ITRC 2008). When appropriate microorganisms are present at the site, biostimulation, the addition of electron donors and/or nutrients to stimulate bacteria, can be used to enhance degradation. Bioaugmentation, the introduction of microorganisms to the subsurface, is used when the microorganisms required to carry out degradation are not present at the site or are not present in large enough concentrations (ITRC 2008).

Freedman and Gossett (1989) were the first to discover that PCE can be readily degraded anaerobically to innocuous ethene. The anaerobic degradation of PCE to ethene is called organohalide respiration and is comprised of a redox process in which anaerobic bacteria use chlorinated ethenes as electron acceptors (Löffler et al. 2013b). In order for the organohalide respiration reaction to proceed, an electron donor, frequently hydrogen or acetate is required (ITRC 2008). In the degradation of PCE or TCE to ethene, chlorine atoms are replaced with hydrogen. The process is shown below in Figure 2.2. Organohalide respiring bacteria gain energy they can use for growth or maintenance from each reductive dechlorination reaction (Simmonds 2007, Löffler et al. 2013a). Several types of organohalide respiring bacteria can dechlorinate PCE to TCE to 1,2-dichloroethene (cis-DCE) such as *Desulfitobacterium* sp., *Desulfuromonas michiganensis*

sp., and *Geobacter lovleyi* (Löffler et al. 2013a). *Dehalococcoides mccartyi* (*Dhc*) strains are the only group known to be able to dechlorinate PCE to ethene (Löffler et al. 2013a).

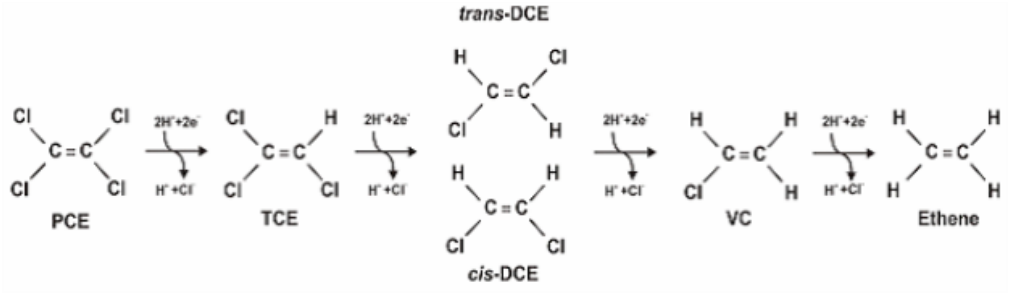

Figure 2.2 Process schematic of biodegradation of PCE to Ethene (ITRC 2008).

Many studies have shown that bioremediation within close proximity to chlorinated solvent DNAPL source zones is possible (Isalou et al. 1998, Harkness et al. 1999, Adamson et al. 2003). For example, Isalou et al. (1998) reported bioremediation of PCE to ethene near the influent of columns with PCE influent concentrations over 600 µM. Additionally, Adamson et al. (2003) were able to bioaugment a near field-scale PCE source area within a 5.49 m by 2.13 m by 1.83 m tank open to the atmosphere. One liter of neat PCE was added to the tank to create residual NAPL and the injected culture dechlorinated PCE to cis-DCE, typically within 24 hours, even in regions containing NAPL (Adamson et al. 2003). Applying bioremediation to the source zone may shorten remediation time by enhancing NAPL dissolution (Yang and McCarty 2000).

One major benefit of bioremediation within the source zone is enhanced dissolution or an increased rate of DNAPL dissolution into the aqueous phase over abiotic dissolution alone. Organohalide respiration acts as a reaction sink, which increases the concentration gradient allowing more DNAPL to dissolve (Yang and McCarty 2000). Additionally, bioremediation degrades PCE to the more soluble TCE and cis-DCE allowing for higher total aqueous concentrations (Yang and McCarty 2000). Equation 2.1 is the Noyes-Whitney Equation which describes the rate of dissolution (Avdeef 2011).

$$\frac{dm}{dt} = A\frac{D}{d}(C_s - C_b) \qquad (2.1)$$

Where, m is the mass of dissolved material, t is time, A is the surface area of the interface between the dissolving substance and the solvent, D is the diffusion coefficient, and d is the thickness of the boundary layer of the solvent at the surface of the dissolving substance. C_S is the mass concentration of the substance on the surface, which is equal to the solubility of the substance when dissolution is limited by diffusion. C_b is the mass concentration of the substance in the bulk of the solvent.

Enhanced dissolution can accelerate source zone contaminant mass depletion and shorten remediation time. There are several examples in the literature of bioremediation being used to enhance PCE dissolution. Yang and McCarty (2000) reported a PCE dissolution rate improvement of approximately 5-fold when flow was coupled with biological dechlorination in a continuous flow column experiment containing neat PCE. Amos et al. (2009) reported an cumulative enhanced dissolution factor of 5.2 in columns containing a mixed NAPL (0.25/0.75 mol/mol PCE dissolved in hexadecane) and inoculated with a PCE-to-ethene dechlorinating consortium (BDI-SZ) with a 20 mM lactate influent. Laboratory experiments with mixed cultures can (bio)enhance PCE DNAPL dissolution 1.4 to 15 fold when compared to abiotic dissolution alone (Amos et al. 2009, Carr et al. 2000, Cope and Hughes 2001, Glover et al. 2007, Sleep et al. 2006, Yang and McCarty 2000). Therefore, source zone bioremediation may be a cost-effective approach to deplete source zone contaminant mass and control contaminant plume formation.

The amount of dissolution enhancement has been shown to be dependent on groundwater flow velocity, transverse dispersivity, degradation kinetics, length scale of reactive zone, and rates of electron donor supply; however, the key determining factors are the extent to

which dechlorinating activity propagates within the source zone and source zone architecture (Chu et al. 2004, Stroo et al. 2012). Microbial reductive dechlorination can only occur within close proximity to the source zone when an electron donor source is also present within the same region.

2.5 Commonly Used Electron Donors

Insufficient supply of electron donor limits the extent of dechlorination (Yang and McCarty 2000, Yang and McCarty 2002, Cupples et al. 2004, Chu et al. 2004). *Dhc* require hydrogen as an electron donor (Yang and McCarty 1998), which is often produced from fermentation of other substrates (Interstate Technology and Regulatory Council [ITRC] 2008). Sugars, organic acids, alcohols, and yeast extract are some common soluble compounds that undergo this fermentation and travel with the groundwater flow after injection, which spreads the electron donor throughout the site. These compounds are often consumed by competitor microorganisms necessitating large quantities and driving up costs (ITRC 2008). These substrates need to be added periodically to maintain sufficient electron donor supply and a safety factor between 2 and 10 is recommended (Harkness 2000, Henry 2010). The amount of electron donor that should be injected is dependent on the electron donor demand of the aquifer and the rate of groundwater flow (ITRC 2008). The electron donor demand of the aquifer includes the concentration of target chlorinated ethenes and the concentration of other electron acceptors not related to dechlorination (i.e., oxygen, nitrate, iron, manganese, and sulfate) (ITRC 2008). Water soluble electron donors, which cost on average $0.5/lb, are less expensive when compared with insoluble electron donors, which cost on average between $5 and $7/lb (McDade et al. 2005). Insoluble electron donors biodegrade slowly over time, which in turn results in a slow fermenting source of hydrogen. These fermentable electron donor substrates include vegetable oil, Hydrogen Release Compound (HRC),

lactic acid polymers, soybean oil, chitin, and wood chips (Aulenta et al. 2006). Insoluble electron donors require fewer injections, but are difficult and costly to inject as they tend to have limited mobility and potentially can cause clogging and changes in groundwater flow patterns (Henry 2010).

One concern with all electron donors is ensuring that sufficient quantities are available for dechlorinating bacteria. The addition of an electron donor also simulates the activity of methanogens, acetogens, sulfate reducers, iron reducers and nitrate reducers (Aulenta et al. 2002). Reactions with competitor microorganisms use up electron donor and could produce unwanted byproducts such as the metals iron(II) and manganese (II) (Aulenta et al. 2002). Ballapragada et al. (1997) found that in a methanogenic dechlorinating population, the dechlorinating bacteria are more efficient than methanogens at scavenging hydrogen at low concentrations or up to a hydrogen partial pressure of 100 ppm. The authors also determined that the methanogens were more sensitive than *Dhc* to high concentrations of chlorinated solvents (Ballapragada et al. 1997). Although electron donors will likely be consumed by all types of microorganisms, maintaining a low concentration of hydrogen at or near the source zone may limit competition.

A viscous electron donor that forms an immobile phase near the DNAPL:water interface could maintain a sustained source of electron donor near the source zone. Previous work suggests that insoluble electron donors that do form an immobile phase near the source zone can support microbial dechlorination and enhance DNAPL dissolution (Yang and McCarty 2002, Fisher and Harkness 2013). For example, emulsified vegetable oil (EVO) has been found to partition into the DNAPL and have long lifetimes in the source zone. Harkness and Fisher (2013) found that in a column with residual TCE DNAPL, a 5% EVO solution was almost entirely captured in the treatment area and was available to

support TCE dechlorination for up to three years. Additionally, Yang and McCarty (2002) compared different electron donors for use in organohalide respiration and found that all of the electron donors tested led to 2-3 fold increases in bioenhanced dissolution, but olive oil premixed with PCE had the highest electron donor efficiency when compared to continuously fed soluble pentanol and insoluble calcium oleate. The main problem with viscous electron donors is that they have a small area of contact and consequently it is difficult to ensure their delivery to the intended target area (ITRC 2008). Currently utilized electron donors are unable to simultaneously supply a sustained release of low concentrations of electron donor and ensure delivery of the electron donor to the intended target.

2.6 Partitioning Electron Donors

The limitations of the current electron donors have led to consideration of partitioning electron donors (PEDs). PEDs are water soluble compounds that favorably partition into the DNAPL (Cápiro et al. 2011). The concept of partitioning of dissolved solutes from the aqueous phase into an immiscible organic phase originated with the use of partitioning interwell tracer tests (PITTs). PITTs are used to estimate DNAPL saturation and distribution in contaminated aquifers (Dugan et al. 2003).

After the PED partitions into PCE- or TCE-DNAPL, the PED and contaminant simultaneously dissolve into the aqueous phase (Cápiro et al. 2011). If the dissolved PED is then hydrolzed or fermented to yield electron donors, the PED could provide a sustained source of electron donor at the DNAPL:aqueous interface. Fatty acid fermentation is thermodynamically constrained, which means that if the PEDs do undergo fermentation to form electron donors, the fermentation of the PEDs or their breakdown products, such as propionate or butyrate, will proceed slowly resulting in a

sustained low level of hydrogen (Schink 2002). This gives organohalide respiring microorganisms the competitive advantage over other microorganisms, such as methanogens (Ballapragada et al. 1997). PEDs also provide a lower viscosity-aqueous phase compared to emulsified liquids or other insoluble electron donors, which facilitates delivery near the source zone without impeding groundwater flow (Cápiro et al. 2011). If PEDs can be effectively introduced near the DNAPL source, they will partition into the DNAPL phase. This partitioning could provide a long-term electron donor source, promote growth of dechlorinating biomass near the DNAPL, and limit the amount consumed by competitor microorganisms as shown in Figure 2.3. These processes can in turn enhance DNAPL dissolution rates of the contaminant after a single injection (Cápiro et al. 2011).

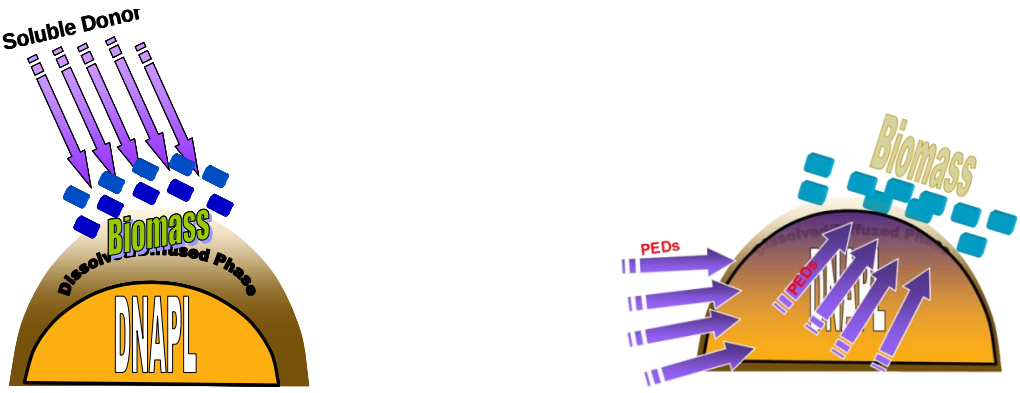

Figure 2.3 The difference between a soluble electron donor and a partitioning electron donor (Cápiro 2012).

The left image shows how a soluble electron donor would interact with the DNAPL and biomass (represented by the blue boxes). Biomass would grow where there is both dissolved electron donor and dissolved phase chlorinated solvent. The image on the right shows how the interaction would change if the electron donor was a PED. The PED would partition into the DNAPL and dissolve into the aqueous phase with the chlorinated solvent. This would promote biomass growth close to the DNAPL, enhancing DNAPL dissolution.

Despite the potential advantages of PEDs in source zone remediation, limited data is available regarding the phase behavior of PEDs at concentrations near solubility and this approach has not been evaluated under conditions that allow for comparison to

conventional electron donors. In order to fill this gap in the literature three candidate PEDs were chosen for further research: n-butyl acetate (nBA), 2-ethyl-1-hexanol (2E1H), and isopropyl propionate (IPP). The first PED candidate, nBA, was chosen based on previous work that showed its ability to partition into TCE (Roberts 2008, Cápiro et al. 2011) and to undergo fermentation or hydrolysis to form potential electron donors (Barton et al. 2000). It has also been shown to sustain TCE organohalide respiration to ethene with a dechlorinating consortium (Harkness et al. 2012). For this project, confirmatory studies with nBA and TCE were used to verify analytical method accuracy, and additional studies were completed with nBA and PCE. 2E1H was chosen based on its use in PITTs, and because its partitioning coefficient into TCE has been previously documented as ranging between 202 and 227 (Istok et al. 2002, Dugan et al. 2003). IPP was chosen because it is a food additive that is similar in structure to nBA. Using these three candidate PEDs, a series of batch reactors and one-dimensional column experiments were completed using both TCE and PCE.

Batch reactor experiments were completed in order to determine liquid-liquid PED mass transfer rates, equilibrium NAPL-water partitioning coefficients (K_{NW}), and equilibrium soil partitioning (K_d) for each of the PED candidates. Column experiments were used to determine dynamic uptake and release behavior and PED lifetime in both residual PCE- and TCE-DNAPL. Biotic batch reactors were used to determine the ability of the PEDs to be utilized by a dechlorinating consortium to reduce PCE to ethene. Based on the ability to sustain organohalide respiration of PCE to ethene and its high partitioning into both PCE and TCE, nBA was chosen for further column experiments containing a dechlorinating consortium. In these column experiments nBA was compared to the commonly used soluble electron donor lactate. These columns considered the frequency

of electron donor addition, extent of dechlorination, and ability of the electron donor to support bioenhanced dissolution.

Chapter 3: Evaluation of PED Mass Transfer Properties under Abiotic Conditions

3.1 Introduction and Objectives

Partitioning electron donors (PEDs) are water soluble organic compounds that favorably partition into non-aqueous phase liquid (NAPL) (Cápiro et al. 2011). In order for a chemical to be a PED, it must both partition favorably into the NAPL phase and the compound itself, or its breakdown products, must be utilized as an electron donor for organohalide respiration of chlorinated ethenes. This chapter seeks to extend beyond previous work performed with n-hexanol and n-butyl acetate (nBA) in the presence of TCE under limited environmentally relevant conditions (Cápiro et al. 2011) by performing an in-depth screening of additional potential PEDs. Three PED candidates 2-ethyl-1-hexanol (2E1H), isopropyl propionate (IPP), and nBA (based on previous encouraging results), were evaluated on the basis of their ability to partition into and then subsequently dissolve out of both tetrachloroethene (PCE) and trichloroethene (TCE) over a broad spectrum of relevant geochemical conditions. A series of abiotic batch reactors and column experiments were designed around the following hypotheses:

1) Based upon previous research describing sustained liquid-liquid partitioning of esters, organic alcohols, and fatty acids (Cápiro et al. 2011), *it is hypothesized that compounds of similar characteristics and structure will have large K_{NW} values, or aqueous-NAPL partitioning into PCE and TCE*.
2) Previous research also suggests that this partitioning is dependent on the ionic strength. For example, surfactants have been shown to have increased partitioning into NAPL with an increase in the ionic strength (Park and Bielefeldt 2003). Similarly, when ionic strength was increased 3-fold, from 10 mM to 30 mM, the K_{NW} for nBA and TCE increased from about 330 to 400 (Cápiro et al.

2011). *Therefore, it is hypothesized that as the ionic strength increases so will the candidate PED partitioning into PCE, and that this effect will be linear over a large range of salinities.*

3) Based on previous research that revealed that both surfactant sorption (Edwards et al. 1994) and chlorinated solvent sorption (Zytner 1991) is dependent upon the organic carbon content of the soil, *it is hypothesized that the candidate PEDs will also sorb to the organic carbon in soils, and as the organic carbon content of the soil increases so will the K_d value, or the solid partitioning coefficient.*

4) Based on previous work demonstrating that PED concentrations can persist beyond the duration of their injection in the presense of entrapped NAPL and that their breakthrough curve are best modeled using non-equilibrium models (Cápiro et al. 2011), *it is hypothesized that the candidate PEDs evaluated will have long lifetimes (25-50x their injection length) in both residual TCE- and PCE-NAPL saturated columns and that the partitioning into the DNAPL is rate limited.*

To test these hypotheses, abiotic batch reactor experiments were completed to determine (i) the phase distribution parameters (K_{NW}), (ii) the mass transfer parameters (k), and (iii) the solid partitioning coefficient (K_d) for the candidate PEDs. The parameters determined in the abiotic batch reactors were used as initial input parameters to model the candidate PED behavior in column experiments that were established to determine the PED partitioning under dynamic flow conditions. The goal of PED screening and identification was to choose soluble compounds that exhibit substantial partitioning into PCE- and TCE-DNAPL for further experiments that will determine their ability to support organohalide respiration. This work seeks to fill gaps in the literature by evaluating additional potential PED compounds over a range of ionic strengths or under dynamic

flow conditions and exploring the potential for these compounds to sorb to organic carbon in aquifer material.

3.2 Candidate PEDs

Three compounds with potential for both high partitioning and the ability to serve as electron donors were screened as potential PEDs. The first candidate PED is n-butyl acetate (nBA), which is a clear, volatile, flammable, organic solvent with a sweet odor and has a solubility near 7,000 mg/L (Pubchem 2014). It is a common food additive and is also used in paints, printing inks, aerosol sprays, fragrances, and cosmetics (DOW 2014). It was chosen because food science literature indicates that it can be hydrolyzed or fermented to nontoxic compounds such as acetate, butyrate, and n-butanol, which could serve as potential electron donors or electron precursors (Barton et al. 2000). The reaction in which nBA undergoes hydrolysis to form acetic acid and butanol is shown below in Figure 3.1 (Williamson 1994, David et al. 2001). Previously completed biotic batch reactors with a dechlorinating consortium indicate that nBA can sustain organohalide respiration of PCE to ethene (Harkness et al. 2012, Roberts 2008). Additionally, previously completed batch reactor experiments have yielded an equilibrium TCE-DNAPL and water partitioning coefficient (K_{NW}) of 330.43 ± 6.7 and first-order liquid-liquid mass transfer rates of 0.22 min^{-1} with nBA concentrations near solubility (Cápiro et al. 2011). The K_{NW} is the ratio of the concentration of nBA in the TCE-DNAPL to the concentration of nBA in the aqueous phase such that a K_{NW} greater than one indicates that partitioning into the NAPL phase occurs preferentially over aqueous-phase partitioning. Therefore, these results indicate that nBA very favorably partitions into TCE-DNAPL.

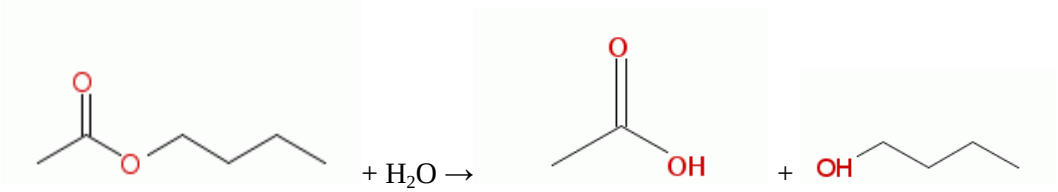

Figure 3.1 Hydrolysis of n-butyl-acetate to form acetic acid and butanol (eMolecules 2014).

The price per pound of nBA is between $0.67 and $0.72 (ICIS 2014), which is similar to the price of lactate, a common soluble electron donor which costs between $0.70/lb and $0.80/lb (ICIS 2014). Based solely on stoichiometry, one mole of nBA can form 16 moles of hydrogen, and four moles of hydrogen are required to reduce PCE to ethene, one mole for each step. Therefore one mole of nBA can reduce 4 moles of PCE to ethene. This is equal to its reducing equivalent. The balanced chemical reaction of nBA reacting with water is shown below in Equation 3.1. Table 3.1 summarizes the relevant chemical properties, price, and reducing equivalents of nBA, the other PED candidates, and lactate.

$$C_6H_{12}O_2 + 10H_2O \rightarrow 16H_2 + 6CO_2 \qquad (3.1)$$

The second PED candidate is 2-ethyl-1-hexanol (2E1H), which is used in the production of plasticizers, coatings, and adhesives (DOW 2014) and has a solubility of around 880 mg/L, the lowest of the three candidate PEDs tested (Pubchem 2014). This chemical was chosen as a potential PED because it is known to partition into TCE. It is commonly used as a partitioning tracer (PITT) and has a TCE-DNAPL and water partitioning coefficient of 227 (Dugan et al. 2003). The price per pound or 2E1H is between $0.62 and $0.65, so it is cost competitive with both nBA and lactate (ICIS 2014). The hydrolysis of 2E1H forms 8 moles of carbon dioxide and 24 moles of hydrogen; this reaction is shown in Equation 3.2. Based on stoichiometry, one moles of 2E1H can reduce 6 moles of PCE to ethene. The relevant chemical properties, price, and reducing equivalents of 2E1H are summarized below in Table 3.1.

$$C_8H_{18}O + 15H_2O \rightarrow 8CO_2 + 24H_2 \qquad (3.2)$$

The third PED candidate, isopropyl propionate (IPP), is a short chain fatty acid. It is colorless with a fruity odor and is the main ingredient in artificial rum extracts and flavorings (DOW 2014). IPP has a solubility of 5,950 mg/L (Pubchem 2014) and was chosen as a potential PED due to its similarity in structure to nBA and because previous studies have indicated the potential for nBA to act as a PED (Roberts 2008, Cápiro et al. 2011). The hydrolysis of IPP forms propionic acid and isopropyl alcohol in the reaction shown below in Figure 3.2 (Williamson 1994).

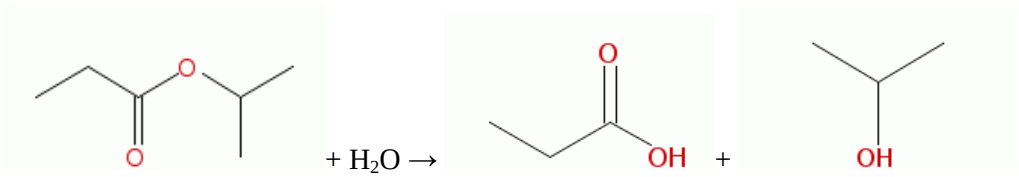

Figure 3.2 Hydrolysis of isopropyl propionate to form propionic acid and isopropyl alcohol (eMolecules 2014).

The price of IPP is not listed on ICIS Chemical Market's list of chemical prices. Based on stoichiometry, one mole of IPP can reduce 4 moles of PCE to ethene. The balanced chemical reaction in which IPP reacts with water is shown below in Equation 3.3. Its relevant chemical properties and reducing equivalents are summarized below in Table 3.1

$$C_6H_{12}O_2 + 10H_2O \rightarrow 16H_2 + 6CO_2 \qquad (3.3)$$

Table 3.1 Summary of chemical properties and prices of the three candidate partitioning electron donors and lactate.

	Molecular Weight (g/mol)	**Density (g/mL)**	**Solubility (mg/L)**	**Price per Pound**	**Reducing Equivalents (mol PCE/ mol PED)**
nBA	116.16	0.88	7,000	$0.67-$0.72	4
2E1H	130.23	0.83	880	$0.62-$0.65	6
IPP	116.16	0.87	5,950	NL	4
Lactate (60% syrup)	112.06	1.31	NA	$0.70-$0.80	1.5

NL= Not Listed, NA= Not Applicable. Chemical property data was obtained from Pubchem (2014). Chemical prices were obtained from ICIS (2014).

3.3 Materials

High Performance Liquid Chromatography (HPLC)-grade PCE and TCE were purchased from Sigma-Aldrich Co. (St. Louis, Missouri). PCE has an equilibrium aqueous phase solubility of 200 mg/L and a liquid density of 1.63 g/cm^3 (Huling and Weaver 1991). TCE has an equilibrium phase solubility of 1,100 mg/L and a density of 1.46 g/cm^3 (Huling and Weaver 1991). PCE and TCE were dyed with 0.4 mM Oil-Red-O, a hydrophobic dye, purchased from Fisher Scientific (Fair Lawn, New Jersey). Hexadecane (HD, 99%), which has an equilibrium aqueous phase solubility of 0.0036 mg/L and a density of 0.77 g/mL, was purchased from Sigma Aldrich (Schwarzenbach et al. 2003). The three PED candidates are IPP (Fisher Scientific Fair Lawn; New Jersey), nBA (Sigma-Aldrich Co.), and 2E1H (Sigma-Aldrich Co.). For use in analytical analyses, HPLC grade isopropyl alcohol was purchased from Fisher Scientific. Calcium chloride was used to increase the ionic strength of the abiotic batch reactors and was purchased from Sigma-Aldrich Co. Sodium bromide was used as a non-reactive tracer and was purchased from Fisher Scientific. All chemicals were of reagent grade or higher purity, and all solutions were prepared using 18 MΩ/cm deionized water (EMD Millipore; Billerica, Massachusetts).

Sorption experiments were completed with Appling soil (University of Georgia Agricultural Experiment Station; Eastville, Georgia), Federal Fine Ottawa sand (US Silica Company; Berkeley Spring, West Virginia), and Webster soil (Iowa State University Agricultural Experiment Station; Ames, Iowa). Appling soil is a natural field soil, classified as silty sand (Wang et al. 2010). Appling soil was sieved using a number 30 sieve so that only particles less than 0.595 mm were used for experiments. Appling soil with particle size less than 0.595 mm has an organic content of 0.66% (wt) (Marcet,

2014). Federal Fine Ottawa Sand is a quartz sand with 0.32 mm mean diameter and an intrinsic permeability of 4.2 X 10^{-11} m^2 (Suchomel et al. 2007). The organic carbon content is 0.01% (wt) (Marcet, 2014). Webster soil is a silt clay loam (Wang et al. 2010). Its organic carbon content is 1.96% (wt) (Marcet, 2014). Additional sorption experiments were completed with glass beads, 40-50 mesh or 0.297 to 0.4 mm (AGSCO Corporation, Wheeling, Illinois). All columns were also packed with Federal Fine Ottawa sand.

3.4 Design and Setup of Abiotic Batch Reactors

The design and setup of all of the abiotic batch reactors including those setup with soil are described below.

3.4.1 Design and Setup of Abiotic Batch Reactors

Batch reactors were setup in 40 mL Teflon screw cap glass vials (VWR International, Westchester, Pennsylvania). Vials were filled at a ratio of 3:1 (v/v) with aqueous PED solution and neat TCE or PCE at an ionic strength of 10 mM. Equilibrium DNAPL and water partitioning coefficients (K_{nw}) were determined after 24 hours of mixing on a LabQuake oscillating shaker table (Barnstead/Thermolyne, Dubuque, Iowa) in vials with eight different initial PED concentrations. Concentrations of nBA, 2E1H, and IPP varied between 0 and 5000 mg/L, 0 and 555 mg/L, and 0 and 4000 mg/L, respectively. After mixing for 24 hours, vials were centrifuged for 5 minutes at 1500 rpm (International Equipment Company (IEC) Centra CL2 centrifuge, Needham Heights, MA). Additional experiments were completed to determine the effect of ionic strength on the K_{NW}. For these experiments, vials were filled at a ratio of 3:1 (v/v) with varying concentrations of nBA and neat PCE. The ionic strength was adjusted between 0 mM and 80 mM by adding the appropriate amounts of calcium chloride.

Another set of experiments were used to obtain the effective mass transfer rates (k) for each PED at an aqueous concentration approaching their aqueous solubility, 5000 mg/L, 550 mg/L, and 4000 mg/L for nBA, 2E1H, and IPP, respectively. The ionic strength of these batch reactors was also 10 mM. Samples were collected from triplicate vials at time intervals of 5, 10, 20, 30, 35, 40, 45, and 50 minutes. It was confirmed that equilibrium was reached by having two consecutive samples with the same concentrations in the aqueous and NAPL phases. At the conclusion of each mixing period the vials were centrifuged for 5 minutes at 1500 rpm. For all batch reactor experiments, samples were taken from triplicate glass vials using a gas-tight syringe. Samples of 250 µL from the NAPL phase and 750 µL from the aqueous phase were transferred from the 40 mL Teflon vials to 2.0 mL glass vials containing 1000 and 750 µL of isopropyl alcohol, respectively, for analysis using a gas chromatograph (GC) equipped with a flame ionization detector (FID), described below. The batch reactor setup is shown in Figure 3.3.

Figure 3.3 Abiotic batch reactors containing a partitioning electron donor and non-aqueous phase liquid, on an oscillating shaker table.

Additionally, abiotic batch reactors were completed to determine equilibrium NAPL and water partitioning coefficients into hexadecane (HD) and NAPLs containing HD to determine the partitioning that would occur in the biotic batch reactors and biotic columns. Batch reactors were set-up and sampled as described above except for changes in the NAPL used and the ionic strength. Batch reactors with nBA concentrations ranging from 0-5000 mg/L were set-up using HD, 0.95 mol HD: 0.05 mol TCE, and 0.75 mol

HD: 0.25 mol PCE at 10 mM ionic strength. These ratios of HD to PCE or TCE were used because they result in aqueous concentrations for both TCE and PCE of about 50 mg/L, or concentrations well below the inhibition level of the dechlorinating microbial population (Amos et al. 2007, Amos et al. 2008). Additional batch reactors were completed for nBA, 2E1H, IPP, and lactate with concentrations ranging from 0 to 5000 mg/L, 0 to 555 mg/L, 0 to 4000 mg/L, and 0 to 3000 mg/L, respectively, with 0.75 mol HD: 0.25 mol PCE mixed NAPL. These batch reactors were run using the same reduced medium solution as used in the biotic batch reactors, described previously (Sung et al. 2003, Amos et al. 2008). The ionic strength of the reduced medium solution is 90 mM.

3.4.2 Design and Setup of Abiotic Batch Reactors with Soil

Additional batch reactors were completed in soil to determine the sorption of the PEDs onto the organic carbon in soil. Initial screening was completed with a solid containing a moderate organic carbon content, Appling soil. The reactors were setup in 40 mL glass vials with Teflon screw caps (VWR International). Vials were filled with 5 grams of Appling soil or glass beads and varying concentrations of aqueous PED solution. PED aqueous concentrations varied from 0 to 6000 mg/L, 0 to 760 mg/L, and 0 to 4500 mg/L for nBA, 2E1H, and IPP, respectively, at 10 mM ionic strength. Vials were mixed on a LabQuake oscillating shaker table for at least 24 hours. At the end of the mixing period vials were centrifuged for 20 minutes at 1500 rpm using an IEC Centra CL2 centrifuge. Samples were collected from triplicate vials. Aqueous samples of 750 µL were taken using a gas-tight syringe and filtered with an Acrodisc nylon 13 mm diameter filter with 0.2 µm pore size purchased from VWR International. Samples were then added to a 2.0 mL glass vial. Excess aqueous PED solution was decanted from the original glass vial and 5 mL of 18 MΩ/cm deionized water was added to ensure the removal of the aqueous PED solution. Vials were centrifuged for 5 minutes at 1500 rpm. Excess liquid was again

decanted and 5 mL of isopropyl alcohol was added to each vial to desorb the PED from the soil. Vials were centrifuged for 5 minutes at 1500 rpm and again sampled using a gas-tight syringe and filtered using an Acrodisc filter. Samples were put in a 2.0 mL glass vial for analysis using a gas chromatograph (GC) equipped with a flame ionization detector (FID), described below. Following these experiments, additional batch reactors were setup to further determine the effects of organic carbon content on the sorption coefficient. These experiments were setup as described above using both nBA and IPP and two additional soils, Federal Fine Ottawa sand, which has an organic carbon content of 0.01%, and Webster soil, which has an organic carbon content of 1.96% (Marcet 2014). The sorption batch setup is shown below in Figure 3.4.

Figure 3.4 Batch reactor containing Appling Soil, mixing on an oscillating shaker table.

3.5 Column Experiment Design and Setup

Six abiotic 1-D column experiments were conducted to quantify PED mass transfer in Federal Fine Ottawa sand containing a uniform distribution of residual PCE- or TCE-DNAPL. One column was completed with each of the three candidate PEDs and PCE and one column was completed with each of the three candidate PEDs and TCE.

3.5.1 Abiotic Column Setup

Borosilicate glass columns (15 cm x 4.8 cm, Kontes Glass Company; Vineland, New Jersey) equipped with Teflon end-plates were packed dry with Federal Fine Ottawa sand. Columns were saturated with 10 mM ionic strength or 500 mg/L calcium chloride. Non-

reactive 10 mM sodium bromide tracers were obtained prior to and after the introduction of NAPL. The sodium bromide solution was pumped into the column for two pore volumes (PVs) and then the system was switched to flush and 10 mM calcium chloride was pumped through the columns for an additional three PVs. A Spectray Chrom Fraction Collector CF-2 (Spectrum Laboratories; Piscataway, New Jersey) was used to collect effluent samples throughout the tracer. An Accumet Model 50 pH/ion/conductivity meter (Fisher Scientific) was used to determine bromide levels of the effluent samples collected. The non-reactive tracer was used to confirm the aqueous PV, the absence of immobile water, and to measure hydrodynamic dispersion within the column.

Prior to the introduction of NAPL, PED breakthrough curves were obtained to determine if there was any interaction with the sand. PED breakthrough curves were obtained by pumping 2 PVs of a PED solution near solubility, 4000-5000 mg/L nBA, 3500-4500 mg/L IPP, or 800-900 mg/L 2E1H, before being switched to flush with background electrolyte solution, 500 mg/L calcium chloride. All aqueous solutions were introduced at approximately 2.5 mL/min or a seepage velocity of 5 m/day, using a Gilson model Minipuls 3 peristaltic pump (Middleton, Wisconsin). The actual flow rate was calculated during the sodium bromide tracer, the average volume collected in each vial of the fraction collector was divided by the time used to collect the sample. The actual flow rates ranged from 1.60 mL/min to 2.81 mL/min. Cápiro et al. (2011) showed that PED partitioning in TCE-DNAPL in similar column experiments is flow rate dependent, but the slope of the dependency is small indicating that these changes in flow rate will have a small effect on the PED partitioning. Effluent samples were taken until no PED was detected; PED detection limits are 1.87 mg/L, 0.97 mg/L, and 0.57 mg/L for nBA, IPP, and 2E1H, respectively and were determined using the Habaux-Vos detection limit

method (Hubaux and Vos 1970). Next TCE-and PCE-DNAPL was stained with 0.4 mM Oil-Red-O and introduced to the columns via a Harvard Apparatus Syringe Infusion Pump 2.2 (Holliston, Massachusetts) at 2 mL/min. Between 80 and 100 mL of neat NAPL were introduced to each column with upward flow followed by downward flushing with 10mM calcium chloride background solution until no NAPL was visible in the column effluent. NAPL saturation was determined from the weight of the column prior to the addition of NAPL and after the addition of NAPL (Wilson et al. 1990). The NAPL saturations ranged from 13.5% to 16.9%, except for the IPP and TCE column which had a NAPL saturation of 19.9%. This higher NAPL saturation could indicate that this column had some NAPL that was not entrapped. A column containing residual NAPL is shown below in Figure 3.5.

Figure 3.5 Abiotic column containing residual tetrachloroethene dyed with Oil-Red-O.

After NAPL saturation, the second non-reactive sodium bromide tracer was completed. Following the tracer, additional PED breakthrough curves were obtained by pumping 2 PVs of the PED solution followed by a flush of 500 mg/L calcium chloride as described

above. Actual flow rates and seepage velocities for each of the columns is listed below in Table 3.2. The experimental set-up is show below in Figure 3.6.

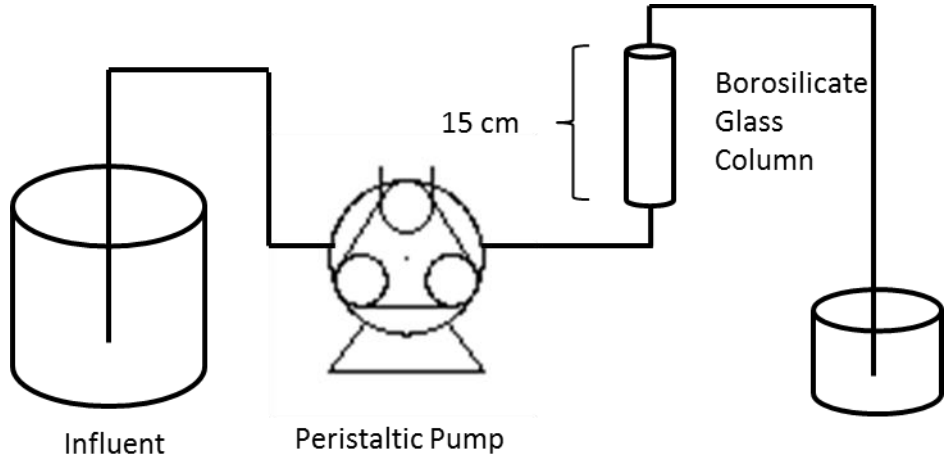

Figure 3.6 Schematic diagram of the column setup.

Column effluent samples were taken in 20 mL screw top glass scintillation vials (VWR) by adding 5 mL of isopropyl alcohol to the vial prior to sampling and adding samples of approximately 5 mL from the column effluent. Effluent samples were taken by using a ring stand to ensure the effluent tubing remained in the sample vial for the sampling time of 2 minutes. Vials were weighed empty, after the addition of isopropyl alcohol, and after sampling and a dilution factor was calculated. Next, 1 mL of the sample was transferred to a 2.0 mL glass vial for analysis using a gas chromatograph (GC) equipped with a flame ionization detector (FID), described below, and was analyzed for PCE or TCE and PED concentrations. During each column experiment, periods of flow interruption, ranging from 3-135 hours, were employed to assess if PED mass transfer between the aqueous phase and the NAPL phase is rate-limited or instantaneous. Samples were taken immediately following each flow interruption. Identical operational procedures were used to run all six columns to allow for direct comparisons between data sets. A summary of the experimental conditions is given below in Table 3.2.

Table 3.2 Summary of experimental conditions for abiotic column experiments.

Experimental Parameter	**TCE**			**PCE**		
Partitioning Electron Donor	**n-butyl acetate**	**2-ethyl-1-hexanol**	**Isopropyl propionate**	**n-butyl acetate**	**2-ethyl-1-hexanol**	**Isopropyl propionate**
Actual Flow Rate (mL/min)	2.50	1.60	2.81	1.99	2.31	2.79
Seepage Velocity (m/day), v_p	5.0	3.3	5.9	4.2	4.8	5.8
Porosity, n	0.39	0.39	0.38	0.38	0.39	0.38
Initial PED Concentration (mg/L), C	4876	843	4917	3976	859	4303
NAPL Saturation (%), S_{NAPL}	13.5	15.9	20.1	16.5	16.9	16.8
Flow Interruption Duration (h)	5-20	3-135	3-92	8-12	8-36	12-18

3.5.2 Column Modeling

For each bromide tracer completed, relative bromide concentrations (C/C_0) were plotted versus the number of PVs eluted from the column. The resulting breakthrough curves (BTCs) were simulated using the mathematical model, Code for Estimating Equilibrium Transport Parameters from Miscible Displacement Experiments (CFITM) as a part of Studio of Analytical Models (STANDMOD) Version 2.2 (available through USDA-ARS U.S. Salinity Laboratory; http://www.ars.usda.gov). PED BTCs were also analyzed using this model along with another STANMOD model, Code for Estimating Non-Equilibrium Transport Parameters from Miscible Displacement Experiments (CFITIM). Both codes provide analytical solutions for semi-infinite columns. CFITIM incorporates a 1-D form of the advection-dispersion-reaction (ADR) solute transport equation. When immobile NAPL is present, the dimensionless form of the 1-D ADR takes the form of Equation 3.4.

$$\frac{R_F \partial C^*}{\partial PV} = \frac{1}{Pe} * \frac{\partial^2 C^*}{\partial X^2} - \frac{\partial C^*}{\partial X} \qquad (3.4)$$

R_F is the solute retardation factor, PV is the dimensionless pore volume eluted from the column, P_e is the Peclet number, and C^* is the relative concentration. Equations 3.5-3.10 below describe each of these variables.

$$R_F = 1 + \frac{K_{NW} S_N}{1 - S_N} \quad (3.5)$$

$$C^* = \frac{C}{C_0} \quad (3.6)$$

$$PV = \frac{v_p t}{L} \quad (3.7)$$

$$Pe = \frac{v_p L}{D_H} \quad (3.8)$$

$$D_H = v_p \alpha \quad (3.9)$$

$$X = \frac{x}{L} \quad (3.10)$$

K_{NW} is NAPL-aqueous partitioning coefficient, S_N is the volumetric NAPL saturation, C is the aqueous concentration (mg/L), C_0 is the initial concentration (mg/L), v_p is the pore-water velocity (cm/min), t is time (min), L is the column length (cm), D_H is the hydrodynamic dispersion coefficient (cm^2/min), α is the dispersivity (cm), and x is the distance parallel to flow. The "two-site" model is also included in CFITIM. This model can be used to describe rate-limited processes such as adsorption and desorption or physical mass transfer limitations such as solute diffusion between regions of mobile and immobile water (van Genuchten and Wagenet 1989). The model is based on the concept that the solid phase of the soil is made up of different constituents, such as soil minerals and organic matter, and that a chemical is likely to interact with the different constituents differently (van Genuchten 1981). The two-site model assumes adsorption sites fit one of two types. The first type of adsorption site is instantaneous and the second is time-dependent (van Genuchten 1981). A two-site adsorption model is considered when modeling rate-limited interactions.

The two-site model introduces two new variables, *k* and F. The parameter *k* describes the first-order rate of sorption and F is the fraction of sites considered to be at equilibrium or sites in which instantaneous adsorption occurs. When the value of F approaches 1 all reaction sites are at equilibrium and when the value of F approaches 0 all reaction sites are at non-equilibrium (van Genuchten and Wagenet 1989). Two new dimensionless parameters are used to incorporate *k* and F. β is a dimensionless partitioning parameter and ω is a dimensionless coefficient for kinetic sorption or mobile-immobile type exchange. Equations 3.11 and 3.12 describe β and ω.

$$\beta R_F = 1 + \frac{FK_{NW}S_N}{(1-S_N)} \qquad (3.11)$$

$$\omega = \frac{k(1-\beta)R_F L}{v_p} \qquad (3.12)$$

3.6 Analytical Methods

All of the abiotic batch reactors and columns were analyzed for PED, PCE, and TCE concentrations. These concentrations were measured using a 7890 GC equipped with a liquid autosampler (HP 7683) and an Agilent DB-5 column (30 m by 0.32 mm OD) connected to a flame ionization detector (FID) (Agilent; Santa Clara, CA).

3.7 Experimental Results and Discussion

Batch experiments were completed to determine the rate and extent of PED partitioning into the NAPL phase and the sorption of PEDs to natural soil.

3.7.1 Abiotic Batch Reactor Results- Equilibrium Partitioning Coefficients

Abiotic batch reactors were completed to determine the equilibrium partitioning coefficient (K_{NW}) or how readily the PEDs partition into the NAPL phase. The equilibrium partitioning coefficients (K_{NW}) are based on the slope of the PED concentration in the NAPL phase versus PED concentration in the aqueous phase line.

The higher the K_{NW} the larger amount of PED that will partition into the NAPL phase. The results of the equilibrium batch experiments, shown in Figures 3.7-3.9, indicate that all three PEDs readily partition into the NAPL phase. All of the PEDs partition more readily into TCE than into PCE. The NAPL-aqueous partitioning coefficients ranged from 95.6 to 352 at an ionic strength of 10 mM. The PED with the highest equilibrium partitioning coefficient was nBA, with equilibrium partitioning coefficients of 352 ± 8.3 and 129 ± 5.0 for TCE and PCE, respectively, as shown in Figure 3.7. The nBA and TCE partitioning coefficient is similar to the value previously reported of 330.43 ± 6.7 (Cápiro et al. 2011). IPP has the next highest partitioning into TCE with equilibrium partitioning coefficients of 277 ± 18.5 and 96 ± 1.4 for TCE and PCE, respectively, as shown in Figure 3.8. The PED with the lowest partitioning into TCE is 2E1H, which has equilibrium partitioning coefficients of 222 ± 4.1 and 137 ± 12.2 for TCE and PCE, respectively, as shown in Figure 3.9. The 2E1H and TCE partitioning coefficient is similar to the previously reported value of 227 (Dugan et al. 2003). Figure 3.7-3.9 show the results of the batch reactor experiments including the K_{NW} values for each PED in both TCE and PCE.

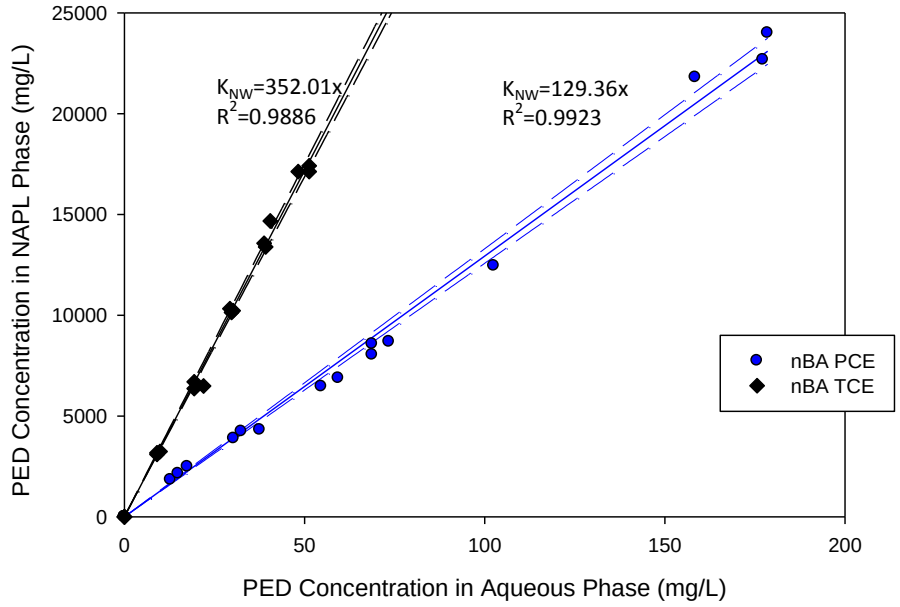

Figure 3.7 Equilibrium partitioning coefficients for n-butyl acetate in both tetrachloroethene and trichloroethene.

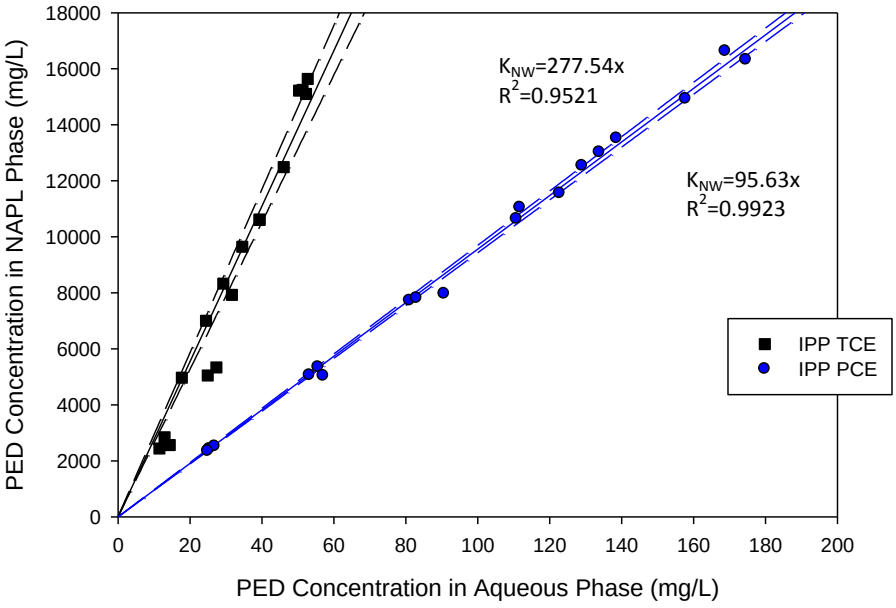

Figure 3.8 Equilibrium partitioning coefficients for isopropyl propionate in both tetrachloroethene and trichloroethene.

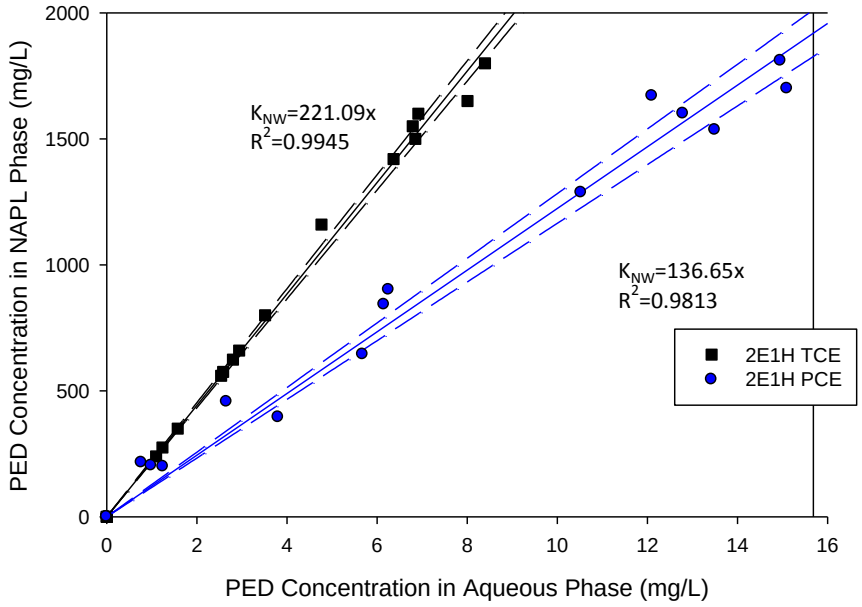

Figure 3.9 Equilibrium partitioning coefficients for 2-ethyl-1-hexanol in both tetrachloroethene and trichloroethene.

The equilibrium partitioning coefficients do not seem to be predictable based on solubility, octanol water partitioning coefficients (K_{OW}), or soil organic carbon content partitioning coefficients (K_{OC}). Meylan et al. (1996) came up with correlations that relate K_{OW} or K_{OC} to solubility. These correlations are listed below in Equations 3.13 and 3.14.

$$-0.834 * LOG(K_{OW}) = LOG(S) + 0.0084(MW) - 0.920 \qquad (3.13)$$

$$LOG(K_{OC}) = -0.55LOG(S) + 3.64 \qquad (3.14)$$

S is the solubility (mg/L) and MW is the molecular weight (g/mol). These correlations were used to calculate K_{OW} and K_{OC} values for each of the PEDs along with another chemical, n-hexanol, whose partitioning into TCE is previously reported at 21.7 ± 6.7 (Cápiro et al. 2011). Hexanol has a high solubility of 5900 mg/L and therefore a low K_{OW} and a low K_{OC} but it also has a very low K_{NW}. From the results obtained using Equations 3.13 and 3.14 and data from these four chemicals, there does not appear to be a trend

between solubility, K_{OW}, or K_{OC} and K_{NW}. The solubility, K_{OW}, K_{OC}, and K_{NW} values are summarized in Table 3.3.

Table 3.3 Octanol-water partitioning (K_{OW}), soil organic content-water partitioning (K_{OC}), and NAPL-water partitioning coefficients (K_{NW}) in trichloroethene for each of the partitioning electron donors and n-hexanol.

Partitioning Electron Donor	**Solubility (mg/L)**	**Kow**	**K_{OC}**	**K_{NW}**
n-Butyl Acetate	7,000	1.52×10^{-5}	33.5	352
2-Ethyl-1-Hexanol	880	2.83×10^{-4}	105	221
Isopropyl Propionate	5,950	3.14×10^{-5}	40.3	277
n-Hexanol	5,900	3.57×10^{-5}	10.2	21.7

The K_{OW} and K_{OC} values are calculated using Equations 3.13 and 3.14. Cápiro et al. (2011) determined the K_{NW} value for n-hexanol of 21.7. All other K_{NW} values were determined experimentally in this study.

Although the equilibrium partitioning coefficient is not predictable, it is directly dependent on ionic strength. As the ionic strength increases so does the equilibrium partitioning coefficient. The batch reactor experiments containing nBA and PCE were setup at four additional ionic strengths. The equilibrium partitioning coefficients were determined to be 112 ± 6.6, 128 ± 11.1, 136 ± 10.5, 169 ± 9.0, and 220 ± 10.6 for 0 mM, 10 mM, 40 mM, 60 mM, and 80 mM ionic strengths, respectively. From these results, the relationship between the ionic strength and equilibrium partitioning coefficient for nBA is fairly linear with a slope slightly larger than one. These results indicate that greater partitioning of PEDs into NAPLs is likely to occur in aquifers formations with higher salt concentrations, and that PED partitioning can be manipulated by changing the ionic strength of the delivery solution. Each of the equilibrium partitioning coefficients is plotted versus its corresponding ionic strength in Figure 3.10.

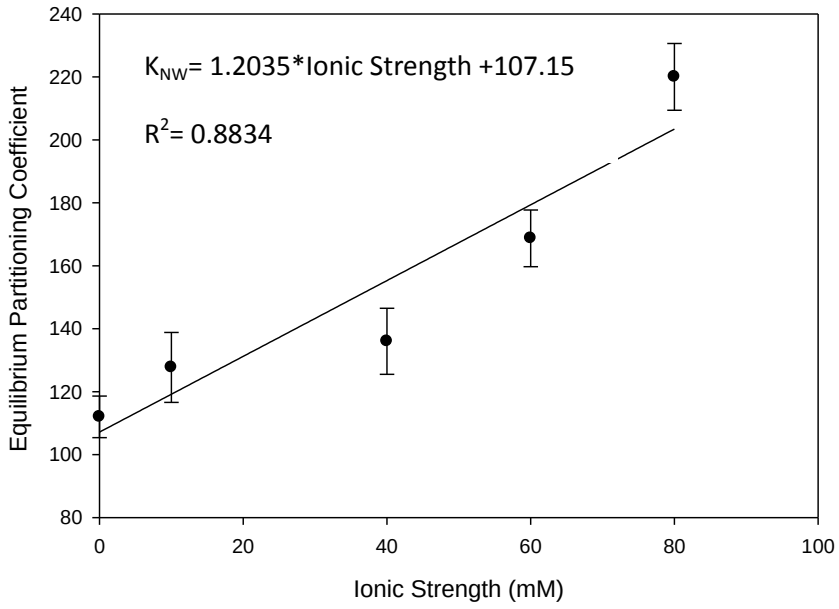

Figure 3.10 The relationship between ionic strength and equilibrium partitioning coefficient for n-butyl acetate and tetrachloroethene batch reactor experiments.

3.7.2 Abiotic Batch Reactors- Mass Transfer Parameters

Abiotic batch reactors were completed to determine the effective mass transfer coefficient (k) or the relative speed in which the PEDs partition into the NAPL phase. The higher the k value the faster the PED partitions into the NAPL phase. The relative effective mass transfer rates for each PED were determined from the aqueous concentrations at various times after mixing. The results of the kinetic batch experiments indicate that all three of the PEDs partition into TCE and PCE at rates between 0.115 min^{-1} and 0.174 min^{-1} and, therefore, all partition at a similar rate. The higher the effective mass transfer rate the more the PED partitions into the NAPL phase in a given amount of time. The PED that exhibited the fastest partitioning into the NAPL phase is nBA, with mass transfer coefficients of 0.174 min^{-1} and 0.126 min^{-1} for TCE and PCE, respectively, as shown in Figure 3.11. IPP has slightly lower mass transfer rates of 0.115 min^{-1} and 0.119 min^{-1} for TCE and PCE, respectively, as shown in Figure 3.12. The mass

transfer rates of 2E1H are 0.161 min^{-1} and 0.116 min^{-1} for TCE and PCE, respectively, as shown in Figure 3.13. The results for the batch reactors including the k values for both TCE and PCE are shown in Figure 3.11-3.13.

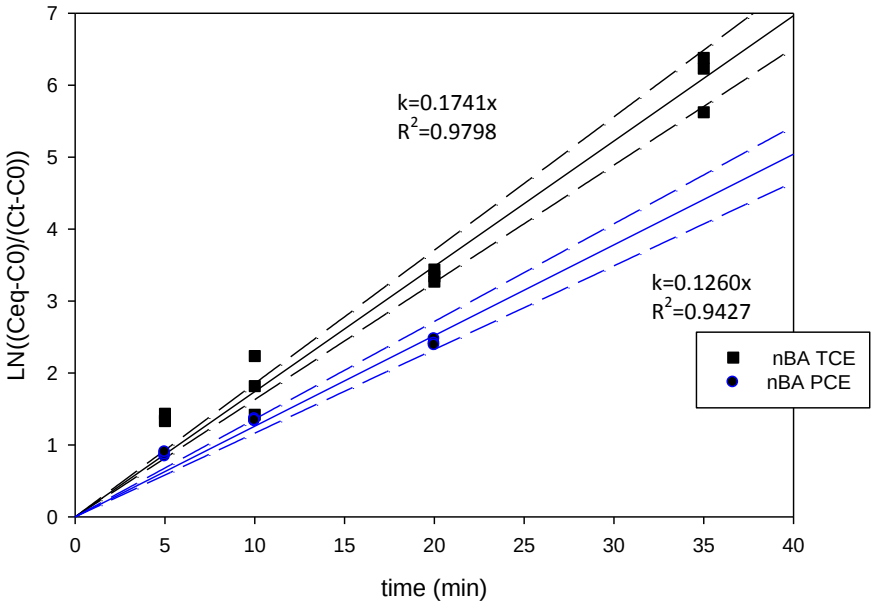

Figure 3.11 Effective mass transfer for n-butyl acetate in both tetrachloroethene and trichloroethene.

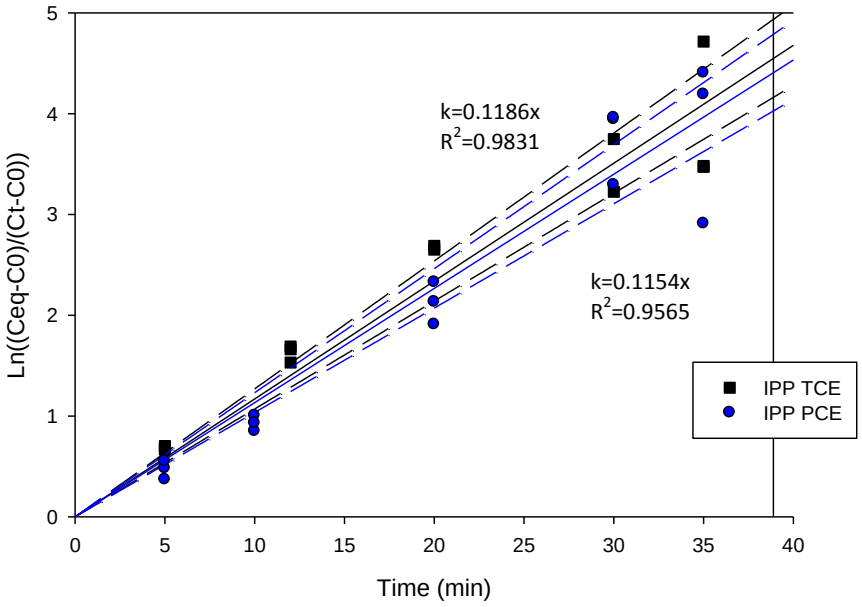

Figure 3.12 Effective mass transfer for isopropyl propionate in both tetrachloroethene and trichloroethene.

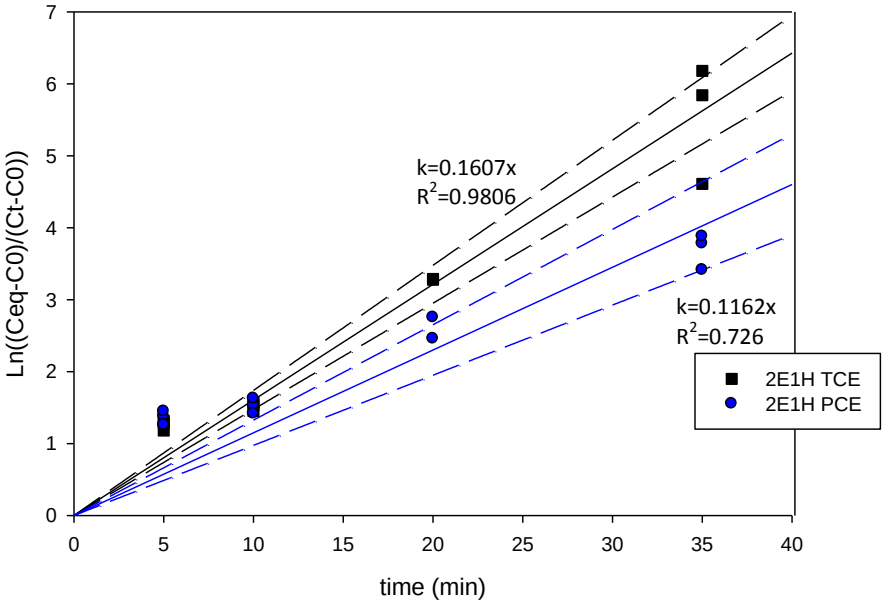

Figure 3.13 Effective mass transfer for 2-ethyl-1-hexanol in both tetrachloroethene and trichloroethene.

3.7.3 Abiotic Batch Reactors with Hexadecane Results

A series of abiotic batch reactors were completed with HD or a NAPL containing HD. First, the nBA partitioning coefficient into pure HD was determined to be 39 as shown in Figure 3.14. Next batch reactors containing nBA and mixed NAPLs of 0.75 mol HD: 0.25 mol PCE and 0.95 mol HD: 0.05 mol TCE at 10 mM were completed. These ratios of HD to PCE or TCE were chosen so that the equilibrium aqueous concentration would be around 50 mg/L for PCE or TCE which is nontoxic to the dechlorinating microbial population (Amos et al. 2007, Amos et al. 2008). The equilibrium aqueous partitioning coefficients are 88 and 46 for nBA with 0.75 mol HD: 0.25 mol PCE and 0.95 mol HD: 0.05 mol TCE, respectively, as shown in Figure 3.14. Since higher partitioning occurred in the HD and PCE NAPL further experiments were completed with this NAPL. Next batch reactors were setup with each of the PEDs and lactate, and 0.75 mol HD: 0.25 mol PCE at 90 mM or the ionic strength of the reduced medium. These batch reactors were used as controls for the biotic batch reactors and biotic columns. The K_{NW} for nBA, IPP, 2E1H, and lactate are 187, 101, 94, and 16, respectively at 90 mM ionic strength as shown in Figure 3.15. As expected, lactate had very little partitioning into the NAPL phase even at high ionic strength. The results of the batch reactors completed at 90 mM ionic strength are shown in Figure 3.15. Note that the 2E1H results are plotted using a different Y-axis than the other electron donors.

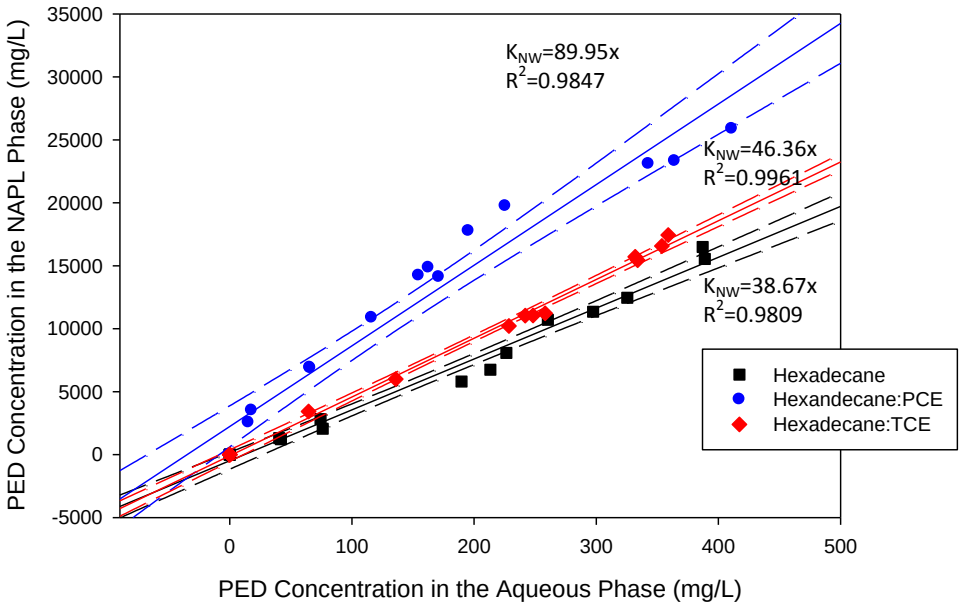

Figure 3.14 Equilibrium partitioning coefficients for n-butyl acetate in hexadecane, 0.75 mol hexadecane: 0.25 mol tetrachloroethene, and 0.95 mol hexadecane: 0.05 mol trichloroethene.

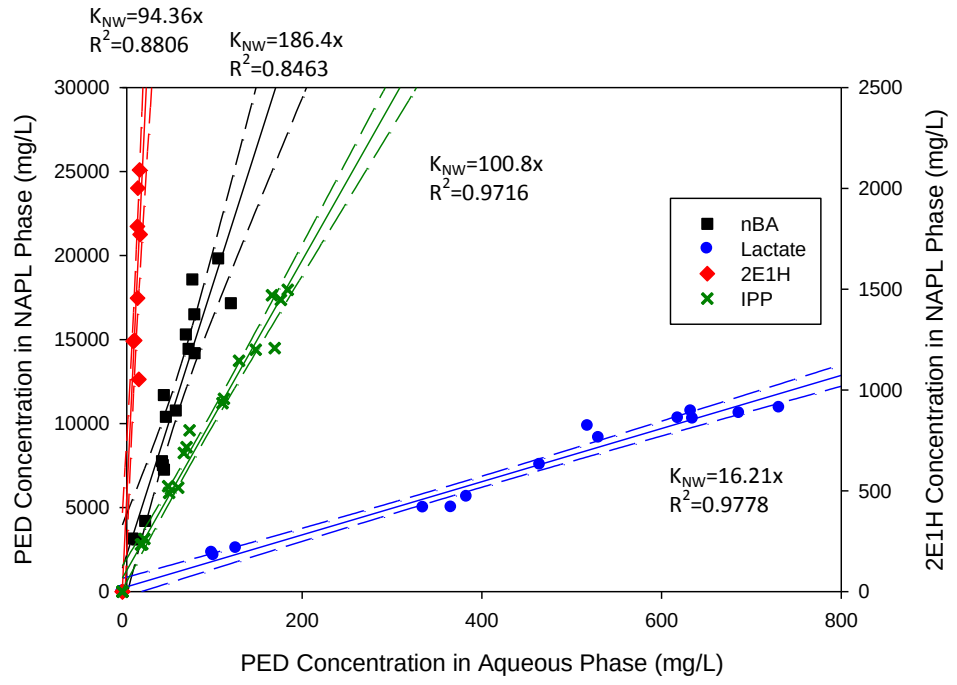

Figure 3.15 Equilibrium partitioning coefficients completed for each of the electron donors and 0.75 mol hexadecane: 0.25 mol tetrachloroethene at 90 mM ionic strength.

3.7.4 Abiotic Batch Reactors- Soil Partitioning Coefficients

An additional set of batch reactors were completed in Appling soil, as a screening with a solid with a moderate organic carbon content, to determine the sorption of the PED to the solid phase. This set of batch experiments determined the soil partitioning coefficient (K_d), which was used to examine potential losses of PEDs to the solid phase. Sorption batch experiments indicate that all three PEDs will adsorb to the organic material in soil, but less than 10% of the total mass will adsorb. Sorption results using the glass beads were used as a control, which revealed no sorption for any of the PEDs. The K_d values for each of the PEDs are reported in L/g and ranged from 0.32 L/kg to 0.81 L/kg. The PED with the highest sorption is 2E1H for Appling soil with a soil partitioning coefficient of 0.81 L/kg. IPP and nBA has similar soil partitioning coefficients of 0.32 L/g and 0.33 L/kg, respectively. The results from the batch reactors with Appling soil including the K_d values are shown below in Figure 3.16.

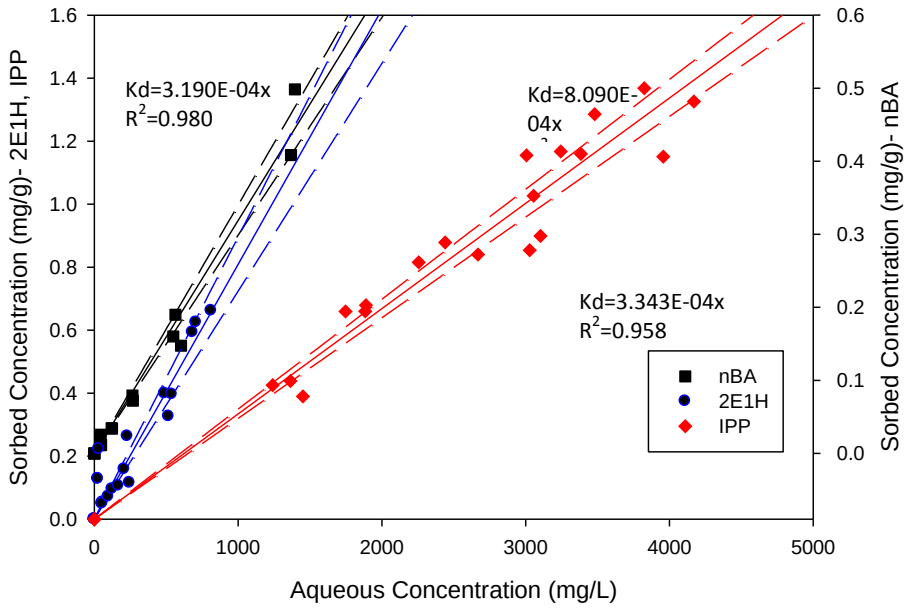

Figure 3.16 Soil partitioning coefficients for each of the partitioning electron donors in Appling Soil.

Additional batch reactors were completed with nBA and IPP in Webster soil and Federal Fine Ottawa sand to further examine the nature of the sorption to organic carbon content relationship. Due to results from the biological analysis, that will be discussed in Chapter 4, in which 2E1H was not utilized by organohalide respiring bacteria, 2E1H was not including in these experiments. In Federal Fine Ottawa sand, the soil with the lowest organic carbon content, the K_d values are 0.04 and 0.08 L/kg for nBA and IPP, respectively. In Webster soil, the soil with the highest organic carbon content, the K_d values are 0.65 and 0.85 L/kg for nBA and IPP, respectively. From these results, the relationship between organic carbon content and the soil partitioning coefficient for nBA and IPP is linear with a positive slope less than one. Figure 3.17 shows the relationship between the soil partitioning coefficient and the organic carbon content for both IPP and nBA.

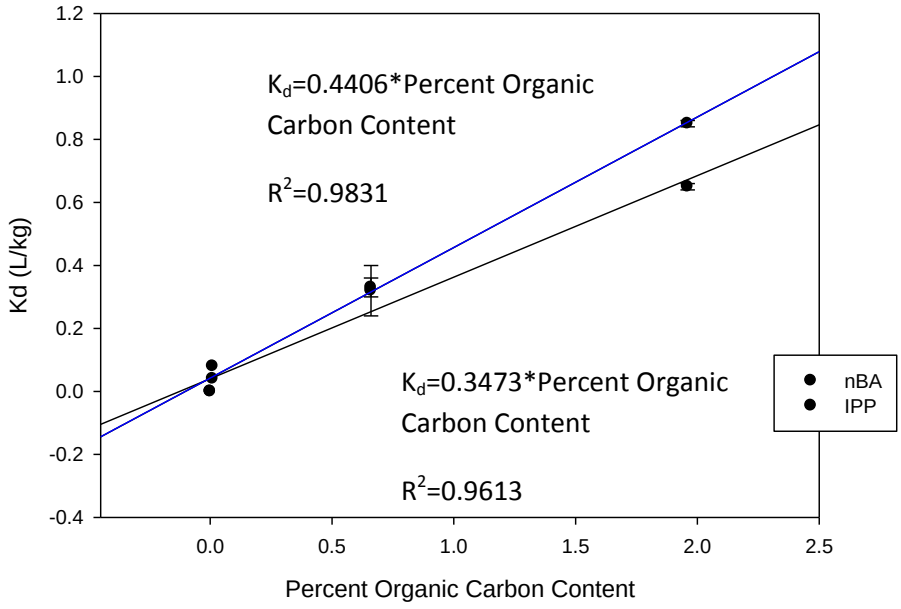

Figure 3.17 The relationship between the soil partitioning coefficient and the organic carbon content for n-butyl acetate and isopropyl propionate.

Less than 10% of the total mass of the PED adsorbed to the soil in all of these experiments. The percent of PED adsorbed to the soil increases as the soil partitioning coefficient increases. The mass of the PED that sorbs to the soil is important in determining the amount that needs to be injected at a field site and is indicative of how much excess PED would have to be injected. A summary of the percent of the PED adsorbed to the soil is shown below in Table 3.4.

Table 3.4 Summary of the average percent of PED adsorbed in the soil batch reactor experiments.

PED/Soil	Federal Fine Ottawa Sand	Appling Soil	Webster Soil
n-Butyl Acetate	0.50% ± 0.05%	3.12% ± 0.67%	5.50% ± 1.11%
Isopropyl Propionate	0.81% ± 0.08%	4.62% ± 0.33%	7.92% ± 0.99%
2-Ethyl-1-Hexanol	NM	7.50% ± 1.16%	NM

NM= Not Measured

3.8 Abiotic Column Results

For all of the abiotic columns, nonreactive tracers and PED breakthrough curves were obtained prior to and after the addition of NAPL. The results from each of these experiments are described below.

3.8.1 Non-reactive Tracer Results

Non-reactive bromide tracers were introduced into the column for 2 PVs both prior to and after the addition of NAPL. Bromide was detected in the column effluent after 1 PV and quickly approached a relative concentration of 1.0. Bromide tracers were symmetric in shape suggesting the absence of regions of immobile water indicating that any observed PED mass transfer limitations were associated with chemical non-equilibrium rather than physical non-equilibrium. The tracers were modeled using CFITM and non-reactive tracer retardation factors of approximately 1.0 were obtained. The pre-NAPL bromide tracers yielded Peclet numbers ranging between 291 and 436 and pre-NAPL pore

volumes between 102 and 107 mL. The post-NAPL bromide tracers yielded Peclet numbers between 106 and 482 and post-NAPL pore volumes between 86 and 92 mL. Post-NAPL Peclet numbers were used to calculate dispersivity values for each of the columns, using Equations 3.8 and 3.9. Dispersivity values ranged from 0.031 to 0.142 cm. The Peclet numbers, pore volumes, and dispersivity for each of the columns are summarized Table 3.5.

Table 3.5 Peclet numbers (PE), pore volumes (PV), and dispersivty (α) for each column.

NAPL Present	PED Present	PE (pre-NAPL)	PV (pre-NAPL) (mL)	PE (post-NAPL)	PV (post-NAPL) (mL)	α (cm)
TCE	**n-butyl acetate**	395	107	345	92	0.043
	2-ethyl-1-hexanol	389	106	482	91	0.031
	Isopropyl propionate	291	104	145	86	0.103
PCE	**n-butyl acetate**	380	102	379	92	0.040
	2-ethyl-1-hexanol	437	105	47	87	0.127
	Isopropyl propionate	261	102	106	92	0.142

3.8.2 PED Breakthrough

PED breakthrough curves were generated prior to and after the addition of NAPL. Prior to the introduction of NAPL, PED breakthrough curves were similar to non-reactive tracer curves, symmetrical and with a retardation factor (R_F) approximately equal to 1.0, indicating the absence of interactions with the solid phase. After the addition of NAPL, effluent samples were analyzed for the PCE or TCE concentrations in addition to the PED concentration. PCE and TCE concentrations were found to be near solubility. For example, in the 2E1H-PCE column, the average PCE concentration was 175 ± 35 mg/L and for the 2E1H-TCE column, the average TCE concentration was 1033 ± 86 mg/L. PED maximum concentrations ranged from 3.9% to 13.6% of the initial PED

concentration over the length of the experiment for each of the six columns completed. Percent PED recovery ranged from 83.2% to 93.0%. A summary of the maximum PED concentrations, PED percent recovery, and NAPL percent recovery can be found in Appendix B in Table B.1.Measurable PED concentrations were initially observed between 5 and 20 PVs depending on both the PED and NAPL used. 2E1H appeared the latest of the three PEDs in PCE and the earliest in TCE, which is consistent with batch observations, indicated that 2E1H has the highest K_{NW} in PCE and the lowest K_{NW} in TCE when compared to IPP and nBA. All three PEDs were observed earlier in PCE (between 5 and 8 PVs) then in TCE (between 14 and 20 PVs) which is also consistent with observed batch results, in which K_{NW} values were higher for each of the PEDs in TCE when compared to PCE. IPP lasted the longest in TCE, 108 PVs, which was 54x its injection length. 2E1H lasted the longest in PCE, 52.2 PVs, which was 26x its injection length. This indicates that PEDs have long lifetimes in TCE- and PCE-DNAPL which means that fewer injections of the PEDs will be required than conventional soluble electron donors. The PVs of initial breakthrough and PVs until washout for each of the PEDs are summarized in Table 3.6.

Table 3.6 Pore Volumes of initial breakthrough and until washout of the PED in each of the column experiments.

NAPL Present	PED Present	PV of initial breakthrough	PV until washout
TCE	**n-butyl acetate**	19.9	104
	2-ethyl-1-hexanol	14.1	73.7
	Isopropyl propionate	14.6	108
PCE	**n-butyl acetate**	5.9	44.7
	2-ethyl-1-hexanol	8.3	52.2
	Isopropyl propionate	6.1	41.6

3.8.3 Flow Interruptions

Flow interruptions ranging from 3-135 hours were used to assess mass transfer limitations under no-flow conditions. For every column completed, flow interruptions on the rising limb of the BTC resulted in a decrease in PED concentration while those of the decreasing side of the BTC resulted in an increase in PED concentration. These concentration changes are indicative of rate-limited PED mass transfer between the aqueous and NAPL phases. All columns had a flow interruption that was approximately 12 hours on both the rising and falling limbs of the BTCs that allowed for comparison of the experimental systems. These results are summarized below in Table 3.7. In general, the results are consistent with results from kinetic batch studies, in which nBA was found to partition into both PCE and TCE the fastest of all the PEDs, and IPP and 2E1H were found to partition at similar rates.

Table 3.7 Percent drops and rise in PED concentration during a 12 hour flow interruption.

NAPL Present	PED Present	Percent Drop in PED Concentration	Percent Rise in PED concentration
TCE	**n-butyl acetate**	5.9%	46.7%
	2-ethyl-1-hexanol	5.7%	34.0%
	Isopropyl propionate	1.6%	32.7%
PCE	**n-butyl acetate**	22.9%	46.4%
	2-ethyl-1-hexanol	14.6%	35.9%
	Isopropyl propionate	16.7%	30.0%

3.8.4 Column Modeling Results

Each of the PED's breakthrough curves was first modeled using CFITM in order to determine if the data fits an equilibrium model. Based on large Sum of Squared Residuals (SSQ), it was determined that none of the PED breakthrough curves could be modeled using an equilibrium model. SSQ is a measure of how well the model fits the data. The

lower the SSQ value the better the model fits the observed the data. The SSQs for the equilibrium models were all higher than those for the non-equilibrium models as shown below in Table 3.8. The PED breakthrough curves were then modeled using CFITIM and the model was used to fit the retardation factor, β, a dimensionless partitioning parameter, and ω, a dimensionless coefficient for kinetic sorption, In TCE, the retardation factors obtained ranged from 44-55 while in PCE, the retardation factors ranged from 19-28. These retardation factors along with the NAPL saturations were used to calculate K_{NW} values using Equation 3.5. The K_{NW} values were found to be very similar to those found in the batch experiments. The β and ω values were used to calculate the effective lumped transfer coefficient (*k*) and the fraction of sites at equilibrium (F) using Equations 3.11 and 3.12. These values are summarized below in Table 3.8. Values of F ranged from 0 to 0.771 indicating that at least 33% of the sites were at non-equilibrium meaning that instantaneous adsorption occurs at, at most 2/3 of the sites. The implication of this is that partitioning is time-dependent, which allows for the long lifetimes in DNAPL source zones. The F value for the nBA and PCE column is equal to 0. This indicates that this graph would be best fit by a one-site non-equilibrium model. The SSQ's for the non-equilibrium models ranged from 0.001 to 0.182. The 2E1H and PCE model has the highest SSQ. Complete graphs showing the observed data, equilibrium model, and non-equilibrium model are shown below in Figure 3.18 and Figure 3.19.

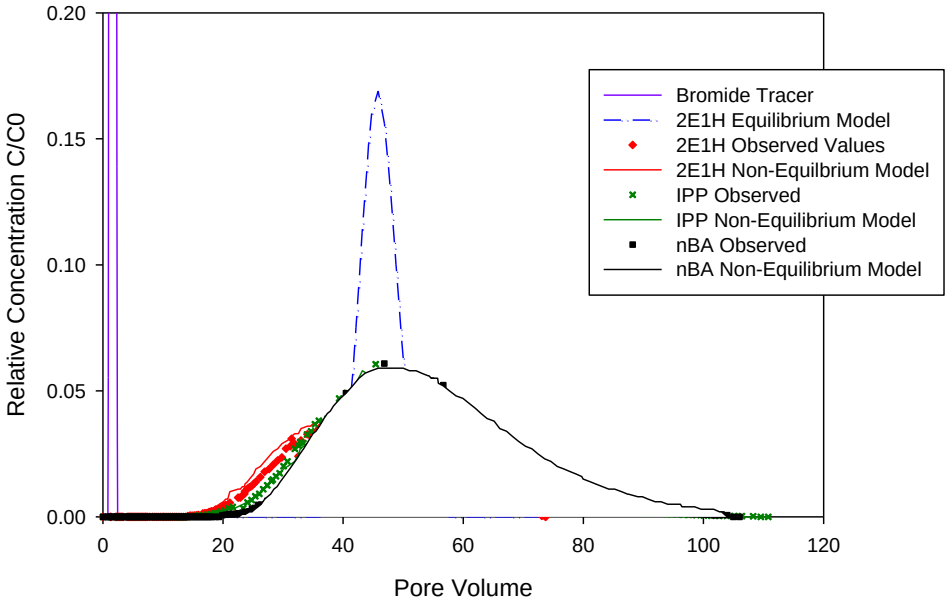

Figure 3.18 Trichloroethene column observed and modeled results for all three partitioning electron donors.

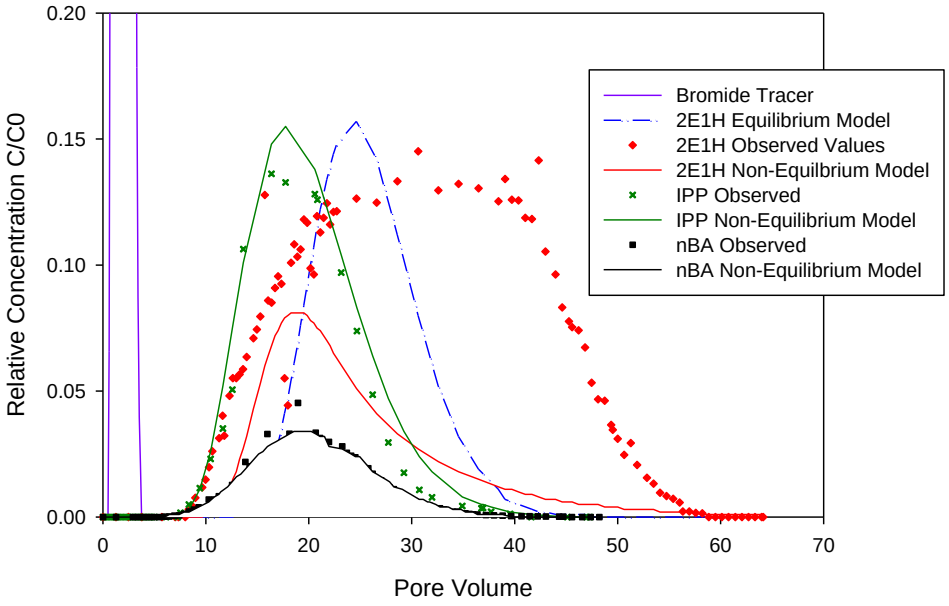

Figure 3.19 Tetrachloroethene column observed and modeled results for all three partitioning electron donors.

Table 3.8 Summary of retardation factors (R_F), NAPL-aqueous partitioning coefficients (K_{NW}), lumped mass transfer coefficients (k), fractions of sites at equilibrium (F), and the sum of squared residuals (SSQ).

NAPL Present	PED Present	R_F	K_{NW}	*k* (min^{-1})	F	SSQ (Equilibrium)	SSQ (Non-Equilibrium)
TCE	**n-butyl acetate**	55.93	343	0.006	0.467	0.222	0.009
	2-ethyl-1-hexanol	44.43	244	0.005	0.318	0.120	0.011
	Isopropyl propionate	56.88	223	0.004	0.494	0.189	0.001
PCE	**n-butyl acetate**	20.64	100	0.024	0	1.46	0.001
	2-ethyl-1-hexanol	25.17	129	0.004	0.771	0.365	0.182
	Isopropyl propionate	20	103	0.021	0.491	0.074	0.003

3.9 Abiotic Batch Reactor and Column Experiment Conclusions

Abiotic batch reactor and column experiments have provided important information about the mass transfer properties and lifetime in the DNAPL source zones of the candidate PEDs. Measured mass transfer parameters demonstrate that all three of the potential PEDs will favorably partition into both PCE and TCE. These results suggest that PEDs could be a cost effective alternative to the currently used electron donors, in the presence of NAPL, because they require a smaller injection of electron donor that could persist for longer periods of time than conventional electron donors. The data collected in the batch reactor experiments have led to the following specific conclusions:

1) All of the candidate PEDs favorably partition into the NAPL phase, and have a higher affinity for TCE than for PCE. Of the three candidate PEDs tested, nBA exhibited the highest NAPL-aqueous partitioning coefficient into TCE, and it also partitioned the fastest into both TCE and PCE as shown in Figure 3.7 and Figure 3.11.

2) Ionic strength directly affects the NAPL-aqueous partitioning coefficient. For nBA and PCE, the relationship between ionic strength and the NAPL-aqueous partitioning coefficient is linear with a positive slope slightly larger than one, as shown in Figure 3.10. Therefore, the salinity of an aquifer will influence the extent of partitioning that will occur, and in practice, PED partitioning behavior could potentially be manipulated by changing the ionic strength of the delivery solution.
3) All of the candidate PEDs examined sorbed to Appling soil, which contains an organic carbon content of 0.66%. The relationship between the organic carbon content of the soil and the sorption coefficient was linear with a positive slope of less than one for IPP and nBA, as shown in Figure 3.17. The total mass absorbed is less than 10% therefore, this sorption is minimal and is unlikely to greatly affect the PED partitioning. A potential asset of PED sorption to soils could be electron donor availability for organohalide respiration of sorbed contaminant, or supply reducing equivalents at the soil:aqueous interface.
4) The breakthrough curves of the candidate PEDs evaluated are best represented by non-equilibrium models indicating rate-limited mass transfer as shown in Figure 3.18 and Figure 3.19. This leads to tailing of the effluent curves and consequently long lifetimes in the DNAPL source zones. This also indicates that PEDs dissolve slowly into the aqueous phase. This thermodynamically restrained availability of the PEDs at the DNAPL:aqueous phase favors organohalide respiring bacteria over methanogens and other competitor microorganisms that cannot effectively compete for hydrogen at the low partial pressures (Ballapreagada et al. 1997).
5) The PEDs evaluated last up to 50x the injection length in TCE and 25x the injection length in PCE as shown in Table 3.5. PED delivery could reduce the

need for frequent or repeated electron donor injections, reducing the cost of remediation.

Chapter 4: PED Utilization by Organohalide Respiring Bacteria and Contribution to Bioenhanced Dissolution

4.1 Introduction and Objectives

The second criteria that determines whether a chemical is a partitioning electron donor (PED) is whether the compound itself, or its breakdown products, is utilized as an electron donor for organohalide respiration of chlorinated ethenes. Chapter 3 showed that the three candidate PEDs, n-butyl acetate (nBA), 2-ethyl-1-hexanol (2E1H), and isopropyl propionate (IPP) all favorably partition into both tetrachloroethene (PCE) and trichloroethene (TCE) dense non-aqueous phase liquid (DNAPL). This chapter seeks to determine if these candidate PEDs are able to support PCE to ethene organohalide respiration in biotic batch reactors. Previously completed biotic batch reactors have shown that nBA is able to support TCE to ethene organohalide respiration (Roberts 2008, Harkness et al. 2012), but similar studies using PCE and any of these candidate PEDs have not been completed. Additionally, no research has been completed that compares PEDs to conventional electron donors in dynamic flow systems. Based upon its persistence in the PCE source zone and its ability to support organohalide respiration, nBA was chosen for further column experiments in which it was compared to lactate, a common soluble electron donor, in terms of duration of PCE to ethene reduction and contribution to bioenhanced dissolution. Biotic batch reactors and column experiments were designed around the following hypotheses:

1) Previous research suggests that the PED and contaminant simultaneously dissolve into the aqueous phase resulting in sustained concentrations within the source zone (Cápiro et al. 2011). Based on this research, *it is hypothesized that PEDs may be able to provide sustained levels of electron donor close to the*

source zone in order to promote organohalide respiration of chlorinated solvents due to their fermentation to acetate or hydrogen.

2) Previous research has shown that in microcosms the duration of PCE to ethene dechlorination is similar when nBA or lactate is used as the electron donor (Harkness et al. 2012) and that an electron donor present at the source zone is able to support bioenhanced dissolution (Yang and McCarty 2002). Based upon this research *it is hypothesized that nBA will both be utilized by organohalide respiring bacteria and provide a bioenhanced dissolution factor similar to lactate.*

To test these hypotheses, biotic batch reactors were setup using each of the PED candidates and lactate in order to determine the ability of organohalide respiring bacteria to utilize the candidate PEDs as electron donors. Additionally, column experiments were setup that allow for a direct comparison between lactate and nBA. Abiotic columns were used to assess the difference in the lifetimes in residual PCE, and biotic columns were used to assess the difference in duration of PCE to ethene dechlorination and in bioenhanced dissolution factors for lactate and nBA. This work seeks to fill gaps in the literature by evaluating the PEDs under conditions that allow for a direct comparison with conventional electron donors in a dynamic flow system.

4.2 Materials

All columns were packed with Federal Fine Ottawa sand (US Silica Company; Berkeley Spring, West Virginia). Federal Fine Ottawa sand is a quartz sand with 0.32 mm mean diameter, intrinsic permeability of 4.2 X 10^{-11} m^2 (Suchomel et al. 2007), and an organic carbon content of 0.001 (Marcet 2014). HPLC-grade PCE was purchased from Sigma-Aldrich Co. PCE has an equilibrium aqueous phase solubility of 200 mg/L and a liquid

density of 1.63 g/cm^3 (Huling and Weaver 1991). Hexadecane (HD; 99% purity) was purchased from Sigma Aldrich Co. HD has an equilibrium aqueous phase solubility of 0.0036 mg/L and a density of 0.77 g/mL. PCE and HD were dyed with 0.4 mM Oil-Red-O, a hydrophobic dye, purchased from Fisher Scientific (Fair Lawn, New Jersey). Sodium bromide was used as a non-reactive tracer and was purchased from Fisher Scientific. The three PED candidates are IPP (Fisher Scientific), nBA (Sigma-Aldrich Co.), and 2E1H (Sigma-Aldrich Co.). The three PEDs were compared to lactate which was purchased as a syrup 60% (w/w) from Sigma Aldrich Co. For use in analytical analyses, HPLC grade isopropyl alcohol was purchased from Fisher Scientific. For analytical standards, TCE (99.5%), cis-dichloroethene (Cis-DCE, 97%), vinyl chloride (VC, 99.9%, gas), and ethene (99.9%, gas) were all purchased from Sigma Aldrich Co. All chemicals were of reagent grade or higher purity, and all solutions were prepared using 18 MΩ/cm deionized water (EMD Millipore; Billerica, Massachusetts).

4.3 Medium Preparation and Inoculum

The background solution for the biotic batch reactors and columns was a reduced medium solution. Reduced anaerobic mineral salt medium was prepared as described previously (Sung, Ritalahti et al. 2003, Amos, Suchomel et al. 2008). The total ionic strength of the solution is 90 mM. For the batch reactors, the reduced medium was prepared in a 2 L, 3-neck round bottom distilling flask (Chemglass Vineland, New Jersey). The batch reactors were performed in serum bottles (160 mL capacity, Wheaton Co., Millville, New Jersey) filled with 100 mL of reduced medium solution. The serum bottles were prepared with nitrogen headspace and sealed with blue butyl-rubber stoppers and aluminum crimp caps (Chemglass). For the columns, the medium was prepared in 4 L Marriotte bottles (Chemglass). Bio-Dechlor INOCULUM (BDI-SZ) was used in the biotic batch reactors and column experiments. BDI-SZ is a PCE-to-ethene dechlorinating

consortium that has been used successfully for bioaugmentation at chlorinated ethene contaminated sites (Ritalahti et al. 2005). It is a microbiologically well-characterized consortium and contains multiple dechlorinators, including three *Dehalococcoides mccartyi (Dhc)* strains, a *Dehalobacter* sp., and *Geobacter lovleyi (G. lovleyi)* strain SZ, without methanogens (Amos et al. 2009).

4.4 Design and Setup of Biotic Batch Reactors

These batch reactors were prepared in 160 mL serum bottles with reduced medium solution (ionic strength of 90 mM), following previously described methods (Amos et al. 2007). In total, 48 biotic batch reactors were completed using each of the three PEDs and a control electron donor, lactate. Each electron donor was added in approximately equal micro-Reducing equivalents per 100 mL. A summary of the electron donor properties and the amount added to each batch reactor is in Table 4.1. Each electron donor was evaluated with PCE dissolved into the aqueous phase, and with a 0.75 mol HD: 0.25 mol PCE-NAPL phase. Abiotic controls were also prepared with each of the electron donors and NAPL combinations in the absence of the microbial consortium. All batch reactors were setup in triplicate. A summary of the batch reactor's setup is shown in Table 4.2. More details about the materials and methods of the biotic batch reactor setup can be found in Bonilla (2015).

Table 4.1 Summary of the electron donor properties and amounts added to each batch reactor.

Electron Donor	**Molecular Weight (g/mol)**	**Density (g/mL)**	**Volume Electron Donor Added (µL)**	**Reducing Equivalent/ Mole**	***µ*Reducing Equivalent/ 100 mL**
nBA	116.16	0.883	30.0	4	8609
2E1H	130.23	0.833	23.9	6	8662
IPP	116.16	0.87	30.5	4	8609
Lactate	112.06	1.32	287.5	1.5	8625

Table 4.2 Summary of biotic batch reactors completed (Bonilla 2015).

		Electron Donor				**Total Reactors per Electron Acceptor**
		nBA	2E1H	IPP	Lactate	
Electron Acceptor	Biotic 300µM Dissolved PCE	3	3	3	3	12
	Biotic 0.25 mol PCE: 0.75 mol HD	3	3	3	3	12
	Abiotic 300µM Dissolved PCE	3	3	3	3	12
	Abiotic 0.25 mol PCE: 0.75 mol HD	3	3	3	3	12
Total Number of Batch Reactors						**48**

4.5 Column Experiment Design and Setup

Four borosilicate glass columns (15 cm x 4.8 cm) equipped with Teflon end-plates were packed wet with autoclaved Federal Fine Ottawa sand using the reduced medium solution, and containing the Bio-Dechlor INOCULUM (BDI-SZ) for the two biotic columns. The columns were packed under anoxic conditions in a Coy Lab glove box (Grass Lake, Michigan). Following packing, reduced medium was continuously flushed through the column at 0.15 mL/min or a seepage velocity of 0.3 m/day. Columns were flushed for about 4 pore volumes (PVs) following packing and the elution of cells was monitored using quantitative real-time polymerase chain reaction (qPCR) and a percent cell recovery was calculated.

In this set of biotic column experiments, a mixed-NAPL comprised of 0.75 mol HD: 0.25 mol PCE was used because the aqueous phase solubility of the PCE in this mixture is about 50 mg/L, which is nontoxic to the dechlorinating microbial population (Amos et al. 2007, Amos et al. 2008). The density of the mixture was 0.86 g/mL. The PCE mixed-NAPL was injected into the column, using a Harvard Apparatus Syringe Infusion Pump 2.2. Between 80 and 100 mL of the mixed NAPL was injected to each column with

downward flow followed by upward flushing with the reduced medium until no NAPL was seen in the effluent. NAPL saturation was determined from the weight of the column prior to the addition of NAPL and after the addition of NAPL (Wilson et al. 1990). Immediately after NAPL addition, an influent containing the reduced medium with 10 mM sodium bromide and 5 mM lactate or about 5000 mg/L nBA was flushed through the column at 0.15 mL/min, or a seepage velocity of 0.3 m/day, using a Gilson model Minipuls 3 peristaltic pump. For the abiotic control columns, the electron donor was only pumped into the column for 2 PVs followed by reduced medium with no electron donor until the lactate and nBA were no longer detected in the effluent. For the biotic columns, lactate was pumped through the column continuously or nBA was pumped through the column for approximately 2 PVs at a time, at PV 0, PV 28, and PV 52. Columns were run at 0.15 mL/min and then adjusted based on dechlorination performance. These flow rates and seepage velocities are summarized below in Table 4.3.

Effluents were connected to a 25 mL glass bulb (G. Finkenbeiner, Inc., Waltham, Massachusetts) and then collected using a Spectray Chrom Fraction Collector CF-2. The glass bulb was used to keep the effluent anoxic and to keep the nBA or the chlorinated solvents from volatilizing. The glass bulb was emptied about once a PV. Samples were analyzed for volatile fatty acids and chlorinated solvents. First, 0.475 mL of sample and 0.025 mL of 0.1 M sulfuric acid was added to a 2 mL glass vials and analyzed on a high-performance liquid chromatograph (HPLC). This sample was analyzed for lactic acid, acetic acid, and propionic acid. An additional 0.5 mL of sample was added to a 2 mL glass vial containing 0.5 mL of IPA to be analyzed on the gas chromatograph (GC) with a flame ionization detector (FID). Another 1.0 mL of sample was added to a 20 mL crimp top vial and analyzed on a gas chromatograph (GC) equipped with a headspace auto sampler and a flame ionization detector (FID). This sample was analyzed for PCE and all

of its daughter products. About 15 mL of the remaining sample was used for microbial analysis. The remaining sample (about 5 mL) was used to analyze pH using an Accumet Model 50 pH/ion/conductivity meter and ORP using an Orion pH/ORP meter model 420 (Thermo Scientific, Waltham, MA). The sample collected using the fraction collector was used to measure bromide concentrations using an Accumet Model 50 pH/ion/conductivity meter. A summary of the experimental conditions is given below in Table 4.3. A schematic of the column setup is shown in Figure 4.1.

Table 4.3 Summary of experimental conditions for control column experiments.

Column	**Abiotic Lactate**	**Abiotic n-Butyl Acetate**	**Biotic Lactate**	**Biotic n-Butyl Acetate**
Actual Flow Rate (mL/min)	0.190	0.156	0.15, 0.10, 0.07	0.15, 0.10, 0.07
Seepage Velocity (m/day), v_p	0.43	0.29	0.32, 0.20, 0.15	0.30, 0.21, 0.15
Porosity, n	0.38	0.38	0.38	0.39
Initial Electron Donor Concentration (mg/L), C_0	147	3592	507, 407, 480, 480	4809, 5084
NAPL Saturation (%), S_{NAPL}	16.9	14.7	11.6	13.3
Initial Cell Recovery (%)	NA	NA	45%	26%

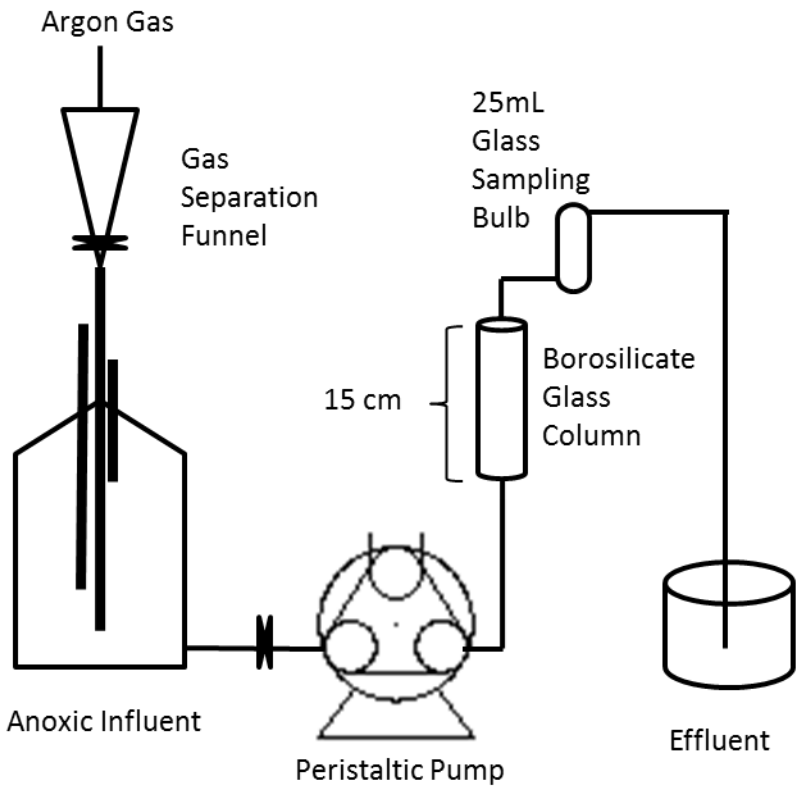

Figure 4.1 Schematic showing the system used to keep the influent anoxic and the glass sampling bulb.

4.6 Analytical Methods

The analytical methods describing both the chemical analysis and the biological analysis for the biotic batch reactors and columns are described below.

4.6.1 Aqueous Phase Chemical Analysis

The PED concentrations were measured using a 7890 gas chromatograph (GC) equipped with a liquid autosampler (HP 7683) and an Agilent DB-5 column (30 m by 0.32 mm OD) connected to a flame ionization detector (FID) (Agilent; Santa Clara, California). Samples were prepared in 2.0 mL glass vials with at least 50% HPLC grade isopropyl alcohol. PCE and its daughter products were measured using an Agilent model 7890 gas chromatograph equipped with Teledyne-Tekmar HT3 headspace auto sampler (Thousand

Oaks, California) and an HP-64 column (60 m by 0.32 mm; film thickness, 1.8 µm nominal) connected to an FID. Samples were prepared by adding 1.0 mL of sample to 20 mL Agilent headspace vials. Analytical standards were completed as described previously (Costanza 2007). Organic acid concentrations were measured using an Agilent 1200 High Performance Liquid Chromatography (HPLC) system equipped with a diode array detector (DAD) operated at 210 nm with an Aminex HPX-87H Ion Exclusion Column (300 mm X 7.8 mm) as described previously (He et al. 2002). Bromide was monitored using an ion-selective probe (Cole-Parmer; Vernon Hills, Illinois) connected to an Accumet Model 50 pH/ion/conductivity meter (Fisher Scientific). An Orion Triode Ag/AgCl combination pH/ATC electrode connected to an Orion 3-star pH meter (Thermo Scientific; Waltham, Massachusetts) was used to measure pH.

4.6.2 Biological Analysis

Aqueous-phase biomass samples were collected from the effluent of the biotic columns. This sample was added to a 15 mL sterile centrifuge tube (VWR) and centrifuged for 30 minutes at 4000 rotations per minute (rpm) at 4°C using an Eppendorf Centrifuge 5810R (Hauppauge, New York). The top 14 mL of liquid was then removed using a pipette and the remaining pellet was re-suspended and added to a 2 mL micro-centrifuge tube. This micro-centrifuge tube was centrifuged for 15 minutes at about 15,000 rpm, using an Eppendorf Centrifuge 5424, and again supernatant was removed and the remaining pellet was stored at -20°C. DNA was extracted using the commercially available QIAmp DNA Mini Kit (Qiagen, Valencia, California) and following the manufacturer-recommended protocol. The extracted DNA was stored at -20°C until qPCR analysis. Bacterial abundance from extracted DNA was measured using an Applied Biosystems Step One Plus qPCR system (Foster City, California). Established protocols for TaqMan-based quantification of *Dhc* 16S rRNA genes have been designed and validated (Ritalahti et al.

2006). *Dhc* 16S rRNA genes were quantified using 6-carboxyfluorescein (FAM) as a reporter and N,N,N',N'-tetramethyl-6-carboxyrhodamine (TAMRA) as a quencher (Ritalahti et al. 2006). The reaction mixture contained 10 µL of TaqMan Universal master mix (Applied Biosystems), 0.06 µL of probe, 0.6 µL of each primer, and 2 µL of template DNA combined in nuclease-free water (MO Bio Laboratories Inc., Carlsbad, CA) for a total reaction volume of 20 µL (Ritalahti et al. 2006). The PCR temperature program was as follows: 2 min at 50°C and 10 min at 95°C, followed by 40 cycles of 15s at 95°C and 1 min at 58°C (Ritalahti et al. 2006). *G. lovleyi* strain SZ 16S rRNA genes were quantified using the SYBR green-based detection chemistry and the Geo196F/Geo535R primer pair as previously described (Amos et al. 2007). The reaction mixture contained 10 µL of Power SYBR green PCR master mix (Applied Biosystems), 0.6 µL of each primer, and 2 µL of template DNA combined in nuclease-free water (MO Bio Laboratories Inc.) for a total reaction volume of 20 µL (Amos et al. 2007). The PCR temperature program was as follows: 2 min at 50°C, 15 min at 95°C followed by 40 cycles of 30s at 94°C, 30s at 50°C and 30s at 72°C (Amos et al. 2007). Standard curves were generated following the procedure previously described (Ritalahti et al. 2006) and used a 10-fold dilution series of quantified plasmid DNA. Each plasmid carried a single copy of the 16S rRNA gene of *Dhc* strain BAVI or the *G. lovleyi* strain SZ. Cell numbers were determined by dividing 16S rRNA gene copy numbers by the 16S rRNA gene copies per genome. Sequenced *Dhc* strains contain a single 16S rRNA gene copy per genome (Kube et al. 2005, Seshadri et al. 2005) and the genome of *G. lovleyi* strain SZ contains two copies of the 16S rRNA gene (GOE Joint Genome Institute, Amos et al. 2007). Cell numbers are reported per mL of sample.

4.7 Biotic Batch Reactor Results

Biotic batch reactors were completed to compare the duration and extent of PCE to ethene reduction when lactate, nBA, IPP, or 2E1H was used as the electron donor. Batch reactors were sampled approximately every other day for two weeks, then twice a week for two weeks, and then sampled weekly for three weeks. An additional sample was taken after 115 days in which pH and hydrogen levels were also analyzed. During each sampling event PCE and daughter product concentrations along with electron donor and fermentation product concentrations were determined.

In all abiotic batch reactors, no PCE degradation was seen. Figure 4.2 shows the chlorinated ethene concentrations for the abiotic batch reactors containing neat PCE and lactate. This graph is representative of all of the abiotic batch reactors. Overtime, there was a slow decrease in PCE concentration, likely due to losses through the rubber stopper. The remaining abiotic batch reactor plots with the chlorinated ethene concentrations can be found in Appendix A.

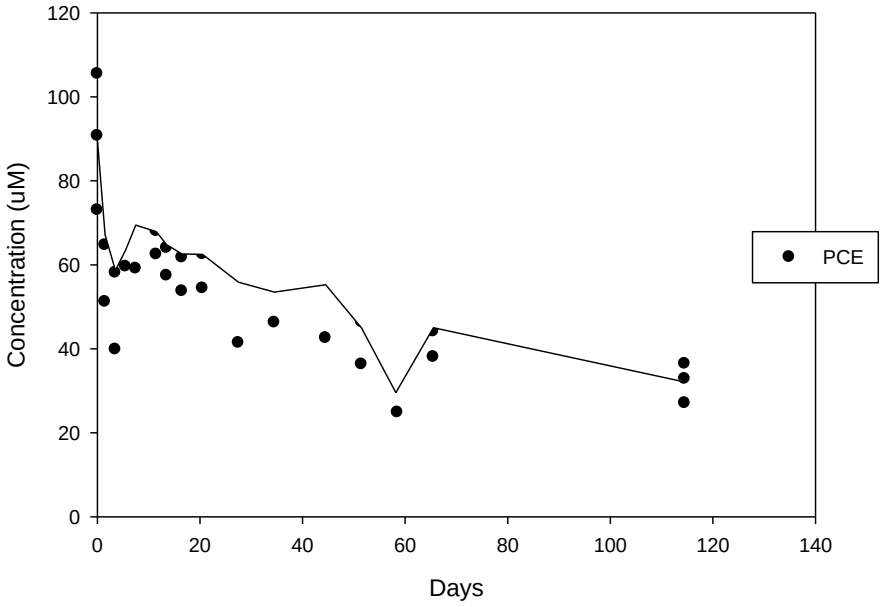

Figure 4.2 The chlorinated ethene concentrations for the abiotic batch reactor Containing lactate and tetrachloroethene.

No dechlorination was seen in the biotic batch reactors containing 2E1H. In Figure 4.3 the chlorinated ethene concentration for the biotic batch reactor containing PCE and 2E1H shows a slight decrease in PCE, but no indication of PCE daughter products. In the abiotic batch reactors containing 2E1H, the concentration of 2E1H remained fairly constant throughout the experiment with an average concentration of 221 ± 41.2 mg/L and 53.5 ± 17.3 mg/L for the batch reactors containing PCE and those containing both PCE and HD, respectively, these graphs can be found in Appendix A. In the biotic batch reactors, 2E1H was broken down to acetate and propionate, so the lack of electron donor was not the reason that dechlorination did not occur, although after the initial spike in acetate and propionate these concentrations remain relatively constant at 50 ± 8.6 mg/L and 51 ± 8.5 mg/L, respectively, indicating that no additional fermentation occurred after the first few days. The electron donor concentration for the biotic batch reactor containing PCE and 2E1H is shown below in Figure 4.4. Similar results were seen in the

biotic batch reactors containing 2E1H and HD and PCE. These graphs can be found in Appendix A.

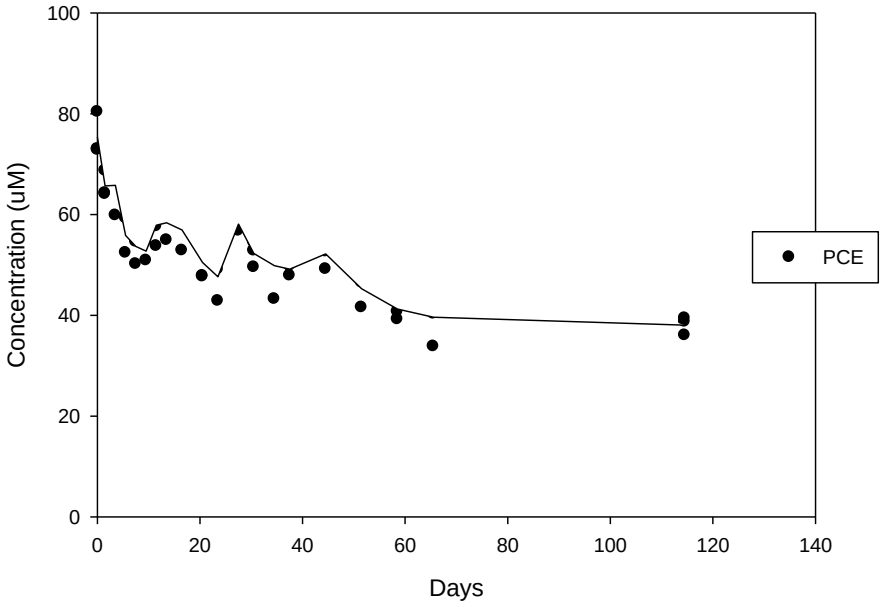

Figure 4.3 Chlorinated ethene concentrations for the biotic batch reactors containing 2-ethyl-1-hexanol and tetrachloroethene.

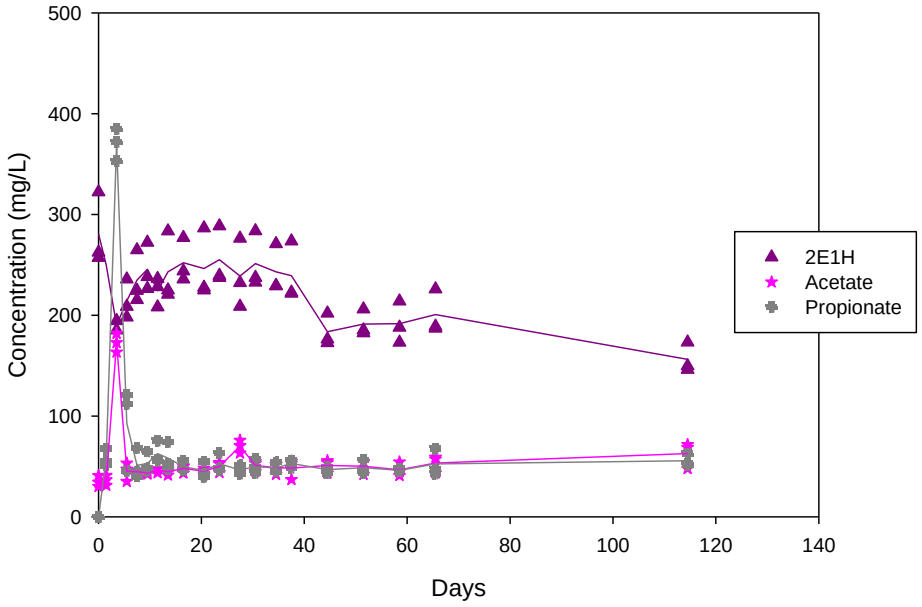

Figure 4.4 Electron donor concentrations for the biotic batch reactors containing 2-ethyl-1-hexanol and tetrachloroethene.

In the batch containing only PCE and lactate, dechlorination from PCE to ethene was observed. At the end of the experiment, only ethene and vinyl chloride (VC) remained in the batch reactor. On the other hand for the biotic batch reactor containing both HD and PCE, dechlorination from PCE to VC was observed and PCE, TCE, cis-DCE, and VC were all present in the reactor at the end of the experiment. Chloroethene concentrations overtime are shown in Figure 4.5 for both of the biotic batch reactors containing lactate.

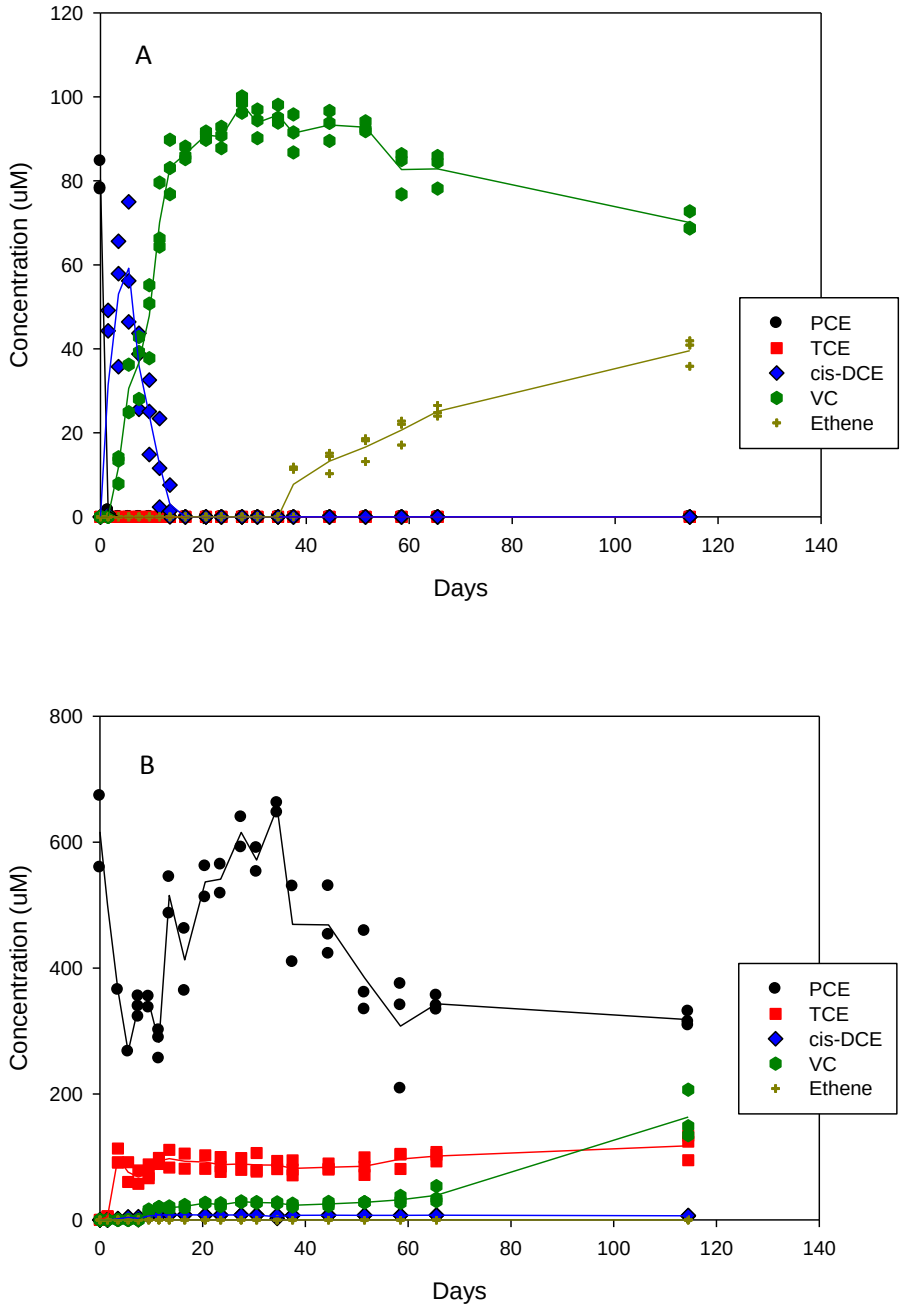

Figure 4.5 Chlorinated ethene concentrations for the biotic batch reactors containing lactate. Graph A shows the lactate and tetrachloroethene results. Graph B shows the lactate and 0.25 mol tetrachloroethene: 0.75 mol hexadecane results.

In the lactate abiotic batch reactors, lactate concentrations remained constant throughout the experiment at an average concentration of 620 ± 31.5 mg/L, these graphs can be

found in Appendix A. In the lactate biotic batch reactors, lactate was immediately broken down to form acetate and propionate. Figure 4.6 shows these electron donor concentrations in the biotic batch reactor containing lactate and PCE. The electron donor concentrations in the biotic batch reactor containing lactate, PCE, and HD is very similar and can be found in Appendix A.

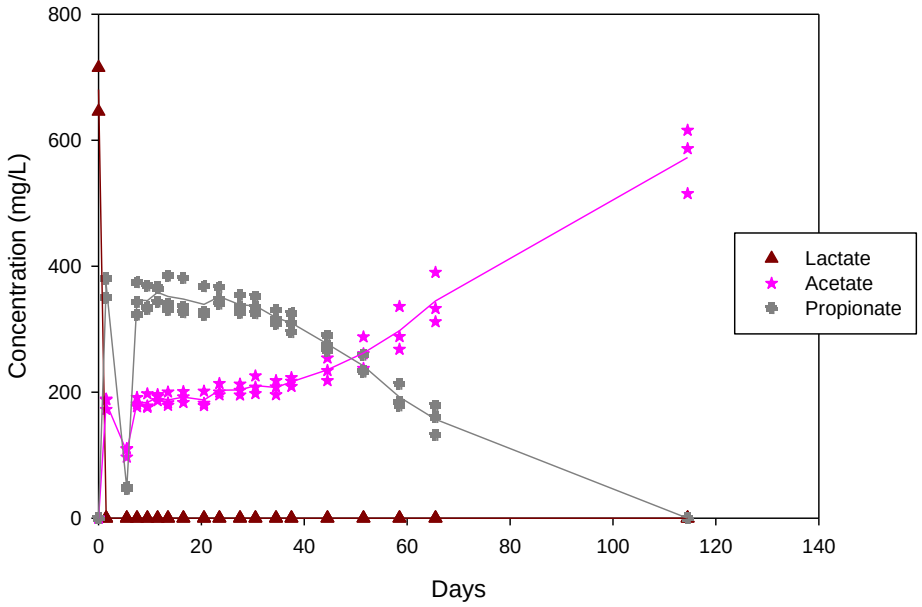

Figure 4.6 Electron donor concentrations in the biotic batch reactor containing lactate and tetrachloroethene.

The results from the batch reactors containing nBA were very similar to those containing lactate. The biotic batch reactor containing PCE and nBA ended with both ethene and VC present; however, unlike the lactate case, TCE was also detected. Similarly to lactate, the batch reactor containing HD, PCE, and nBA did not produce ethene and concentration of PCE, TCE, cis-DCE, and VC were all present at the end of the experiment. Chlorinated ethene concentrations for the batch reactors containing nBA is shown below in Figure 4.7.

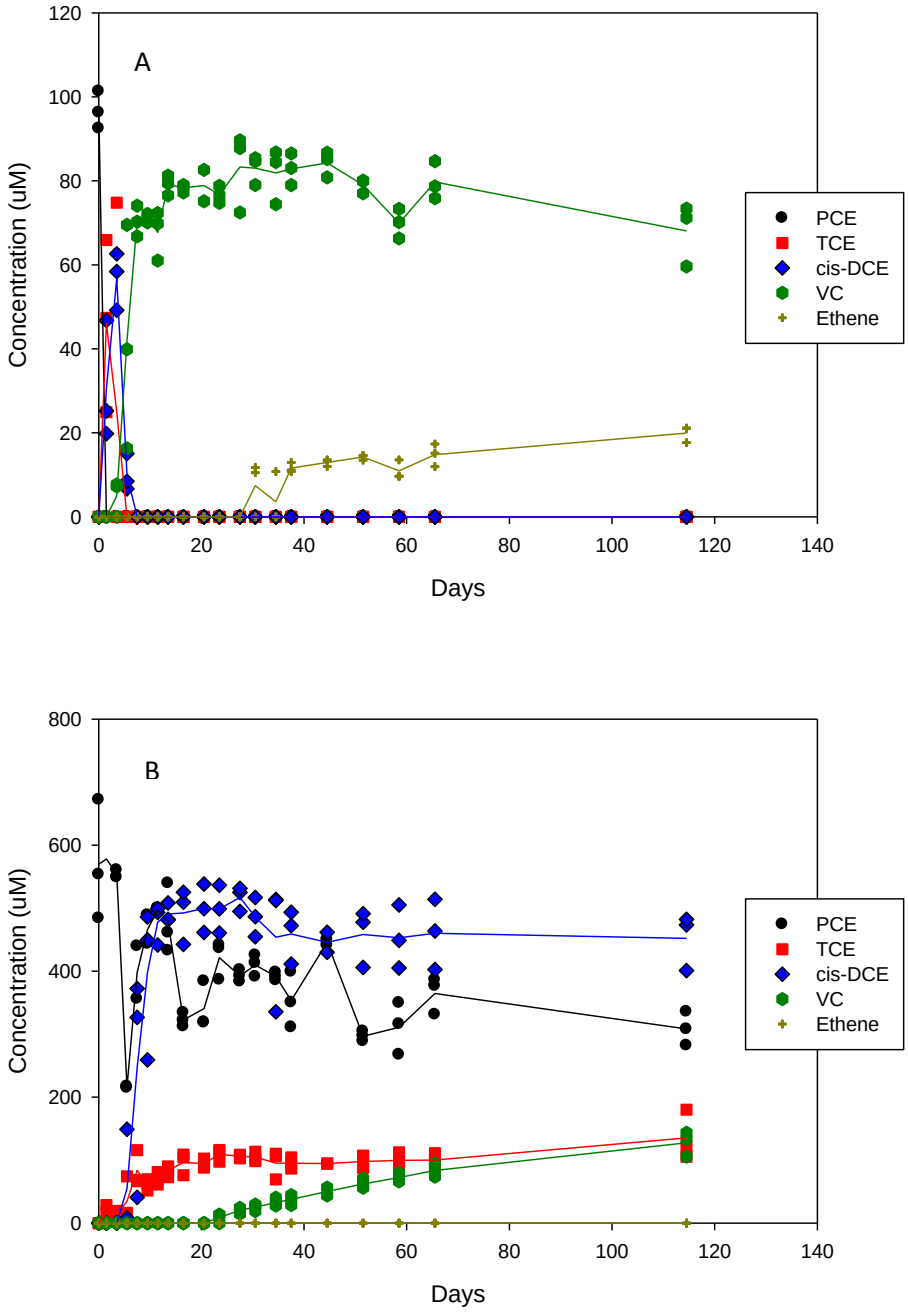

Figure 4.7 Chlorinated ethene concentrations for the biotic batch reactors containing n-butyl acetate. Graph A shows the n-butyl acetate and tetrachloroethene results. Graph B shows the n-butyl acetate and 0.25 mol tetrachloroethene: 0.75 mol hexadecane results.

In the abiotic batch reactors containing nBA, acetate and butanol were detected, indicating that nBA breaks down to form acetate and butanol through hydrolysis, not

fermentation. Figure 4.8 shows that the concentration of nBA slowly decreased over time, while the concentrations of butanol and acetate slowly increased over time. A similar trend was seen in the abiotic batch reactor containing nBA, PCE, and HD. This graph can be found in Appendix A.

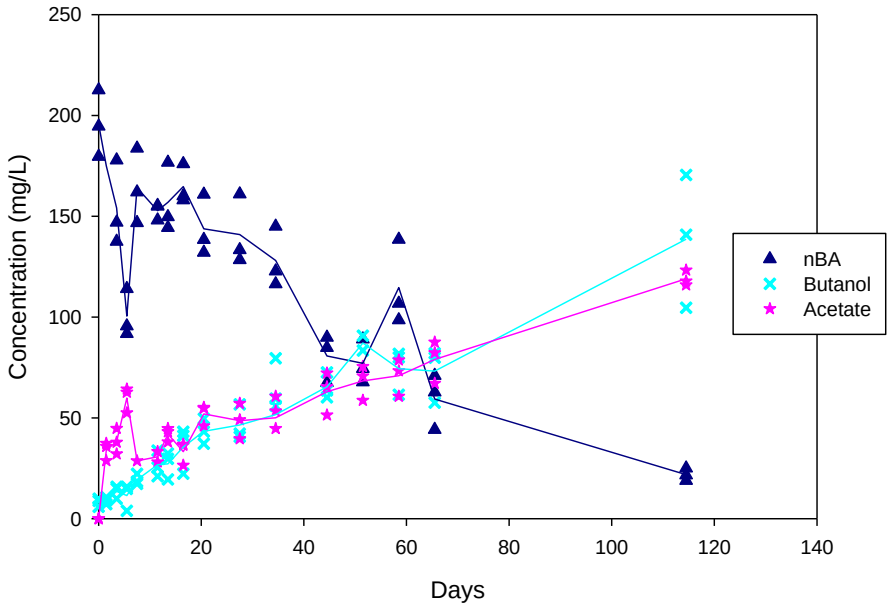

Figure 4.8 Electron donor concentrations in the abiotic batch reactor containing n-butyl acetate and tetrachloroethene.

In the biotic batch reactors containing nBA, butanol, acetate, and propionate were all detected. In the biotic batch reactor containing only nBA and PCE, the concentration of nBA slowly decreased overtime, while the concentration of acetate slowly increased overtime. The concentration of propionate remained relatively constant at an average concentration of 45 ± 8.7 mg/L. Butanol concentrations were small with concentrations below 10 mg/L. The concentration of nBA, butanol, acetate, and propionate in the biotic batch reactor containing nBA and PCE are shown in Figure 4.9 In the biotic batch reactor containing nBA, PCE, and HD, the concentration of nBA remained relatively constant at a concentration equal to about ¼ of the concentration in the biotic batch containing only

nBA and PCE, or an average concentration of 59 ± 14.8 mg/L, indicating that nBA partitioned into the NAPL phase. Acetate and propionate concentrations spiked within the first week of the experiment, but then were negligible for most of the rest of the experiment. Butanol concentrations remained small concentrations less than 10 mg/L. The concentrations of nBA, acetate, propionate, and butanol in the biotic batch reactor containing nBA, PCE, and HD are shown in Figure 4.9.

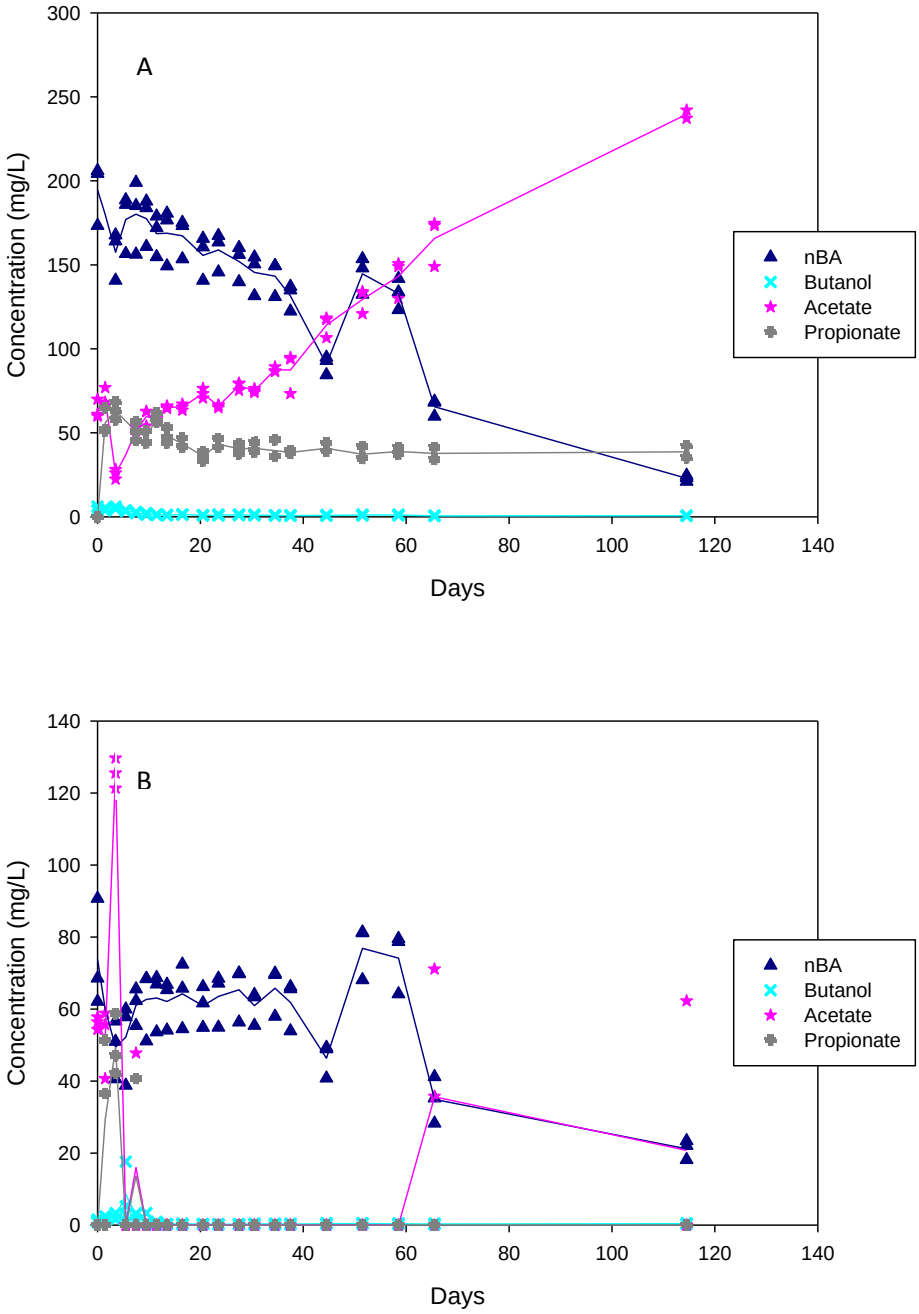

Figure 4.9 Electron donor concentrations in the biotic batch reactors containing n-butyl acetate. Graph A shows the n-butyl acetate and tetrachloroethene results. Graph B shows the n-butyl acetate and 0.25 mol tetrachloroethene: 0.75 mol hexadecane results.

Dechlorination was observed in the biotic batch reactors containing IPP. In the biotic batch reactor containing IPP and PCE, only VC and ethene remained at the end of the

experiment. Ethene was not detected until 115 days into the experiment. On the other hand, the biotic batch reactor that contained IPP, PCE, and HD stalled at cis-DCE and PCE, TCE, and cis-DCE were all present at the end of the experiment. Figure 4.10 shows the chlorinated ethene concentrations in the biotic batch reactors containing IPP.

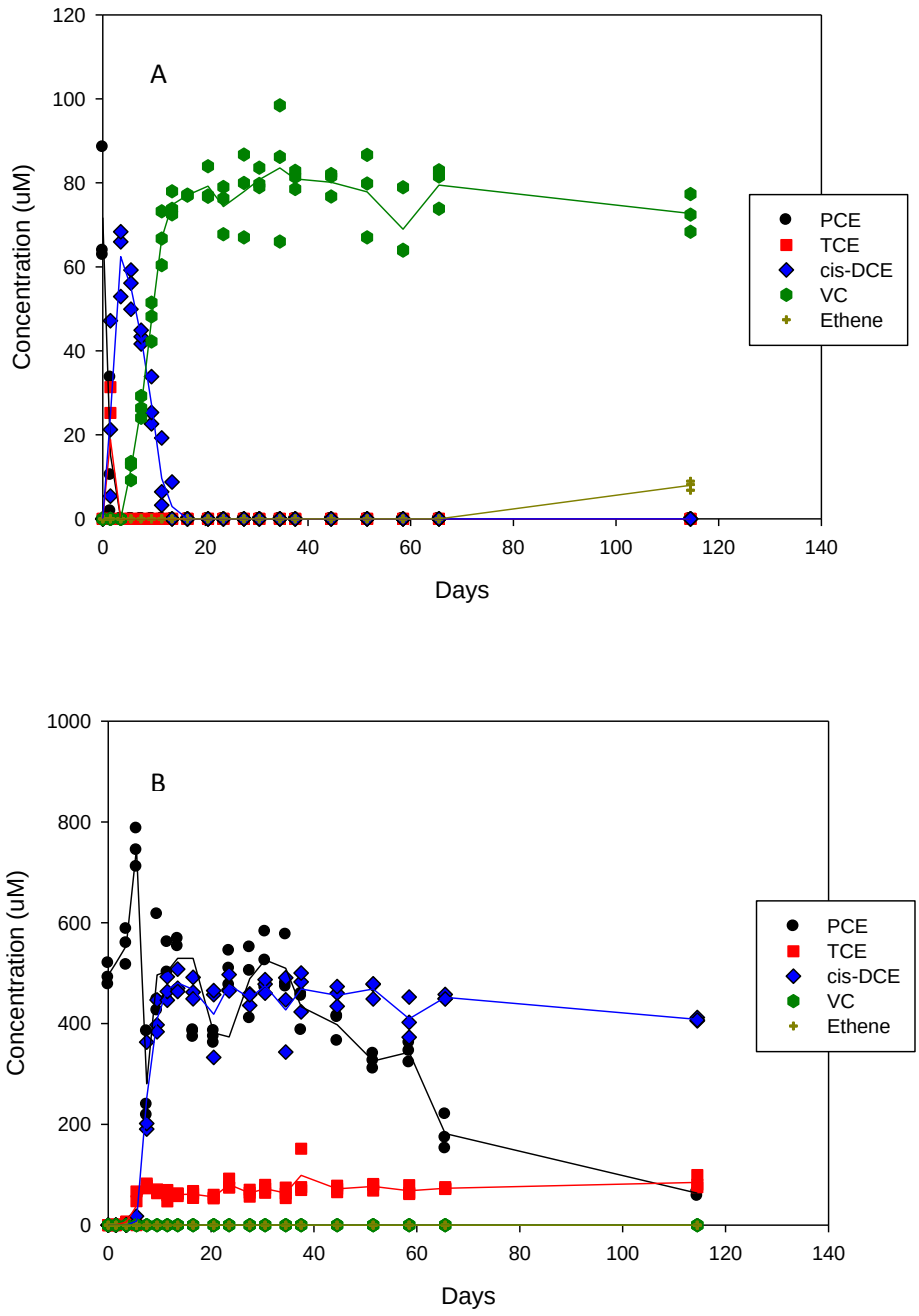

Figure 4.10 Chlorinated ethene concentrations for the biotic batch reactors containing isopropyl propionate. Graph A shows the isopropyl propionate and tetrachloroethene results. Graph B shows the isopropyl propionate and 0.25 mol tetrachloroethene: 0.75 mol hexadecane results.

In the abiotic batch reactors containing IPP, the concentration of IPP remained fairly constant throughout the experiment with an average concentration of 147 ± 32.2 mg/L. Graphs showing the IPP concentration over time for both sets of abiotic batch reactors can be found in Appendix A. In the biotic batch reactors containing IPP, IPP was broken down to acetate and propionate, although only a slight decrease in the total concentration of IPP was observed. Figure 4.11 shows the concentration of IPP, propionate, and acetate in the biotic batch reactor containing IPP and PCE. In the biotic batch reactor containing IPP, PCE, and HD the concentrations of acetate and propionate were close to 0 mg/L after an initial spike in these concentrations. The IPP concentrations were substantially smaller than in the batch containing only IPP and PCE, indicating partitioning into the NAPL phase. The electron donor concentrations in the biotic batch reactor containing IPP, PCE, and HD are shown below in Figure 4.11.

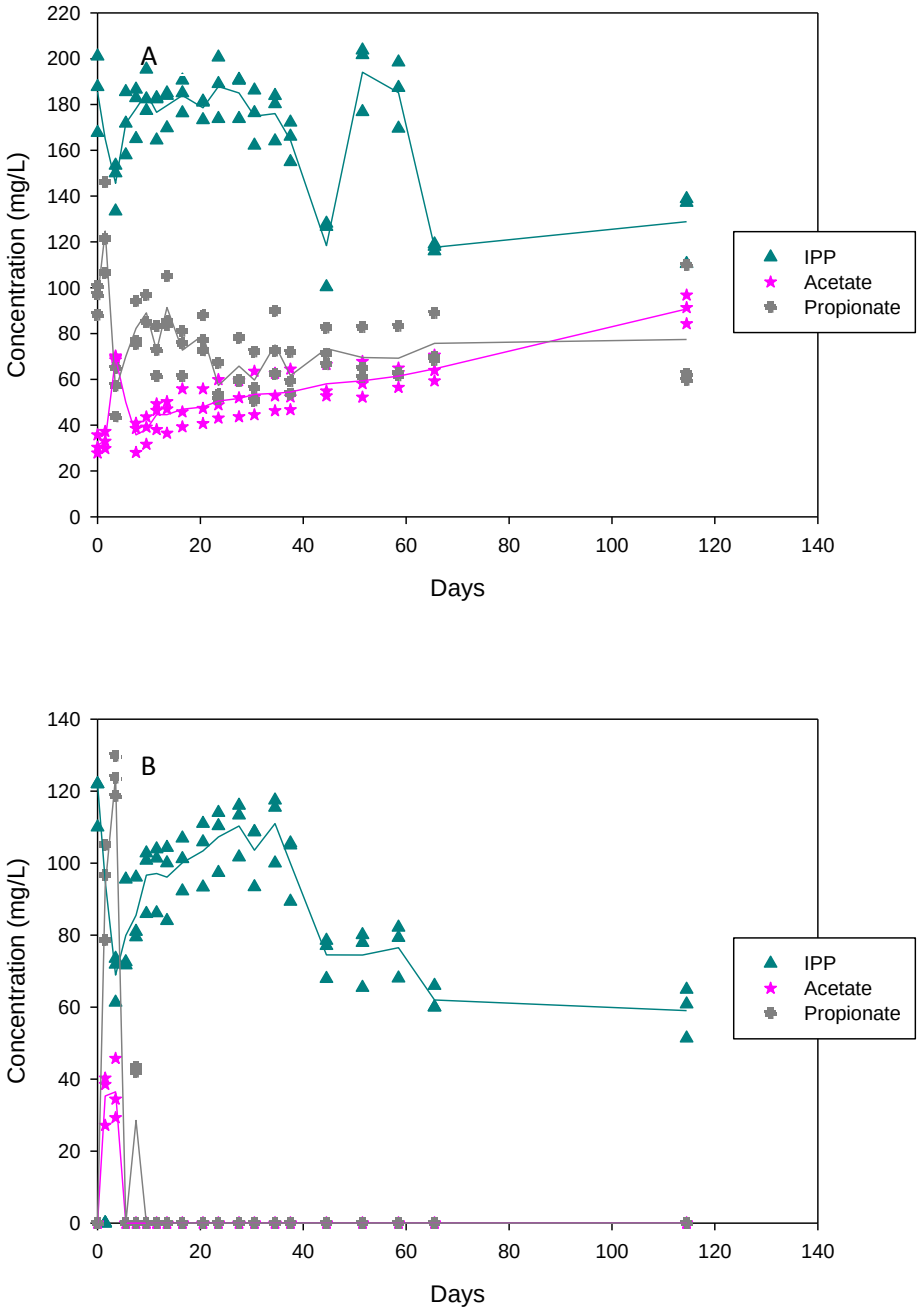

Figure 4.11 Electron donor concentrations in the biotic batch reactors containing isopropyl propionate. Graph A shows the isopropyl propionate and tetrachloroethene results. Graph B shows the isopropyl propionate and 0.25 mol tetrachloroethene: 0.75 mol hexadecane results.

The duration of dechlorination were similar when lactate and nBA were used as the electron donor. Although TCE was not detected when lactate was used an electron donor, overall, nBA may have allowed for a slightly faster rate of dechlorination, since the duration at which cis-DCE disappeared and ethene appeared was shorter, when compared to the other biotic batch reactors. One reason that TCE may have only been detected when nBA and IPP were used as the electron donor is because the culture was maintained with lactate as the electron donor, so dechlorination may have been slower in the first few days while the culture adjusted to the new electron donor. Overall, dechlorination was slower in the biotic batch reactors containing HD. This maybe because the PCE levels were higher in these batch reactors than those containing only PCE. Additionally, since the electron donor concentrations were generally lower in the batch reactors containing HD compared to those without, the dissolution rate from the NAPL phase may have been the rate-limiting step. A comparison of the times that each chlorinated ethene appeared or disappeared is summarized in Table 4.4 and Table 4.5.

Table 4.4 A comparison of the time (days) of disappearance and appearance of each of the chlorinated ethenes in the biotic batch reactors containing tetrachloroethene.

300 µM PCE	Lactate	n-Butyl Acetate	Isopropyl Propionate
PCE Last Appearance	3.5	1.5	3.5
TCE First Appearance	-	1.5	1.5
TCE Last Appearance	-	5.5	3.5
cis-DCE First Appearance	1.5	1.5	1.5
cis-DCE Last Appearance	16.5	7.5	16.5
VC First Appearance	3.5	3.5	5.5
VC Last Appearance	-	-	-
Ethene First Appearance	37.5	30.5	114.5

Table 4.5 A comparison of the time (days) of disappearance and appearance of each of the chlorinated ethenes in the biotic batch reactors containing 0.25 mol tetrachloroethene: 0.75 mol hexadecane.

300 μM PCE	Lactate	n-Butyl Acetate	Isopropyl Propionate
PCE Last Appearance	-	-	-
TCE First Appearance	1.5	1.5	1.5
TCE Last Appearance	-	-	-
cis-DCE First Appearance	3.5	3.5	3.5
cis-DCE Last Appearance	-	-	-
VC First Appearance	9.5	23.5	-
VC Last Appearance	-	-	-
Ethene First Appearance	-	-	-

The ideal pH for *Dhc* is neutral, between 6.5 and 8 (ITRC 2008). The pH was measured on day 115. The average pH ranged from 6.97 to 8.58. In general the abiotic batch reactors had higher pH than the biotic batch reactors. The average pH ranged from 7.9 to 8.58 and 6.97 to 8.10 for the abiotic and biotic batch reactors, respectively. The process of bioremediation of chlorinated solvents lowers the pH because hydrochloric acid is a by-product of organohalide respiration (ITRC 2008).The biotic batch reactors containing 2E1H had higher pH than those containing other electron donors because no dechlorination occurred. The pH in the biotic batch reactors containing HD had lower pH than those containing only PCE. A summary of the average pH is shown below in Figure 4.12.

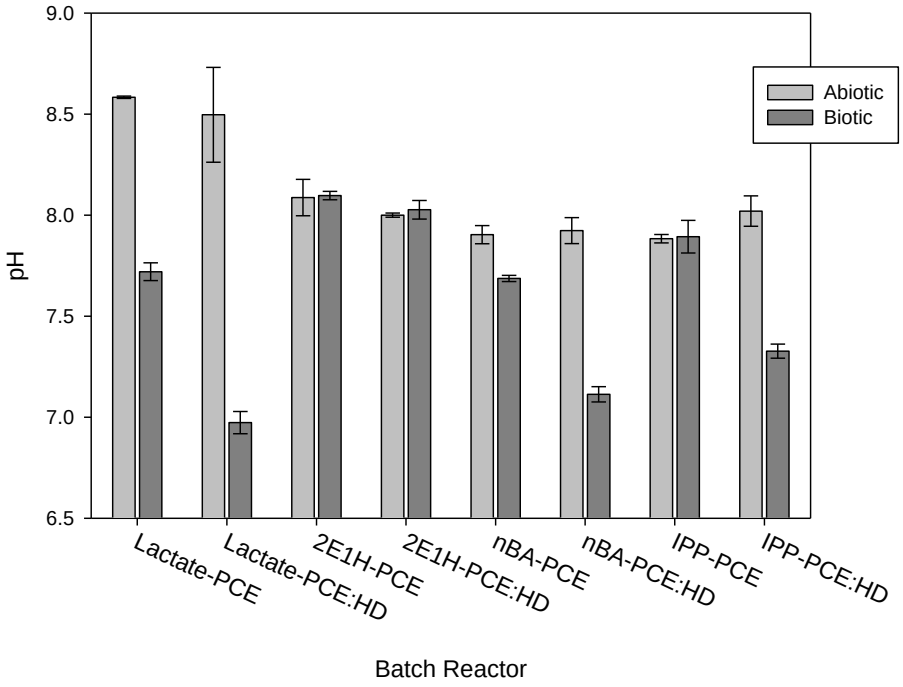

Figure 4.12 pH levels in the batch reactors.

Hydrogen levels were also measured on day 115. Hydrogen concentrations are important, because hydrogen is the only electron donor that *Dhc* use and is indicative of complete fermentation of the electron donors (Löffler et al. 2013a). Hydrogen was not detected in any of the 2E1H bottles, where dechlorination was not observed. Hydrogen levels were highest in the biotic batch reactors containing nBA, PCE, and HD with an average concentration of 127 ± 75.2 ppmv. Hydrogen was not detected in the biotic batch reactors containing lactate, PCE, and HD even though VC was detected. The hydrogen might have been consumed as quickly as it was formed in these reactors. Hydrogen was detected in the biotic batch reactors containing only PCE at concentrations of 52 ± 11.9 ppmv, 70 ± 8.5 ppmv, and 105 ± 9.4 ppmv for lactate, nBA, and IPP, respectively. The hydrogen levels are shown below in Figure 4.13

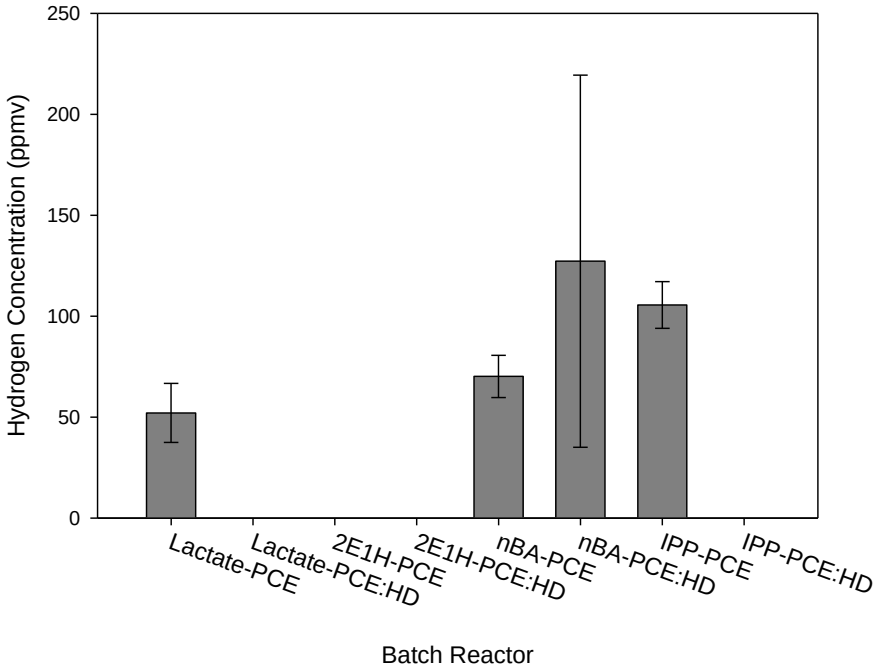

Figure 4.13 Hydrogen concentrations in the biotic batch reactors.

4.8 Biotic Column Results

The results for both the abiotic negative control columns and the biotic columns are summarized below.

4.8.1 Negative Control Column Results

Effluent samples were analyzed for lactate, nBA, butanol, acetate, and PCE. PCE concentrations in both the nBA and the lactate column ranged from 26 to 57 mg/L. The expected aqueous PCE concentration of the HD and PCE mixture is 50 mg/L. The bromide tracers were symmetrical with a R_F close to 1.0. Lactate broke through at PV 0.99, similar to the bromide tracer. The lactate concentrations reached 147 mg/L or 100% of the concentration entering the column. The lactate lasted until PV 3.2, about a PV longer than the bromide tracer. A total of 95.7% of the lactate was recovered. Neither the equilibrium model nor the non-equilibrium model fits this data perfectly, but the non-

equilibrium model fits the tailing that was observed in the lactate concentrations. The Sum of Squared Residuals (SSQ) is a measure of how well the model fits the observed data, and the lower the SSQ value the better the model fits data. The non-equilibrium model had an SSQ of 0.277 and the equilibrium model had an SSQ of 1.13 indicating the non-equilibrium model fits this data better than the equilibrium model. The non-equilibrium model was used to fit the retardation factor (R_F), beta (β), and omega (ω) and these values were used to calculate the equilibrium aqueous:NAPL partitioning coefficient (K_{NW}), effective mass transfer (k), and the fraction of sites at equilibrium (F) values. All of these variables are explained in Chapter 3 Section 3.5.2. The K_{NW} was calculated to be 0.77. This is an order of magnitude lower than the K_{NW} calculated using the batch reactor results of 16.2. The F value was calculated to be 0 which indicates that all of the sites are at non-equilibrium or the partitioning is time dependent, but that this data is best fit by a "one-site" model. This data is summarized in Table 4.6. The observed lactate concentration, bromide tracer, equilibrium model, and non-equilibrium model are plotted below in Figure 4.14.

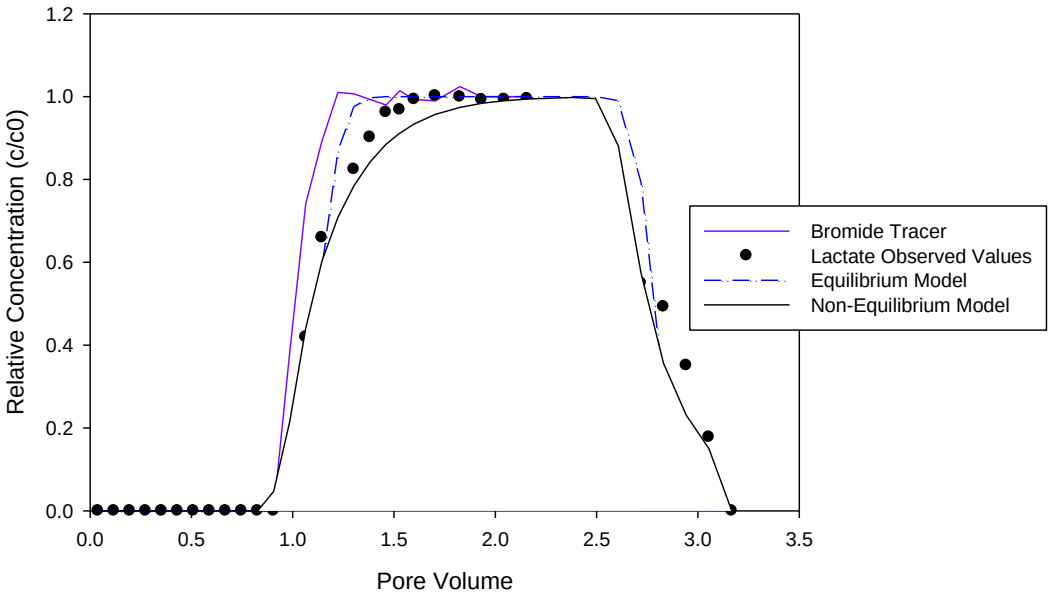

Figure 4.14 Column results for the abiotic column with lactate and 0.25 mol tetrachloroethene: 0.75 mol hexadecane showing the observed lactate relative concentrations, bromide tracer, equilibrium modeling results, and non-equilibrium modeling results.

On the other hand, nBA broke through at PV 5.2 and lasted until PV 24.9. This is substantially longer than lactate, but shorter than nBA in the column with pure PCE. The highest concentration of nBA observed was 96 mg/L or 23.4% of the influent concentration. Butanol and acetate were also observed in the effluent samples indicating that nBA was breaking down to form these compounds through hydrolysis. In total 82.9% of the nBA was recovered; 70.4% was recovered as nBA. Figure 4.15 shows the amount, in moles of nBA, that was recovered as nBA and as butanol in each sample.

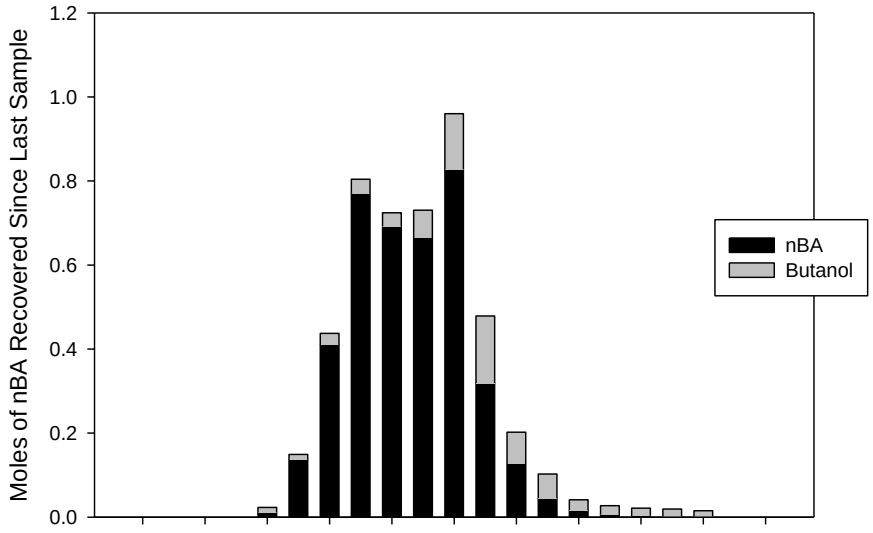

Figure 4.15 The total number of moles recovered of n-butyl acetate, as n-butyl acetate and as butanol, between each sample**.**

The nBA concentration data was modeled using both the equilibrium and non-equilibrium models. The equilibrium model, SSQ of 0.041, did not fit the data as well as the non-equilibrium model, SSQ of 0.008, as shown in Figure 4.16. The K_{NW} value was calculated to be 48.5. This is also an order of magnitude lower than the K_{NW} value of 186, calculated using the batch reactor data. The F value was calculated to be 0 which indicates that all of the sites are at non-equilibrium or the partitioning is rate limited and the data is best fit by a "one-site" model. This data is summarized in Table 4.6. The observed nBA concentration, bromide tracer, equilibrium model, and non-equilibrium are plotted below in Figure 4.16.

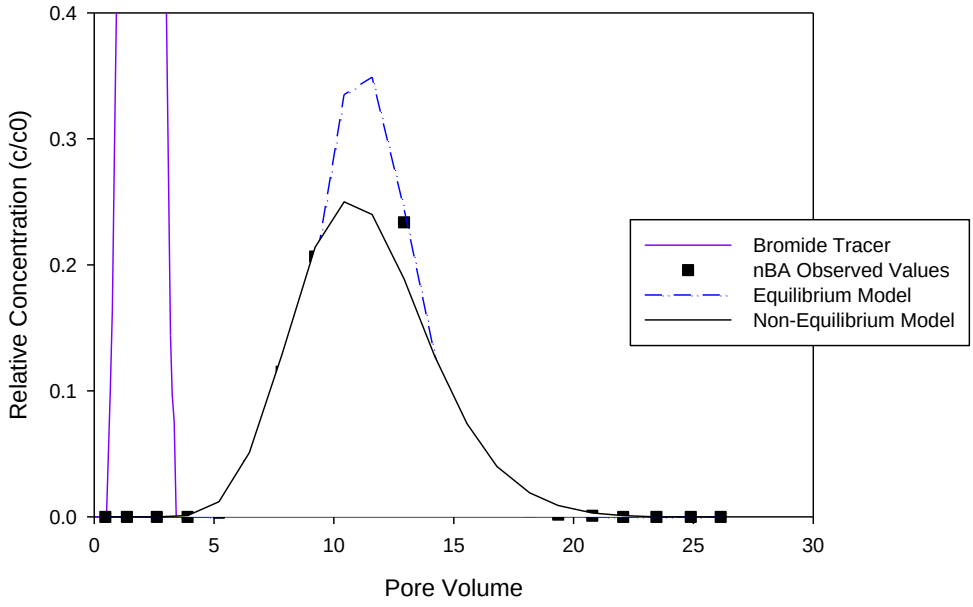

Figure 4.16 Column results for the abiotic column with n-butyl acetate and 0.25 mol tetrachloroethene: 0.75 mol hexadecane showing the observed n-butyl acetate relative concentrations, bromide tracer, equilibrium modeling results, and non-equilibrium modeling results.

Table 4.6 Summary of the peclet numbers (PE), dispersivity (α), retardation factor (R_F), NAPL-aqueous partitioning coefficient (K_{NW}), lumped mass transfer coefficient (k), and fractions of sites at equilibrium (F).

Electron Donor	**PE**	**α (cm)**	**R_F**	**K_{NW}**	***k* (min^{-1})**	**F**	**SSQ (Equilibrium)**	**SSQ (Non-Equilibrium)**
n-butyl acetate	61.3	0.245	10.5	48.5	0.094	0	0.041	0.008
Lactate	364.7	0.041	1.16	0.77	0.002	0	1.13	0.277

4.8.2 Microbial Elution Phase

Prior to NAPL addition in the biotic columns, the columns were run for about 4 PVs with reduced medium with no electron donor to monitor the elution (i.e. washout) of both the

Dhc and the *G. lovleyi*. The BDI-SZ consortium used as the inoculum for the lactate column contained (4.6 ± 0.3) X 10^7 *Dhc* cells/mL and (4.4 ± 0.5) X 10^9 *G. lovleyi* cells/mL. This resulted in a total addition of (4.8 ± 0.3) X 10^9 *Dhc* cells and (4.6 ± 0.5) X 10^{11} *G. lovleyi* cells to the column. The number of *Dhc* and *G. lovleyi* cells in the column effluent prior to NAPL addition, are shown below in Figure 4.17. The *Dhc* and *G. lovleyi* in the first effluent sample were 4x and 3x lower than those measured in the inoculum, respectively. The amount of cells in the effluent decreased sharply after 2 PVs of flushing. At the conclusion of the 4.5 PVs prior to NAPL addition, 45% of the *Dhc* cells were recovered which suggests that 2.6 X 10^9 cells remained associated with the column material. On the other hand, 51% of the *G. lovleyi* cells were recovered and 2.4 X 10^{11} cells remained associated with the column material.

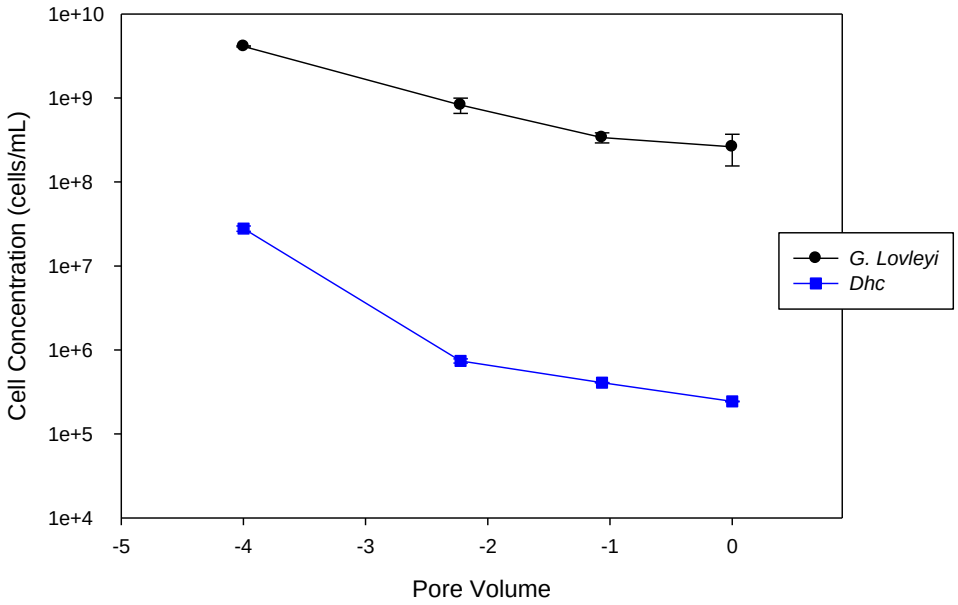

Figure 4.17 *Dehalococcoides mccartyi (Dhc)* and *Geobacter Lovleyi (G. lovleyi)* cells in lactate column effluent samples prior to NAPL addition.

The BDI-SZ consortium used as the inoculum for the nBA column contained (1.9 ± 0.02) X 10^8 *Dhc* cells/mL and (1.8 ± 0.2) X 10^9 *G. lovleyi* cells/mL. This resulted in a total

addition of (2.0 ± 0.3) X 10^{10} *Dhc* cells and (1.9 ± 0.2) X 10^{11} *G. lovleyi* cells to the column. The number of *Dhc* and *G. lovleyi* cells in the column effluent, prior to the NAPL addition, are shown below in Figure 4.18. The *Dhc* and *G. lovleyi* in the first effluent sample were 3x and 2x lower than those measured in the inoculum, respectively. At the conclusion of the 4.5 PVs prior to NAPL addition, 25% of the *Dhc* cells were recovered which suggests that 1.5 X 10^{10} cells remain associated with the column material. On the other hand, 45% of the *G. lovleyi* cells were recovered and 1.1 X 10^{11} cells remained associated with the column material.

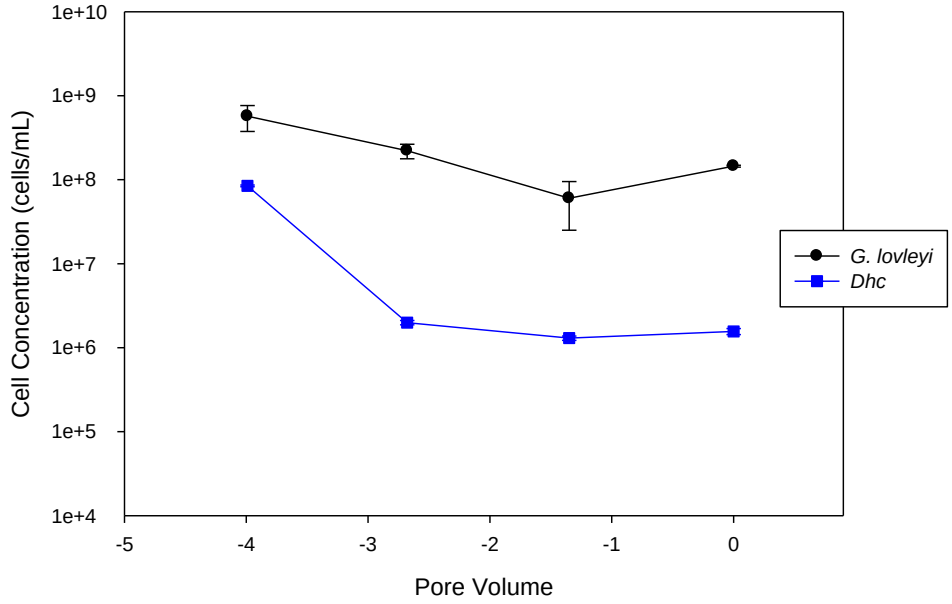

Figure 4.18 *Dehalococcoides mccartyi (Dhc)* and *Geobacter lovleyi (G. lovleyi)* cells in n-butyl acetate column effluent samples prior to NAPL addition.

4.8.3 NAPL Dissolution Phase

During the NAPL dissolution phase concentrations of PCE and its daughter products were monitored. Flow was started at a rate of 0.15 mL/min or a seepage velocity of 0.3 m/day. At this flow rate minimal dechlorination was detected in either column. Flow interruptions were used to determine if slowing of the flow rate would increase the

amount of dechlorination that occurred. A flow interruption of 12 hours occurred at PV 10 and a flow interruption of 72 hours occurred at PV 30. After both flow interruptions, increases in TCE and cis-DCE concentrations were detected indicating that slowing the flow rate would in fact increase the rates of organohalide respiration. After the first flow interruption, the flow was reduced from 0.15 mL/min to 0.10 mL/min, or a seepage velocity of 0.3 m/day to 0.2 m/day. After the second flow interruption the flow was decreased from 0.10 mL/min to 0.07 mL/min, or a seepage velocity of 0.2 m/day to 0.15 m/day.

In the lactate column, the PCE concentration for the first 36.6 PVs was an average of 244 ± 43.4 µM. The expected PCE concentration if no dechlorination was occurring, based on the molar ratio of the NAPL phase, is 300 µM. After 36.6 PVs the concentration of PCE detected in the effluent slowly decreased. TCE was first detected after 4 PVs and hit a maximum of 135 µM at PV 32.7 (after the long flow interruption). The concentration of cis-DCE continuously increased, after its original detected at 15.6 PVs, throughout the remainder of the experiment to a maximum of about 1500 µM. VC was first detected at PV 45.7 and ethene was first detected at PV 40.7. The concentrations of VC and ethene never increased above 60 µM. The chlorinated ethene concentrations along with the timing of flow interruptions and flow reductions are shown below in Figure 4.19

The amount of *G. lovleyi* cells in the lactate column effluent samples increased, while the number of *Dhc* cells in the effluent decreased, throughout the experiment. From PV 10 until PV 37 the *G. lovleyi* cell concentration increased by 2 orders of magnitude and a total of 1.5 X 10^{12} cells were recovered. This is 672% of the 2.2 X 10^{11} cells that remained in the column after the microbial elution phase. This demonstrates that the *G. lovleyi* were growing within the column. On the other hand, from PV 10 until PV 37, the

Dhc cell concentrations decreased by a factor of 2. The total *Dhc* cell recovery is 4.8 X 10^8 cells which is 18.3% of the cells that remained in the column after the microbial elution phase. After the first flow interruption the concentration of *G. lovleyi* cells doubled, while the concentration of *Dhc* cells increased by about 10%. After the second flow interruption the *G. lovleyi* cell concentration increased by a factor of 2 and the *Dhc* cell concentration increased by an order of magnitude. The cell concentrations in the lactate column are shown below in Figure 4.20.

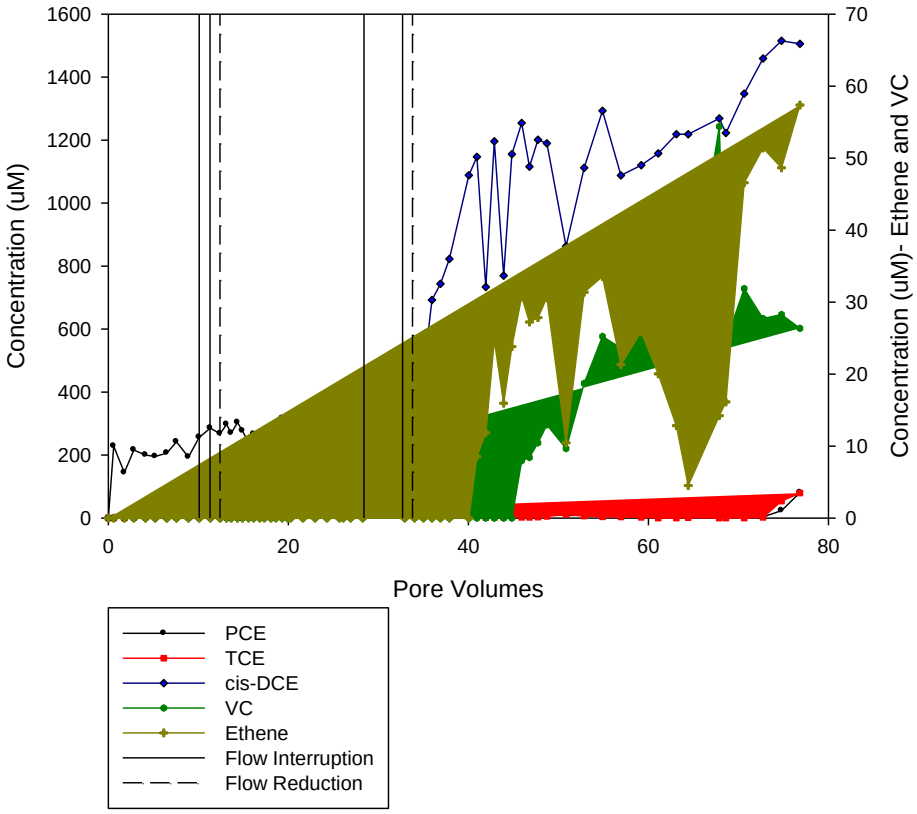

Figure 4.19 Chlorinated ethene concentrations, flow interruptions, and flow reductions for the column containing lactate.

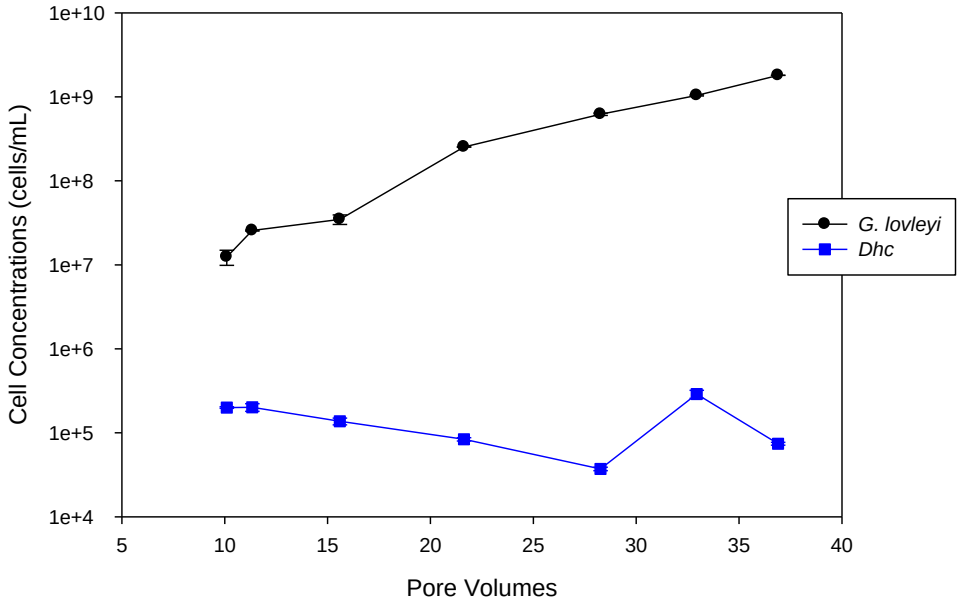

Figure 4.20 *Dehalococcoides mccartyi (Dhc)* and *Geobacter lovleyi (G. lovleyi)* cell concentrations in the effluent of the lactate column.

In the nBA column, the PCE concentration for the first 37 PVs was an average of 218 ± 56.0 µM. It is expected that the concentration in the nBA column is slightly lower than in the PCE column because the HD:PCE NAPL added to this column had a slightly smaller mole ratio of PCE. The expected PCE concentration, based solely on this mole ratio, is about 250 µM. After 37 PVs the PCE concentration in this column slowly decreased. TCE was first detected after 1.2 PVs and reached a maximum of 275 µM at PV 35.7 (after the long flow interruption). TCE appeared earlier and had a higher maximum in the nBA column than in the lactate column. This is expected based on the results of the biotic batch reactors. In the biotic batch reactors, TCE was detected in the reactors containing nBA but it was not detected in the reactors containing lactate. The concentration of cis-DCE increased after its detection at PV 4.3 to a maximum of about 460 µM. In the nBA column, cis-DCE was detected sooner than in the lactate column, but did not reach as high of a maximum. VC was first detected at 35.7 PVs, which is sooner than in the lactate

column. The earlier detection of cis-DCE and VC in the nBA column could indicate that dechlorination is happening faster in the nBA column than in the lactate column. Ethene was only just detected at about PV 60, which may be due cis-DCE inhibition.

It is likely the high concentrations of cis-DCE inhibited the production of ethene. High concentrations of cis-DCE have been shown to inhibit Dhc and VC to ethene dechlorination even at concentrations less than 50 µM cis-DCE in microcosms containing PM and EV, anaerobic mixed cultures (Yu and Semprini 2004, Yu and Semprini 2005). Amos, Suchomel et al. (2009) ran a column using this same mixed HD and PCE NAPL and BDI-SZ inoculum. Ethene was not detected in the column effluent until cis-DCE concentrations decreased to 6 µM indicating that the high concentrations of cis-DCE inhibited VC dechlorination to ethene (Amos, Suchomel et al. 2009), although future work is needed to explore the influence cis-DCE inhibition of completed dechlorination of PCE using the BDI-SZ culture. The chlorinated ethene concentrations along with timing of flow interruptions, flow reductions, and additions of nBA are shown below in Figure 4.21.

Both the amount of *G. lovleyi* cells and *Dhc* cells in the nBA column effluent samples increased, throughout the experiment. From PV 6 until PV 47 the *G. lovleyi* cell concentration increased by 1 order of magnitude and a total of 1.3×10^{12} cells were recovered. This is 1287% of the 1.0×10^{11} cells that remained in the column after the microbial elution phase. This proves that the *G. lovleyi* were growing within the column. From PV 6 until PV 47, the *Dhc* cell concentrations also increased by 1 order of magnitude. The total *Dhc* cell recovery is 1.1×10^{9} cells which is 7% of the cells that remained in the column after the microbial elution phase. After the first flow interruption, the concentration of *G. lovleyi* and *Dhc* cells were both 1.5 times larger than the

concentrations prior to the flow interruption. After the second flow interruption, the *G. lovleyi* cell concentration increased by 0.5 orders of magnitude and the *Dhc* cell concentration doubled. The cell concentrations in the nBA column are shown below in Figure 4.22.

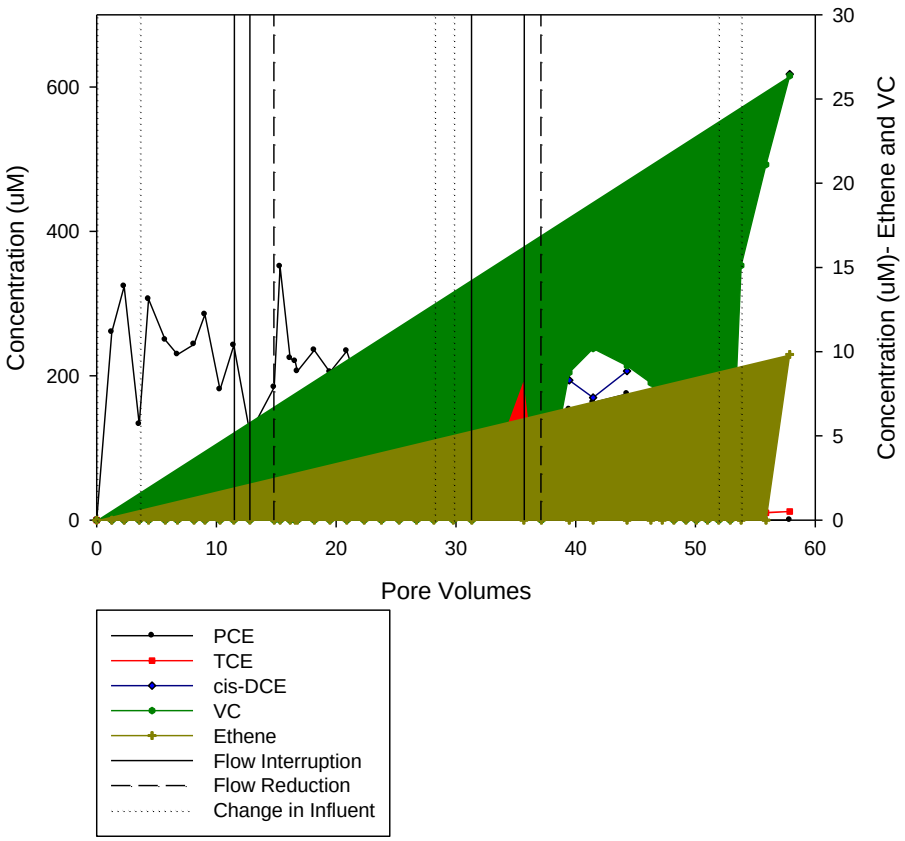

Figure 4.21 Chlorinated ethene concentrations, flow interruptions, flow reductions, and n-butyl acetate additions for the column containing n-butyl acetate.

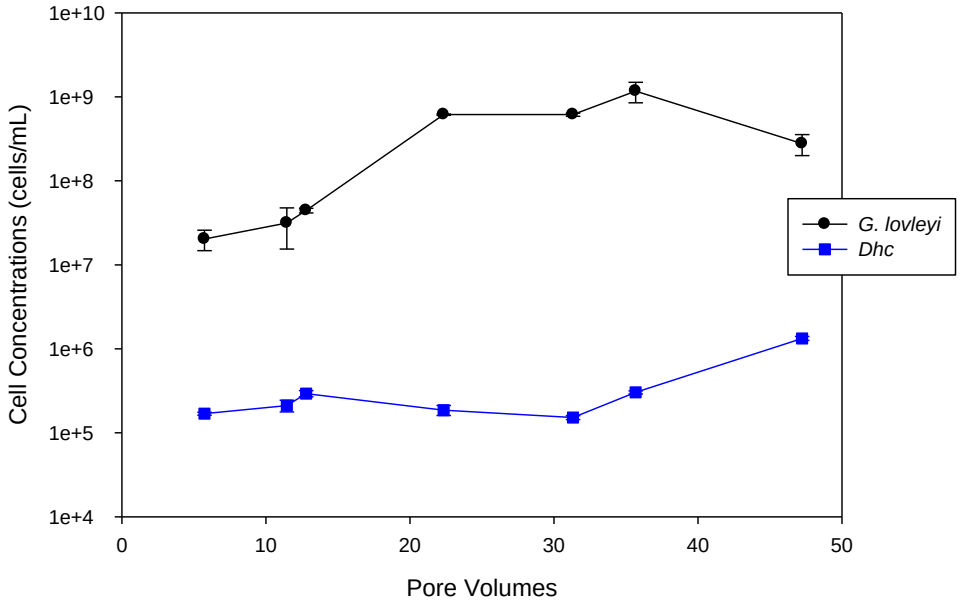

Figure 4.22 *Dehalococcoides mccartyi (Dhc)* and *Geobacter lovleyi (G. lovleyi)* concentrations in the effluent of the n-butyl acetate column.

Throughout the experiment the pH in the lactate column was an average of 7.03 ± 0.18. The lowest pH, 6.67 occurred after the long flow interruption, around PV 37. VC and ethene were not detected until after PV 40, in which the pH had returned to a pH of 7. The pH is shown below in Figure 4.23. The pH in the nBA column was an average of 7.21 ± 0.19. The lowest pH 6.74 occurred after the long flow interruption, around PV 36. After this flow interruption the pH immediately returned to a pH above 7.0. The pH for the nBA column is shown below Figure 4.23.

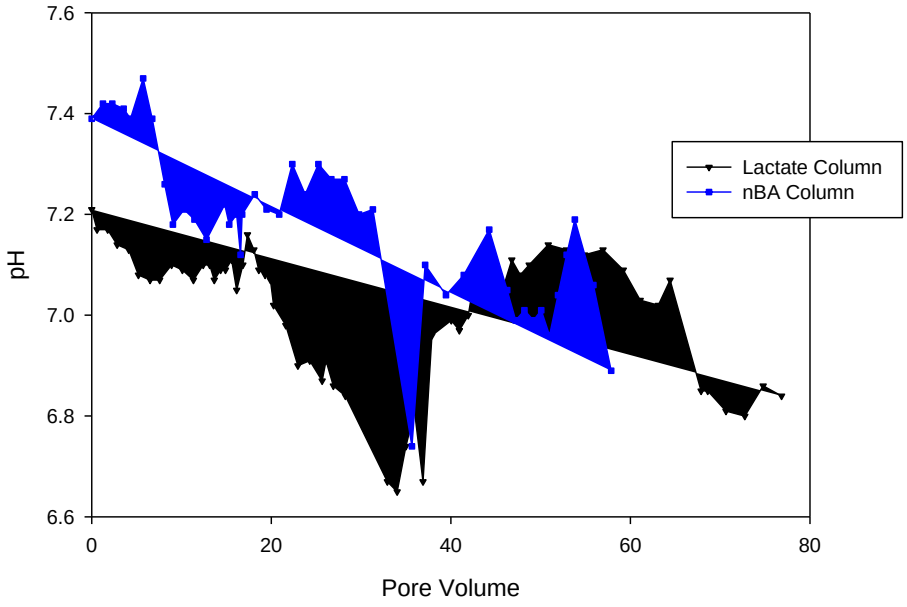

Figure 4.23 pH in the lactate and n-butyl acetate columns**.**

4.8.4 Electron Donor Concentrations

For each of the columns the concentration of electron donors was also monitored. For the lactate column, lactate quickly approached a maximum of 433 mg/L which is 85.4% of the influent concentration. By PV 6.5 the concentration of lactate in the effluent was no longer detectable. The concentration of acetate remained fairly constant throughout the experiment, except for after the long flow interruption when the concentration dropped to zero. The concentration of acetate ranged between 0 and 165 mg/L or 2.7 milli-reducing equivalents/L. The concentration of propionate varied more throughout the experiment, but followed the same trend and was also zero after the long flow interruption. The maximum concentration was 360 mg/L which corresponds to a milli-reducing equivalent/L of 8.6. In total, 176 mmol of hydrogen was added to the column in the form of lactate. In the effluent samples, 137 mmol of hydrogen was recovered as lactate,

acetate, and propionate for a total recovery of 78%. The milli-reducing equivalents of lactate, acetate, and propionate are shown below in Figure 4.24.

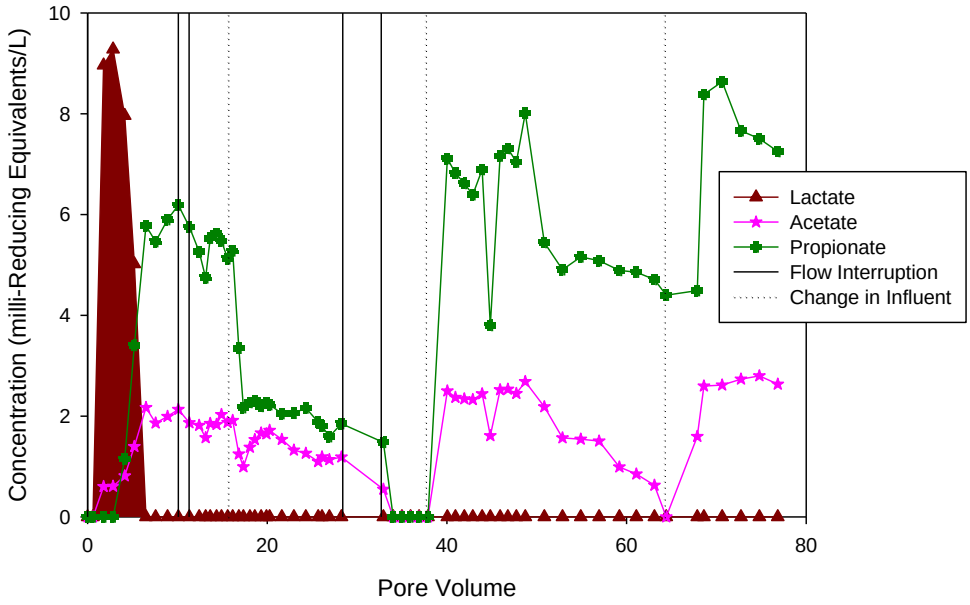

Figure 4.24 Concentrations of lactate, acetate, and propionate in milli-reducing equivalents/L for the lactate column.

In the column containing nBA, nBA was added in about 2 PV increments at about 5000 mg/L at PV 0, PV 28, and PV 52. After the first addition of nBA, nBA lasted from PV 4.3 to PV 23.8. The maximum concentration of nBA observed is 666 mg/L or 13.8% of influent concentration. Butanol and acetate concentrations were similar throughout the experiment. Butanol ranged from 0 mg/L to 130 mg/L or a milli-reducing equivalent/L of 5.3. Acetate ranged from o mg/L to 140 mg/L or a milli-reducing equivalent/ L of 2.4. When the concentration in the effluent of nBA, butanol, and acetate were all under 2 mg/L, nBA was added a second time. The second addition of nBA occurred just before the long flow interruption and final flow reduction. After this second addition, nBA was detected in the effluent from PV 37 until PV 44, although the maximum nBA concentration was similar at 736 mg/L or 14.5% of the influent concentration. The longer

delay until the detection of nBA, after its addition, and the shorter time that it lasted in the column is most likely due to the increase in microbial activity due to the long flow interruption and reduction in flow. Butanol and acetate were also detected for shorter amounts of PVs than after the first nBA addition. In total, 450 mmol of hydrogen were added to the column in the form of nBA. A total recovery of 210 mmol hydrogen or 48% as nBA, butanol, and acetate occurred. The milli-reducing equivalents/L of nBA, butanol, and acetate are shown below in Figure 4.25.

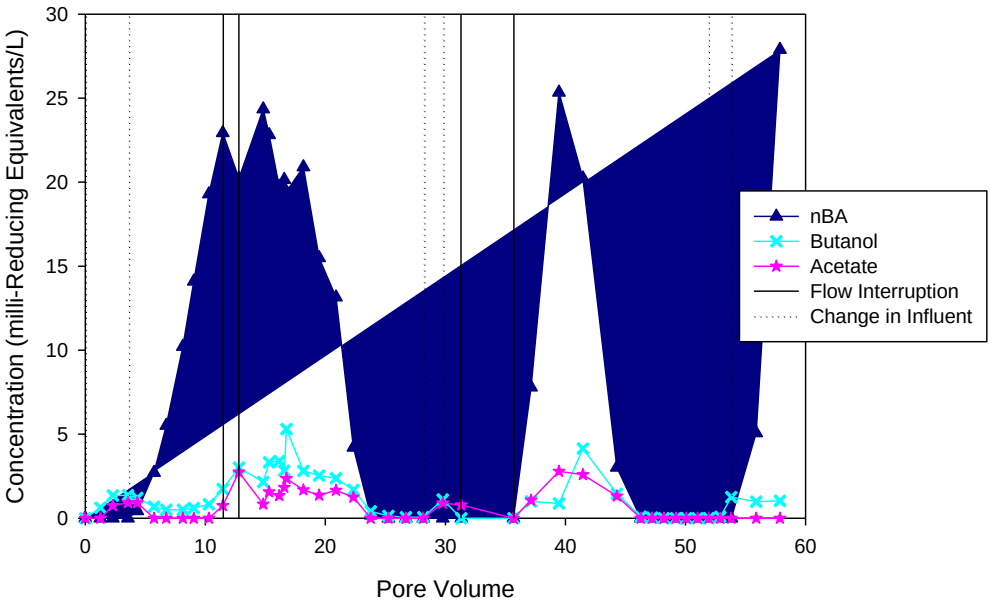

Figure 4.25 Concentrations of n-butyl acetate, acetate, and butanol in milli-reducing equivalents/L in the n-butyl acetate column**.**

4.8.5 Comparative Cumulative Mass Recoveries and Mass Transfer Enhancement Factor

One goal of this work is to compare the bioenhanced dissolution of PCE when using lactate or nBA as the electron donors. The expected PCE recovery is based on the aqueous phase solubility of the PCE in the PCE and HD mixed NAPL. The solubility is dependent on the mole ratio of the PCE and HD. Since the solubility of HD is so small, it

was assumed that the amount of HD in the column remained the same throughout the experiment. The molar ratio of PCE in the NAPL decreased as PCE was recovered. The experimental recovery and expected recovery for both columns was about the same until PV 30 when the long flow interruption occurred and the flow rate was slowed for the final time. After PV 30 the experimental recovery gets exponentially larger than the expected recovery as shown below in Figure 4.26 and Figure 4.27.

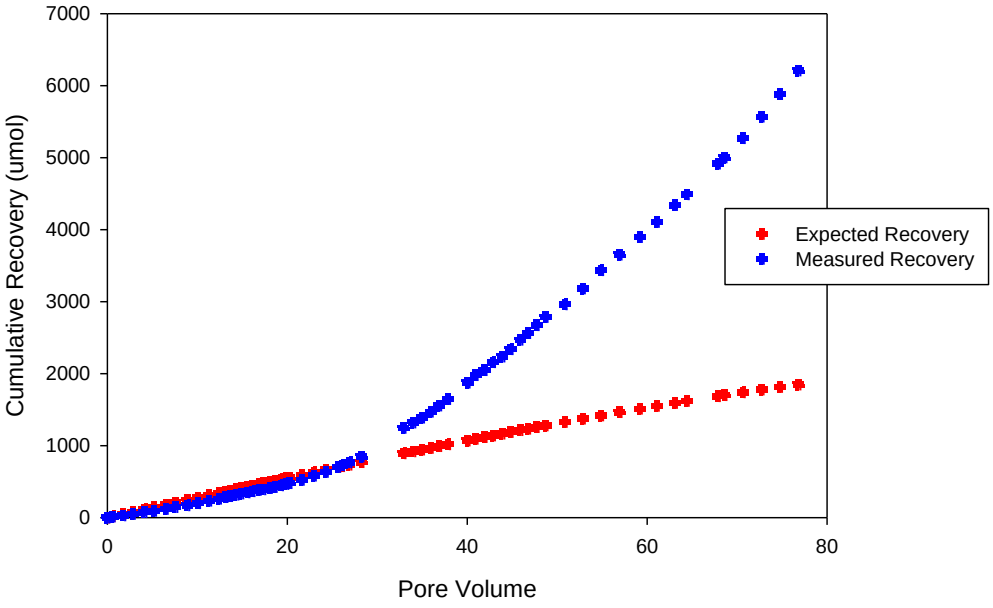

Figure 4.26 Cumulative mass recovery of tetrachloroethene in the lactate column.

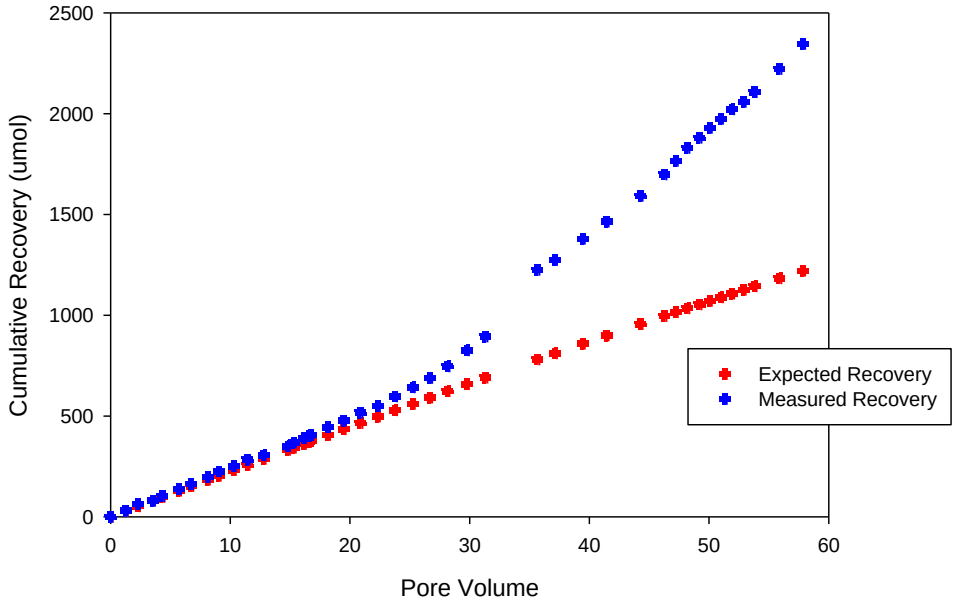

Figure 4.27 Cumulative mass recovery of tetrachloroethene in the n-butyl acetate column.

At PV 60, the cumulative and maximum mass transfer enhancements were compared for the lactate and nBA columns. The enhancement factors and the experimental and expected recoveries of each chlorinated ethene are summarized below in Table 4.7. The expected abiotic mass recovery is 11.1% and 10.7% for the lactate and nBA columns, respectively. The difference in abiotic recoveries and total PCE mass in the columns is due to the difference in NAPL saturations in these columns and difference in initial PCE to HD molar ratios. Both columns recovered under 1000 µmols or 10% of the total mass as PCE. In the nBA column, about twice as much was recovered as TCE than in the lactate column. This is consistent with biotic batch results in which more TCE was detected in the batch reactors containing nBA than in the batch reactors containing lactate. Most of the recovery for both columns was as cis-DCE. The lactate column recovered about three times more cis-DCE than the nBA column. VC and ethene accounted for less than 1% of the total recovery in both columns. The cumulative mass

transfer enhancement factor for the lactate column was 2.3, which was slightly larger than the cumulative mass transfer enhancement factor of 1.8 found for the nBA column. The maximum mass transfer enhancement factor is calculated by comparing the experimental effluent concentrations to the abiotic effluent concentrations. Maximum mass transfer enhancement factors are commonly higher the cumulative mass transfer enhancement factors. The maximum enhancement factor for the lactate column is 4.9, which is larger than for the nBA column, which is 3.7. Previous cumulative and maximum enhancement factors have been published for this same 0.75 mol HD:0.25 mol PCE NAPL, BDI-SZ inoculum, and lactate as the electron donor as a cumulative and maximum bioenhanced dissolution factor range of 4.6-5.2 and 13.6-21, respectively (Amos et al. 2008, Amos et al. 2009). It is predicted that the bioenhanced dissolution factor will continue to increase as the ratio of PCE to HD in the columns decrease, because the aqueous phase PCE concentration will decrease. The lower aqueous phase PCE concentration will promote *Dhc* growth (Löffler et al. 2013a). As a result, it is predicted that the bioenhancement factors in these columns, prior to 100% PCE recovery, will be similar to those found previously by Amos et al. (2008, 2009).

Table 4.7 Cumulative chlorinated ethene recoveries and mass transfer enhancement factors for the lactate and n-butyl acetate columns at pore volume 60.

Lactate Column	**Mass (µmol)**	**Mass (%)**	**nBA Column**	**Mass (µmol)**	**Mass (%)**
PCE Loading	13600	100	PCE Loading	11800	100
Experimental Recovery			**Experimental Recovery**		
PCE	831	6.1	PCE	939	8.0
TCE	211	1.6	TCE	415	3.5
cis-DCE	2789	20.5	cis-DCE	1044	8.8
VC	23.6	0.2	VC	25	0.2
Ethene	41.4	0.3	Ethene	2	<0.1
Total	3896	28.7	Total	2425	20.5
Expected Recovery (Abiotic)			**Expected Recovery (Abiotic)**		
PCE	1511	11.1	PCE	1258	10.7
Cumulative Enhancement Factor = 2.6 Maximum Enhancement Factor = 5.1			**Cumulative Enhancement Factor = 1.9 Maximum Enhancement Factor = 3.7**		

The lactate column was run for about 15 more PVs than the nBA column. At PV 77 the cumulative enhancement factor was about a third larger than at PV 60 for the lactate column. A similar trend is expected for the nBA column. The total recovery of PCE for the lactate column is 46%. More than 75% of this total recovery is as cis-DCE. The enhancement factors and chlorinated solvent recoveries for the lactate column are summarized below in Table 4.8.

Table 4.8 Cumulative chlorinated ethene recoveries and mass transfer enhancement factors for the lactate column at pore volume 77.

Lactate Column	**Mass (µmol)**	**Mass (%)**
PCE Loading	13600	100
Experimental Recovery		
PCE	854	6.3
TCE	237	1.7
cis-DCE	4950	36.4
VC	77	0.6
Ethene	92	0.7
Total	6209	45.7
Expected Recovery (Abiotic)		
PCE	1848	13.6
Cumulative Enhancement Factor = 3.4 **Maximum Enhancement Factor =9.4**		

4.9 Column Experiment Conclusions

Biotic batch reactors and column experiments have provided important information about the ability of the candidate PEDs to support PCE to ethene organohalide respiration and to provide reducing equivalents at the DNAPL:aqueous interface, leading to bioenhanced dissolution by a dechlorinating inoculum. Results suggest that both nBA and IPP can support PCE to ethene organohalide respiration, and nBA results in similar duration of PCE to ethene reduction and bioenhanced dissolution as lactate. The data collected in these experiments have led to the following specific conclusions:

1) IPP and nBA are utilized by organohalide respiring bacteria to reduce PCE to ethene. Ethene was produced first in the batch reactors containing nBA as shown

in Table 4.4. The addition of nBA as an electron donor could decrease the time to complete reduction to ethene over lactate and the other candidate PEDs tested in this chapter.

2) Lactate acted similarly to the non-reactive tracer in the 0.75 mol HD:0.25 mol PCE NAPL, even at the higher ionic strength of 90 mM as shown in Figure 4.14. This demonstrates that lactate exhibits little to no partitioning into the NAPL phase, and suggests that lactate has to be injected continuously in order to be effective for enhancing bioremediation of the NAPL.
3) The use of nBA as an electron donor lead to a cumulative and maximum bioenhanced dissolution factors of 1.9 and 3.7, respectively, as shown in Table 4.7. This bioenhanced dissolution factor is predicted to increase as the experiment continues because the PCE to HD ratio will continue to decrease and consequently so will this PCE aqueous phase concentration, which will promote *Dhc* growth (Löffler et al. 2013a). This trend has already been observed in the lactate column. Bioenhanced dissolution reduces the time to source zone removal, consequently reducing the time to site closure and costs associated with remediation.
4) Lactate and nBA were comparable, in the column experiments completed, in terms of utilization by organohalide respiring bacteria and bioenhanced dissolution, but nBA could be added in a single or few injections whereas lactate has to be added continuously. Even in the presence of the organohalide respiring bacteria, nBA remained in the source zone for 15x its injection length. Consequently, nBA could reduce the cost of remediation because it has the benefit of requiring fewer injections than soluble electron donors while the injection is still in the aqueous phase eliminating the difficulties associated with injecting insoluble electron donors. The PED, nBA, could be most advantageous

in sites where NAPL exists in bedrock, because it would be easy to inject and would travel within the cracks in the bedrock until reaching the NAPL, where the nBA would favorably partition and last for long periods of time.

Chapter 5: Engineering Implications and Recommendations

5.1 PED Significance and Engineering Implications

The work completed thus far indicates that partitioning electron donors (PEDs) have potential to reduce the need for frequent electron donor injections due to their long lifetime (i.e. 25 to 50 x their injection length) in dense non-aqueous phase liquid (DNAPL) source zones. Organohalide respiring bacteria require an electron donor (e.g., acetate and/or hydrogen) to reduce tetrachloroethene (PCE) to ethene (Löffler et al. 2013a) but, currently used electron donors are unable to simultaneously supply a sustained release of low concentrations of electron donor and ensure delivery of electron donor to the intended target. This leads to a decreased efficiency in the use of the electron donor and could limit the amount of bioremediation that occurs. PEDs could meet these goals by favorably partitioning into the DNAPL and then slowly dissolving into the aqueous phase with the chlorinated solvent promoting biomass growth at the aqueous:DNAPL interface. This favors organohalide respiring bacteria that are able to withstand higher concentrations of chlorinated solvents than other bacteria that use hydrogen (e.g., methanogens) (Ballapragada et al. 1997).

Batch reactor experiments completed suggest that all three of the tested PED candidates, n-butyl acetate (nBA), isopropyl propionate (IPP), and 2-ethyl-1-hexanol (2E1H), favorably partition into both PCE and trichloroethene (TCE). Of these three PEDs, nBA exhibits the highest NAPL-aqueous partitioning coefficient into TCE and partitions the fastest into both PCE and TCE. This partitioning is directly affected by the ionic strength. In this work, it was shown that the relationship between the ionic strength and the NAPL-aqueous partitioning coefficient for nBA and PCE is linear with a positive slope slightly larger than one. This suggests that the salinity of an aquifer will influence the amount of

partitioning that will occur, and in practice, PED partitioning could be manipulated by changing the ionic strength of the delivery solution.

Experiments were also completed to determine the amount of the PEDs that will sorb to the organic matter in soil. For both IPP and nBA, chosen because they were utilized by organohalide respiring bacteria to reduce PCE to ethene, it was determined that the relationship between the organic carbon content of the soil and the sorption coefficient is linear with a positive slope less than one. The highest sorption observed was to Webster soil which has an organic carbon content of 1.96%, but the sorption to this soil was still less than 10% of the total PED mass. This means that the sorption to the organic matter in an aquifer is minimal and is unlikely to greatly affect the amount of PED that will partition into the NAPL. The sorption of the PEDs to the soil is important to consider because it means that the PED could potentially be used as an electron donor to support dechlorination of sorbed contaminants.

Column studies completed thus far have determined PED lifetime in residual PCE and TCE. PED breakthrough curves indicate rate-limited mass transfer from the DNAPL to the aqueous phase, which leads to long lifetimes in the DNAPL source zones. The PEDs evaluated lasted up to 50x their injection length in TCE and 25x their injection length in PCE. This extended lifetime in DNAPL source zones, beyond the injected pulse, indicates that PEDs could require smaller volume injections than conventional electron donors, which could reduce the overall cost of remediation. Additionally, PEDs slowly dissolve into the aqueous phase and fatty-acid fermentation is thermodynamically restrained, which favors organohalide respiring bacteria over methanogens and other competitor microorganisms that are unable to effectively compete for hydrogen at low partial pressures and high chlorinated solvent concentrations (Ballapragada et al. 1997).

Biotic batch reactors were used to evaluate the ability of organohalide respiring bacteria to utilize the PEDs as electron donors. In batch reactors containing nBA and IPP, organohalide respiring bacteria were able to reduce PCE to ethene. On the other hand, 2E1H did not support dechlorination in these experiments despite measured fermentation to acetate and propionate (i.e., available electron donor or electron precursors). Ethene was produced at least one week sooner in the biotic batch reactors containing nBA, when compared to the other PEDs and lactate. Due to these results, and the high partitioning observed in the other experiments, nBA was chosen for further comparison to lactate. In abiotic control columns lactate did not last much longer than the non-reactive tracer indicating little to no partitioning into the NAPL phase. This reinforces that lactate has to be continuously injected in order to be an effective electron donor source.

In columns amended with the inoculum BDI-SZ, nBA led to bioenhanced dissolution. Bioenhanced dissolution is a benefit of using bioremediation to treat the source zone because it reduces the time to source zone removal by creating a reaction sink near the DNAPL which increases the PCE concentration gradient. PCE dissolution can be greatly enhanced (1.4-15x) (Amos et al. 2009, Carr et al. 2000, Cope and Hughes 2001, Glover et al. 2007, Sleep et al. 2006, Yang and McCarty 2000) via microbial reductive dechlorination to less-chlorinated daughter products because these have 5.5-17.5x higher solubilities than PCE (Interstate Technology and Regulatory Council [ITRC] 2008). Bioenhanced dissolution can reduce the time to site closure and consequently, the potential costs associated with remediation. Lactate and nBA were comparable in duration of PCE to ethene reduction and bioenhanced dissolution, but nBA supplied electron donor for 15x its injection length. Therefore, nBA has the benefit of requiring fewer injections to maintain electron donor at the DNAPL:water interface.

PEDs incorporate the desirable attributes of both soluble and insoluble electron donors because PEDs are water soluble compounds, which could require smaller volume injections than conventional soluble electron donors. Additionally, PEDs supply a continuous slow release of hydrogen, which is ideal for *Dhc* and could allow *Dhc* to out compete other microorganisms that consume hydrogen (e.g., methanogens). PEDs also contribute to bioenhanced dissolution, which reduces the time to site closure and the overall costs of remediation. PEDs could be most advantageous at sites where NAPL exists in bedrock. The PEDs would be easy to inject into the bedrock and easily travel within the cracks in the bedrock until reaching the NAPL. The PEDs would then favorably partition into the NAPL where they would last for long periods of time. Due to these attributes, PEDs could be a cost effective alternative to commonly used electron donors.

5.2 Future Work

To strengthen the case for the use of PEDs as electron donors, further work should be completed. First, in this work the PEDs were only compared to a common soluble electron donor, lactate. The PEDs should also be compared to an insoluble electron donor such as EVO to determine if the PEDs will also support bioenhanced dissolution by dechlorinating populations similarly to an insoluble electron donor. Second, most aquifers are not entirely made up of sand so similar abiotic columns to those completed in this study should be completed using natural soil containing higher organic carbon contents. These could evaluate the impacts on the organic carbon content on the PED partitioning. It is hypothesized, based on the batch reactors with soil completed in this study, that the presence of soil organic matter will reduce PED partitioning into the DNAPL because less PED will be available in the aqueous phase, but the extent of this is unknown.

Additionally, this study only evaluated source zones. In order to evaluate plume evolution impact (60 cm) columns with side ports could be used. These columns could also determine the temporal and spatial distribution of biomass, organic acids, hydrogen, and pH. Lastly, a two-dimensional aquifer cell could be used to measure mass transfer and microbial distribution in systems containing heterogeneous DNAPL ganglia and pools as a function of the PED delivery and release. It is unlikely that an aquifer would have uniform flow field and NAPL saturation, but would more likely have heterogeneous flow fields and NAPL saturations of both ganglia and saturated pools. It is hypothesized that PED delivery at the DNAPL:aqueous interface will promote microbial colonization within ganglia regions and near pooled zones. Aquifer cells could also be used to evaluate more realistic PED delivery, where targeted PED delivery would be used instead of flushing the entire source region. Work from these additional experiments could further the argument the PEDs could be a cost effective alternative to the currently used electron donors.

Appendix A: Biotic Batch Reactor Results

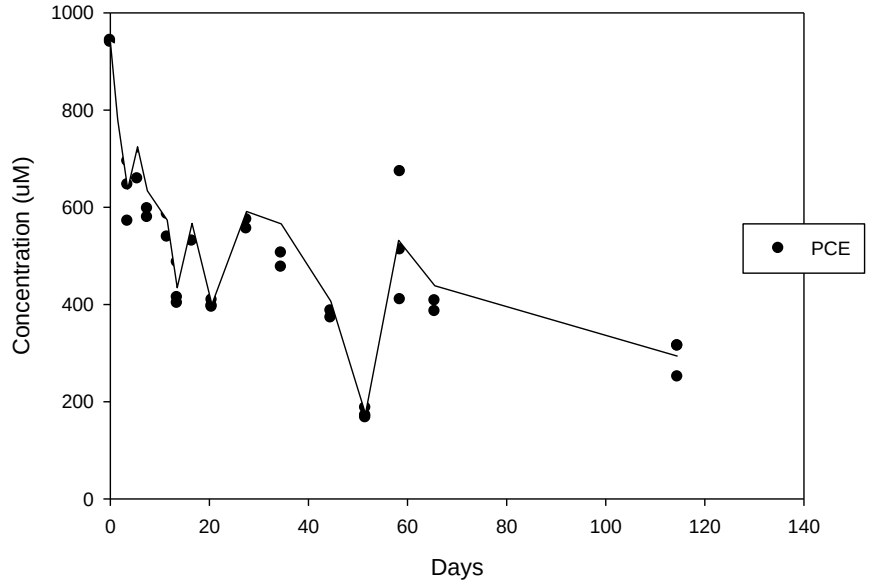

Figure A.1 Chlorinated ethene concentrations in the abiotic batch reactor containing lactate and 0.25 mol tetrachloroethene:0.75 mol hexadecane.

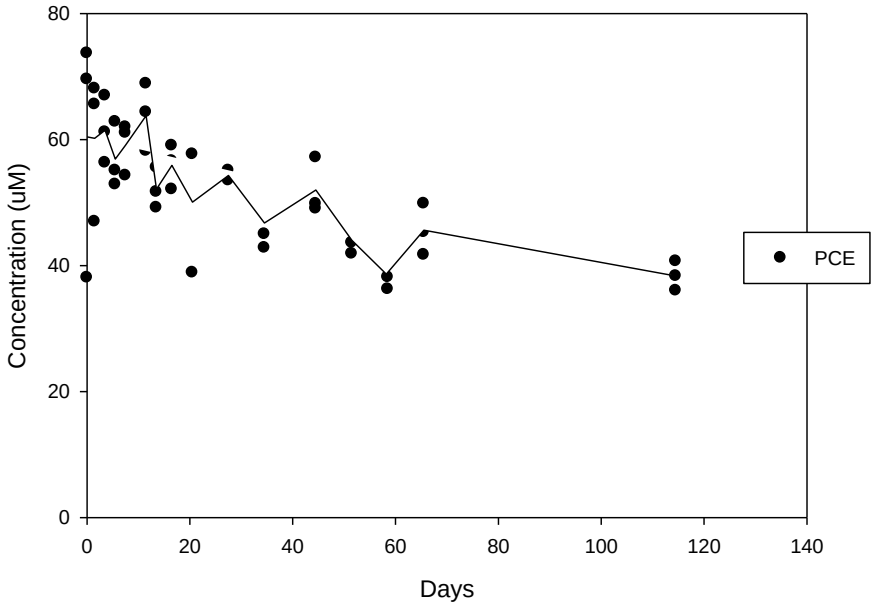

Figure A.2 Chlorinated ethene concentrations in the abiotic batch reactor containing 2-ethyl-1-hexanol and tetrachloroethene.

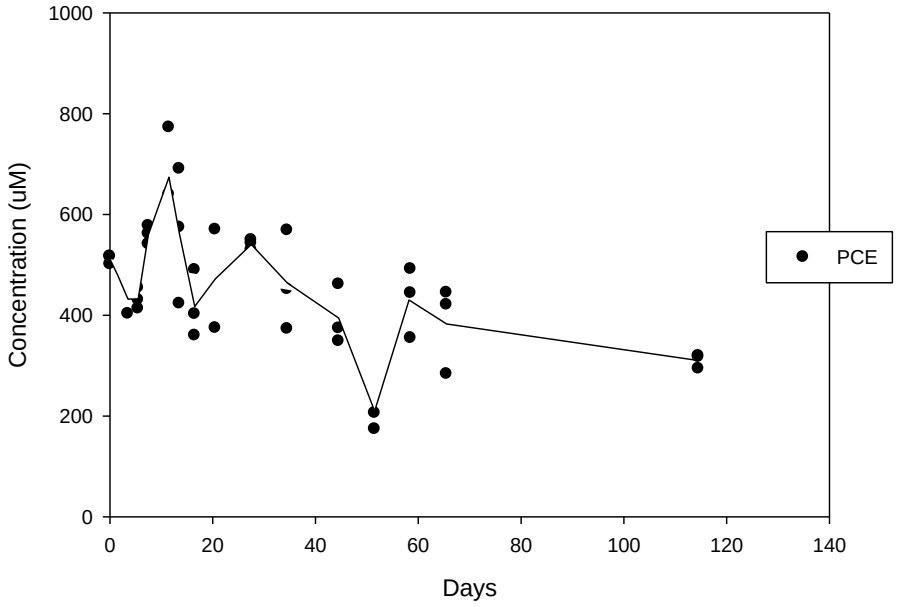

Figure A.3 Chlorinated ethene concentrations in the abiotic batch reactor containing 2-ethyl-1-hexanol and 0.25 mol tetrachloroethene: 0.75 mol hexadecane.

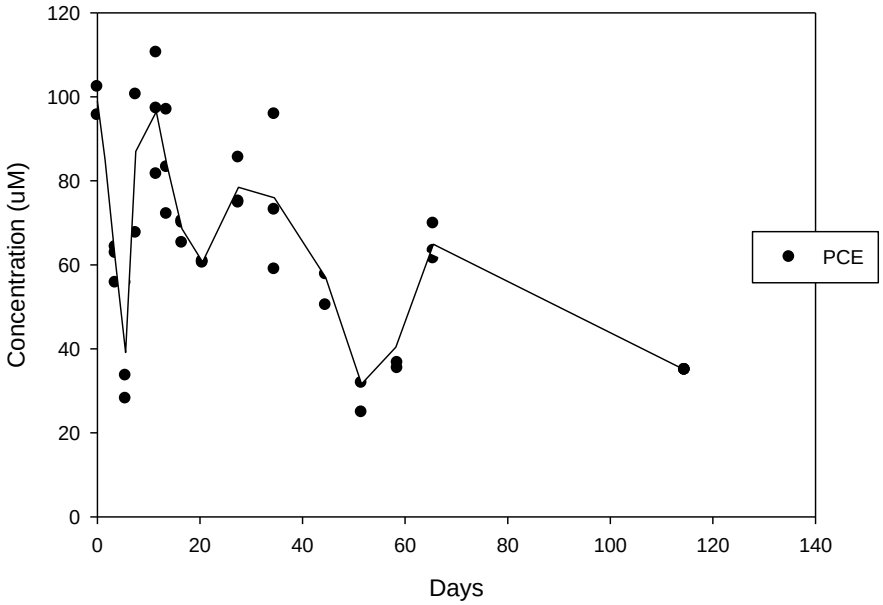

Figure A.4 Chlorinated ethene concentrations in the abiotic batch reactor containing n-butyl acetate and tetrachloroethene.

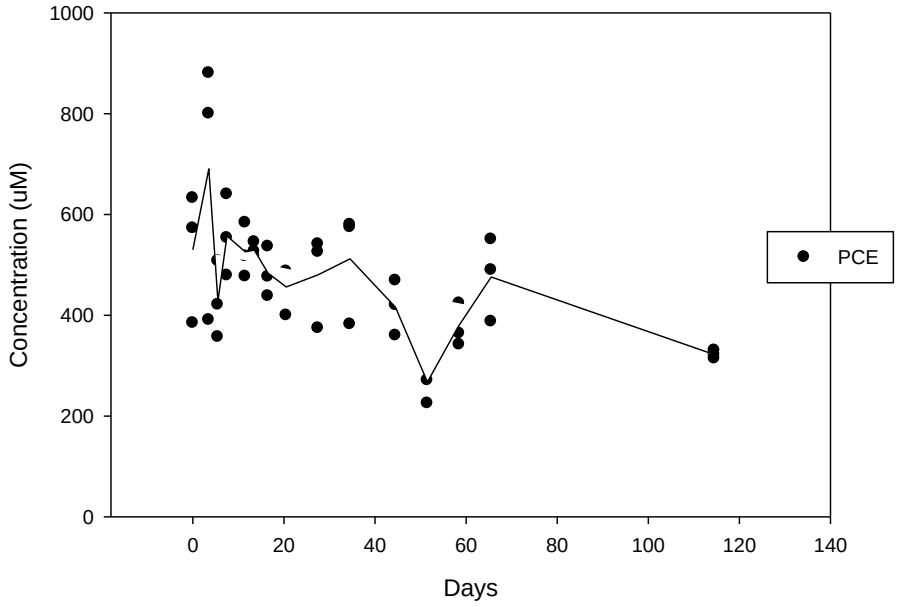

Figure A.5 Chlorinated ethene concentrations in the abiotic batch reactor containing n-butyl acetate and 0.25 mol tetrachloroethene: 0.75 mol hexadecane.

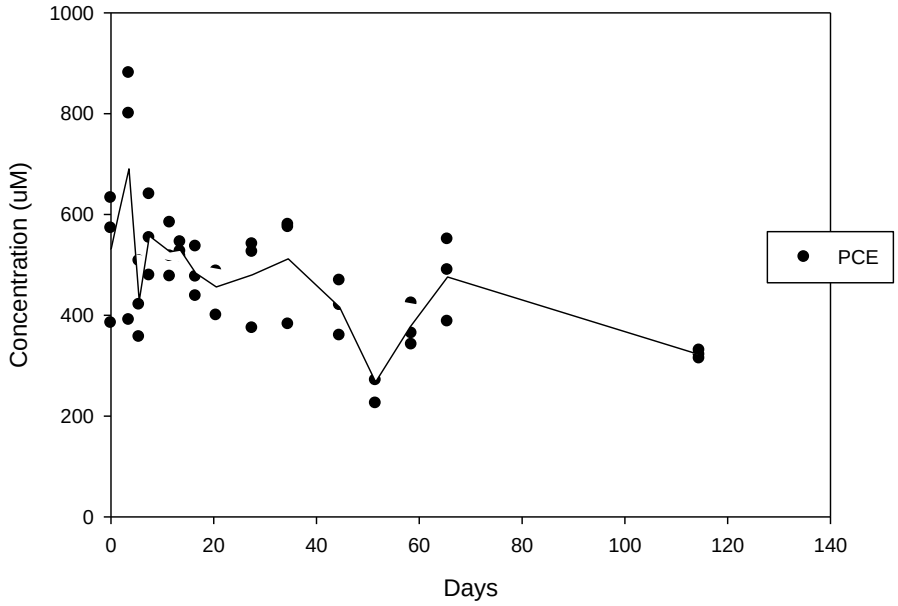

Figure A.6 Chlorinated ethene concentrations in the abiotic batch reactor containing isopropyl propionate and tetrachloroethene.

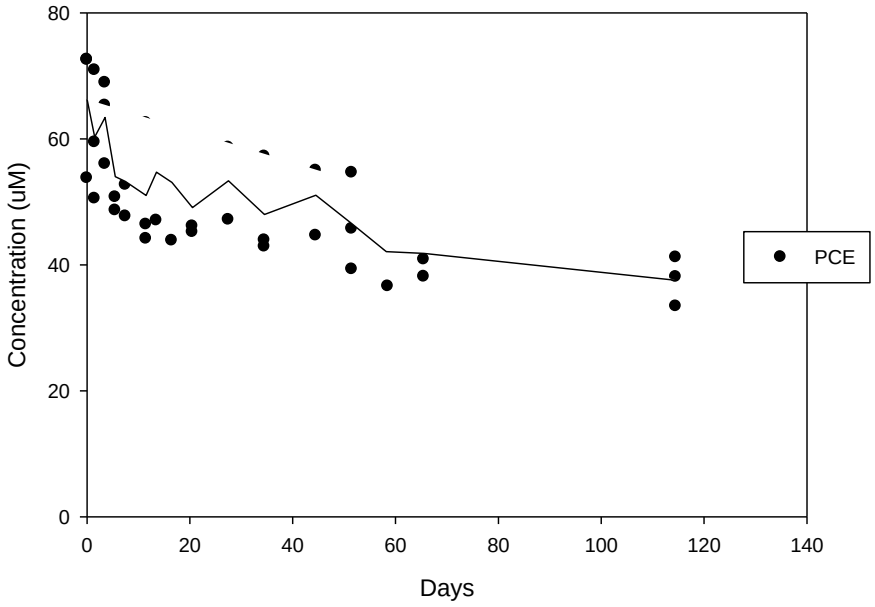

Figure A.7 Chlorinated ethene concentrations in the abiotic batch reactor containing isopropyl propionate and 0.25 mol tetrachloroethene: 0.75 mol hexadecane.

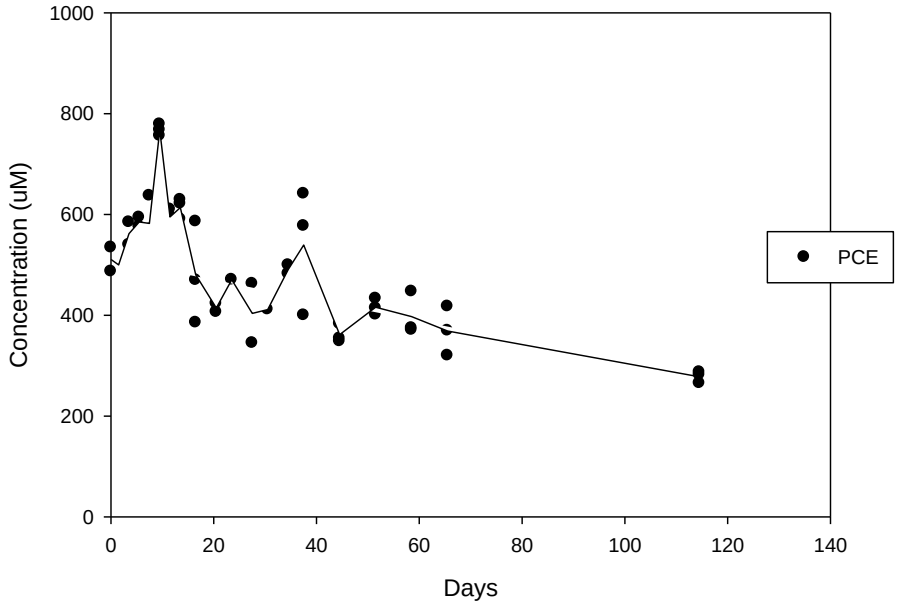

Figure A.8 Chlorinated ethene concentrations in the biotic batch reactor containing 2-ethyl-1-hexanol and 0.25 mol tetrachloroethene: 0.75 mol hexadecane.

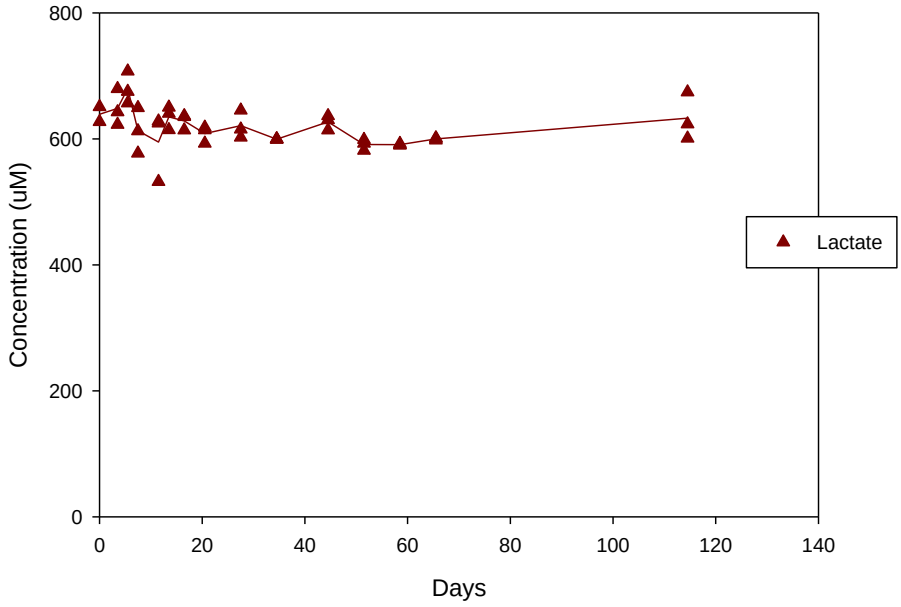

Figure A.9 Lactate concentrations in the abiotic batch reactor containing lactate and tetrachloroethene.

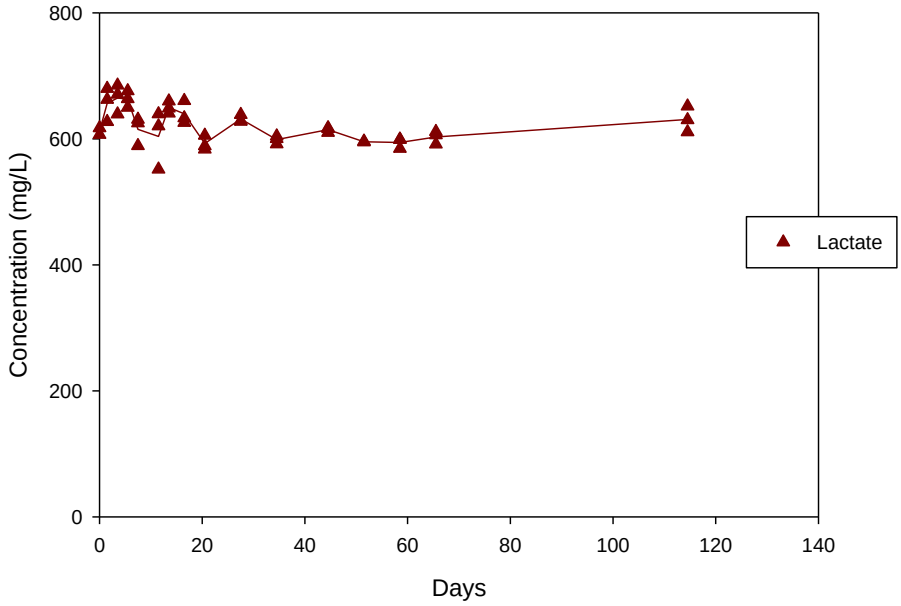

Figure A.10 Lactate concentrations in the abiotic batch reactor containing lactate and 0.25 mol tetrachloroethene: 0.75 mol hexadecane.

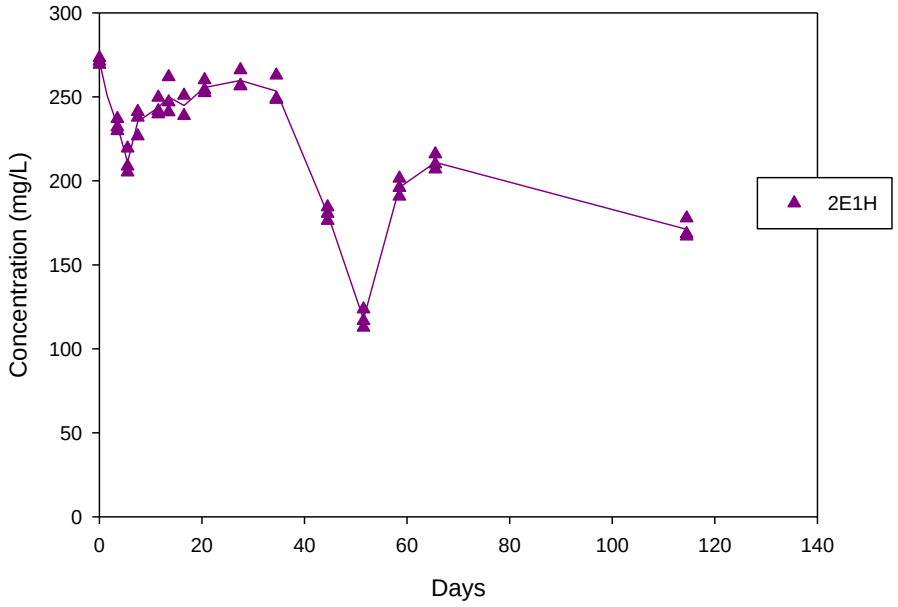

Figure A.11 2-ethyl-1-hexanol concentrations in the abiotic batch reactor containing 2-ethyl-1-hexanol and tetrachloroethene.

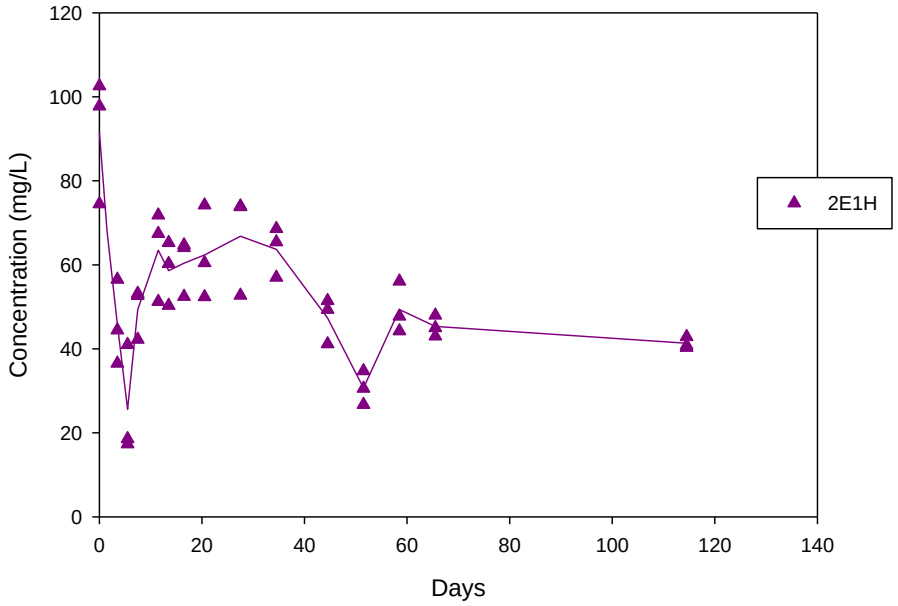

Figure A.12 2-ethyl-1-hexanol concentrations in the abiotic batch reactor containing 2-ethyl-1-hexanol and 0.25 mol tetrachloroethene: 0.75 mol hexadecane.

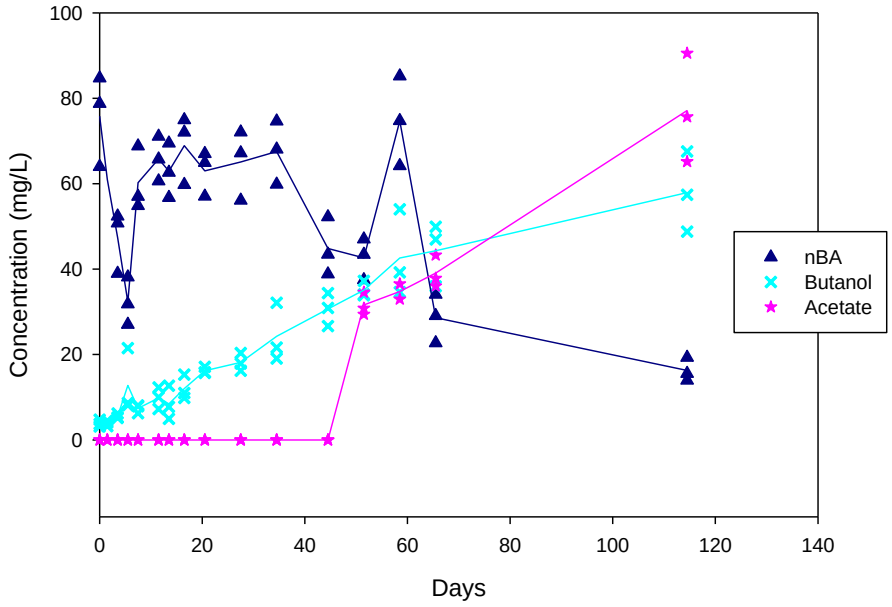

Figure A.13 n-butyl acetate, butanol, and acetate concentrations in the abiotic batch reactor containing n-butyl acetate and 0.25 mol tetrachloroethene: 0.75 mol hexadecane.

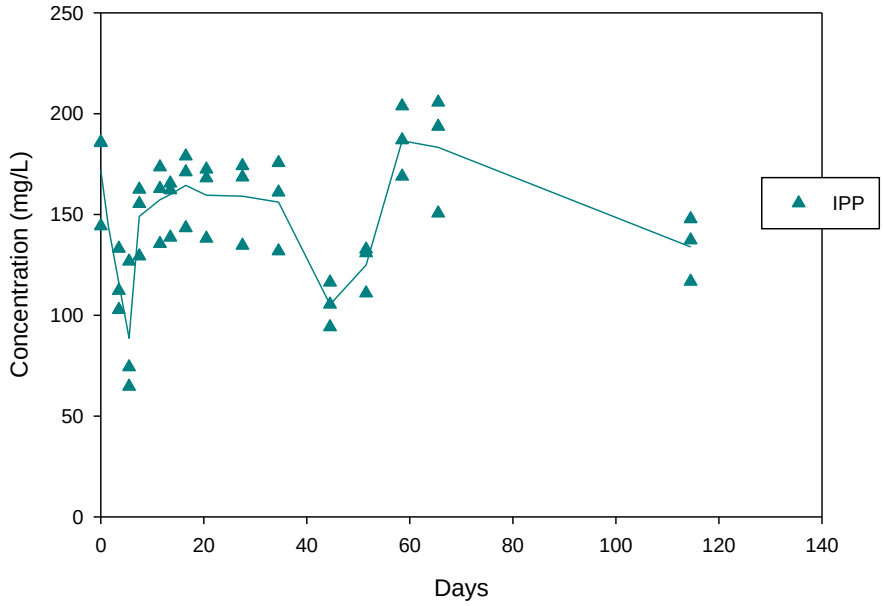

Figure A.14 Isopropyl propionate concentrations in the abiotic batch reactor containing isopropyl propionate and tetrachloroethene.

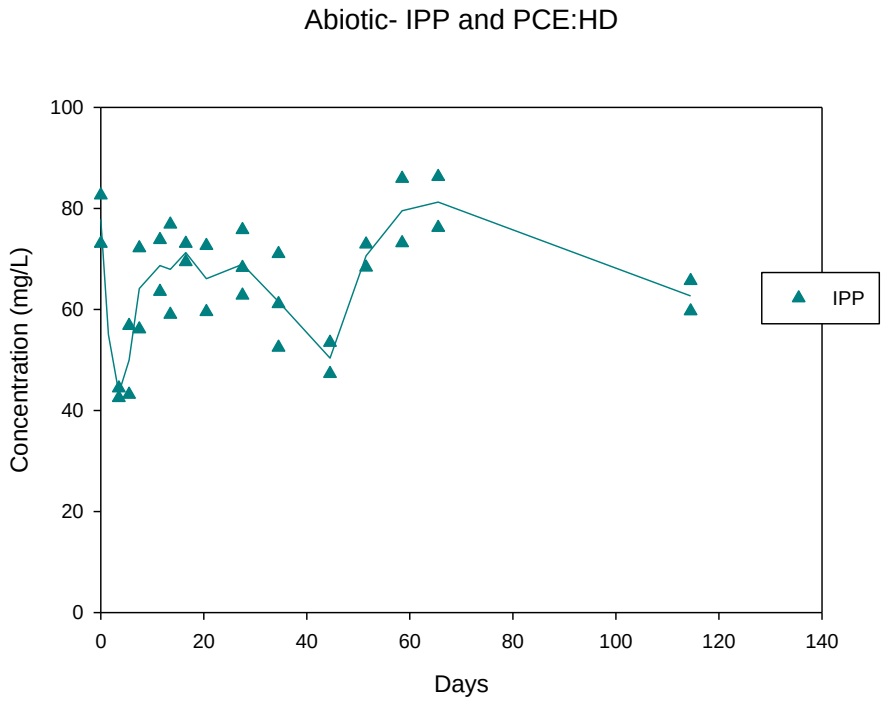

Figure A.15 Isopropyl propionate concentration in the abiotic batch reactors containing isopropyl propionate and 0.25 mol tetrachloroethene: 0.75 mol hexadecane.

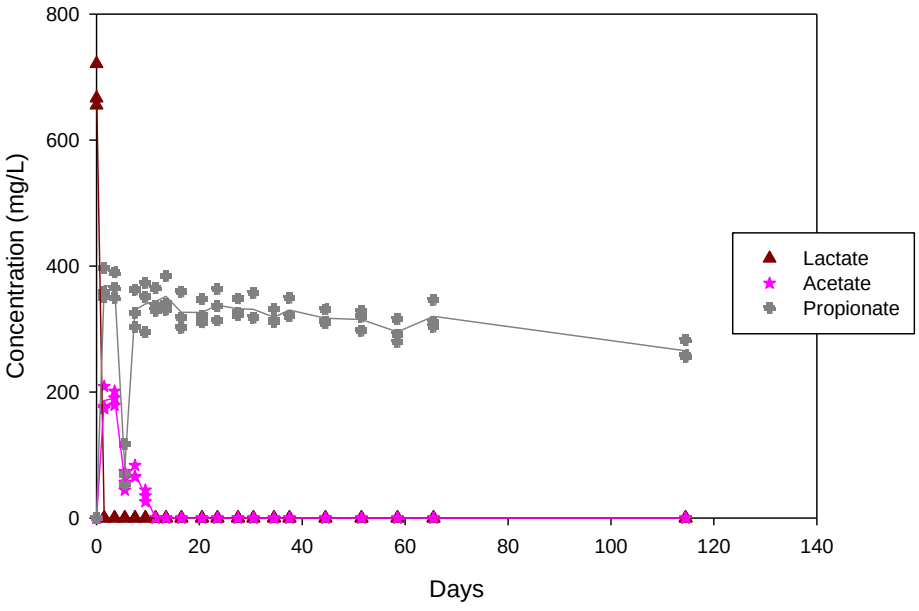

Figure A.16 Lactate, acetate, and propionate concentrations in the biotic batch reactor containing lactate and 0.25 mol tetrachloroethene: 0.75 mol hexadecane.

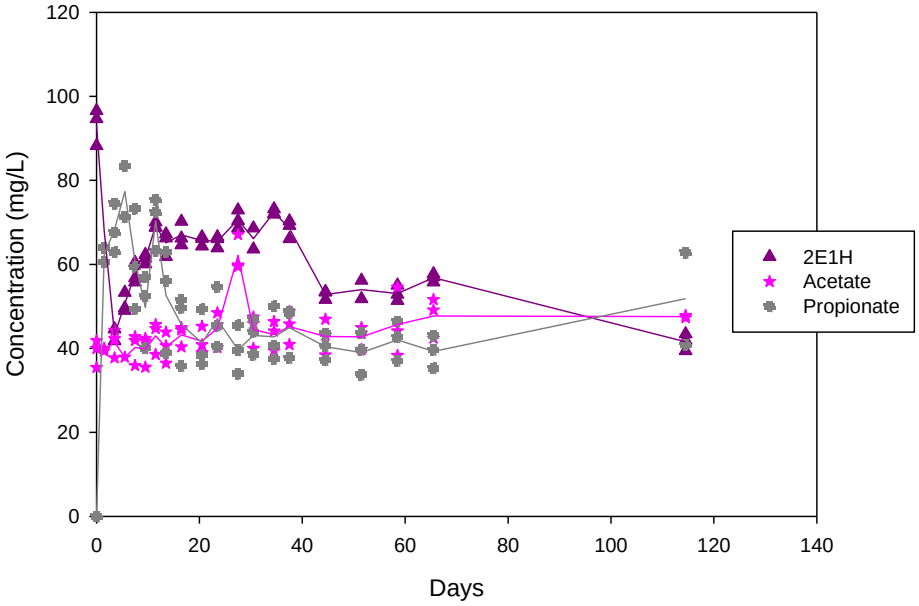

Figure A.17 2E1H, acetate, and propionate concentrations in the biotic batch reactor containing 2-ethyl-1-hexanol and 0.25 mol tetrachloroethene: 0.75 mol hexadecane.

Appendix B: Column Results

Table B.1 Summary of PED maximum concentration, PED recovery, and NAPL recovery for each abiotic column experiment.

NAPL Present	PED Present	PED C_{max} (mg/L)	PED C_{max} (%)	PED Mass Recovery (%)	NAPL Mass Recovery (%)
TCE	n-butyl acetate	297	6.1%	83.2%	28.6%
	2-ethyl-1-hexanol	32.7	3.9%	83.5%	4.3%
	Isopropyl propionate	297	6.1%	93.0%	13.0%
PCE	n-butyl acetate	180	4.5%	86.3%	1.6%
	2-ethyl-1-hexanol	183	13.5%	90.8%	0.6%
	Isopropyl propionate	585	13.6%	84.3%	0.7%

References

Adamson, D. T., J. M. McDade and J. B. Hughes (2003). "Inoculation of a DNAPL source zone to initiate reductive dechlorination of PCE." Environmental Science & Technology **37**(11): 2525-2533.

Amos, B. K., J. A. Christ, L. M. Abriola, K. D. Pennell and F. E. Löffler (2007). "Experimental evaluation and mathematical modeling of microbially enhanced tetrachloroethene (PCE) dissolution." Environmental Science & Technology. **41**: 963-970.

Amos, B. K., E. J. Suchomel, K. D. Pennell and F. E. Loffler (2008). "Microbial activity and distribution during enhanced contaminant dissolution from a NAPL source zone." Water Resources **42**(12): 2963-2974.

Amos, B. K., E. J. Suchomel, K. D. Pennell and F. E. Loffler (2009). "Spatial and temporal distributions of *Geobacter lovleyi* and *Dehalococcoides spp*. during bioenhanced PCE-NAPL dissolution." Environmental Science & Technology **43**(6): 1977-1985.

Amos, B. K., Y. Sung, K. E. Fletcher, T. J. Gentry, W.-M. Wu, C. S. Criddle, J. Zhou and F. E. Loffler (2007). "Detection and quantification of *Geobacter lovleyi* strain SZ: implications for bioremediation at tetrachloroethene- and uranium- impacted Sites." Applied and Environmental Microbiology **73**(21): 6898-6904.

Agency for Toxic Substances & Disease Registry [ATSDR]. (2013). Toxicology Profile for Trichloroethylene Amendment. In: United States Department of Health and Human Services.

Aulenta, F., M. Majone and V. Tandoi (2006). "Enhanced anaerobic bioremediation of chlorinated solvents: environmental factors influencing microbial activity and their relevance under field conditions." Journal of Chemical Technology & Biotechnology **81**(9): 1463-1474.

Aulenta, F., M. Majone, P. Verbo and V. Tandoi (2002). "Complete dechlorination of tetrachloroethene to ethene in presence of methanogenesis and acetogenesis by an anaerobic sediment microcosm." Biodegradation **13**(6): 411-424.

Aulenta, F., A. Pera, S. Rossetti, M. Petrangeli Papini and M. Majone (2007). "Relevance of side reactions in anaerobic reductive dechlorination microcosms amended with different electron donors." Water Resources **41**(1): 27-38.

Avdeef, A. (2011). "Dissolution Theory." Retrieved March 30th, 2015, from http://www.in-adme.com/dissolution_theory.html.

Ballapragada, B. S., H. D. Stensel, J. A. Puhakka and J. F. Ferguson (1997). "Effect of hydrogen on reductive dechlorination of chlorinated ethenes." Environmental Science & Technology **31**(6): 1728-1734.

Barton, H. A., P. J. Deisinger, J. C. English, J. M. Gearhart, W. D. Faber, T. R. Tyler, M. I. Banton, J. Teegaurden and M. E. Anderson (2000). "Family approach for estimating reference concentration/doses for series of related organic chemicals." Toxicological Sciences **54**(1): 251-261.

Bonilla, E. X. (2015). Comparison of Contaminant Paritioning Short Chain Fatty Acids versus Lactate as Electron Donor Sources to Support Dechlorinating Bacteria., Senior Honors Thesis, Tufts University, Medford, MA.

Cápiro, N. L. (2012). Assessment of Partitioning Electron Donors (PEDs) for Enhanced Source Zone Bioremediation: Abiotic Mass Transfer.

Cápiro, N. L., E. K. Granbery, C. A. Lebron, D. W. Major, M. L. McMaster, M. J. Pound, F. E. Löffler and K. D. Pennell (2011). "Liquid-liquid mass transfer of partitioning electron donors in chlorinated solvent source zones." Environmental Science & Technology **45**(4): 1547-1554.

Carr, C. S., S. Garg and J. B. Hughes (2000). "Effect of dechlorinating bacteria on the longevity and composition of PCE-containing nonaqueous phase liquids under equilibrium dissolution conditions."Environmental Science & Technology **34**: 1088-1094.

Christ, J. A., C. A. Ramsburg, L. M. Abriola, K. D. Pennell and F. E. Löffler (2005). "Coupling aggressive mass removal with microbial reductive dechlorination for remediation of DNAPL source zones: a review and assessment." Environmental Health Perspective **113**(4): 465-477.

Chu, M., P. K. Kitanidis and P. L. McCarty (2004). "Possible factors controlling the effectiveness of bioenhanced dissolution of non-aqueous phase tetrachloroethene." Advances in Water Resources **27**: 601-615.

Cope, N. and J. B. Hughes (2001). "Biologically-enhanced removal of PCE from NAPL source zones." Enivronmental Science & Technology **35**: 2014-2021.

Costanza, J. (2007). "Headspace Method."

Cupples, A. M., A. M. Spormann and P. L. McCarty (2004). "Vinyl Chloride and *cis*-Dichloroethene Dechlorination Kinetics and Microorganism Growth under Substrate Limiting Conditions." Environmental Science & Technology **38**: 1102-1107.

Cweirtny, D. M. and M. M. Scherer (2010). Chapter 2 Chlorinated Solvent Chemistry: Structures, Nomenclature and Properties. In Situ Remediation of Chlorinated Solvent Plumes. H. F. Stroo and C. H. Ward, Springer New York: 29-37.

Da Silva, M.I., R.C. Daprate, D.E. Gomez, J.B. Hughes, C.H.Ward, and P.J. Alvarez (2006). "Comparison of bioaugmentation and biostimulation for the enhancement of dense nonaqueous phase liquid source zone bioremediation." Water Environment Research **78**:2456-2465.

David, R. M., T. R. Tyler, R. Ouellette, W. D. Faber and M. I. Banton (2001). "Evaluation of subchronic toxicity of n-butyl acetate vapor." Food Chemical Toxicology **39**(8): 877-886.

DOW. (2014). "Product Safety Assessment." Retrieved June, 2014, from http://msdssearch.dow.com/PublishedLiteratureDOWCOM.

Dugan, P. J., J. E. McCray and G. D. Thyne (2003). "Influence of a solubility-enhancing agent (cyclodextrin) on NAPL-water partition coefficients, with implications for partitioning tracer tests." Water Resources Research **39**(5): 1123.

Edwards, D., Z. Liu and R. Luthy (1994). "Surfactant solubilization of organic compounds in soil/aqueous systems." Journal of Environmental Engineering **1**(5): 5-22.

eMolecules. (2014). Retrieved January 28th, 2015, from https://www.emolecules.com/cgi-bin/search.

Freedman, D. L. and J. M. Gossett (1989). "Biological reductive dechlorination of tetrachloroethylene and trichloroethylene to ethylene under methanogenic conditions." Applied and Environmental Microbiology **55**(9): 2144-2151.

Glover, K. C., J. Munakata-Marr and T. H. Illangasekare (2007). "Biologically enhanced mass transfer of tetrachloroethene from DNAPL in source zones: experimental evaluation and influence of pool morphology." Environmental Science & Technology **41**: 1384-1389.

Harkness, M. R. (2000). Economic Considerations in Enhanced Anaerobic Degradation. 2nd International Conference Remediation of Chlorinated and Recalcitrant Compounds, Monterey, CA.

Harkness, M. R., A. A. Bracco, M. J. Brennan, K. A. DeWeerd and J. L. Spivack (1999). "Use of bioaugmentation to stimulate complete deductive dechlorination of trichloroethene in dover soil columns." Environmental Science & Technology **33**(7): 1100-1109.

Harkness, M., A. Fisher, L. D. Michael, E. E. Mack, J. A. Payne, S. Dworatzek, J. Roberts, C. Acheson, R. Herrmann and A. Possolo (2012). "Use of statistical tools to evaluate the reductive dechlorination of high levels of TCE in microsom studies." Journal of Contaminant Hydrology **131**: 100-118.

Harkness, M. and A. Fisher (2013). "Use of emulsified vegtable oil to support bioremediation of TCE DNAPL in soil columns." Journal of Contaiminant Hydrology **151** 16-33.

He, J., Y. Sung, M. E. Dollhopf, B. Z. Fathepure, J. M. Tiedje and F. E. Löffler (2002). "Acetate versus hydrogen as direct electron donors to stimulate the microbial reductive dechlorination process at chloroethene-contaminated sites." Environmental Science & Technology **36**(18): 3945-3952.

Henry, B. M. (2010). CHAPTER 12: BIOSTIMULATION FOR ANAEROBIC BIOREMEDIATION OF CHLORINATED SOLVENTS. In Situ Remediation of Chlorinated Solvent Plumes. Denver, Colorado, Parsons Corporation: 357-424.

Hubaux, A. and G. Vos (1970). "Decision and detection limits for linear calibration curves." Analytical Chemistry **42**(8): 849-855.

Huling, S. and Weaver, J. W. (1991). Ground Water Issue: Dense Nonaqueous Phase Liquids (EPA/540/4-91-002). US Environmental Protections Agency, Washington, DC.

ICIS. (2014). "Indicative Chemical Prices A-Z." Retrieved June, 2014, from http://www.icis.com/chemicals/channel-info-chemicals-a-z/

Isalou, M., B. E. Sleep and S. N. Liss (1998). "Biodegradation of high concentrations of tetrachloroethene in a continuous flow column system." Environmental Science & Technology **32**(22): 3579-3585.

Istok, J. D., J. A. Field, M. H. Schroth, B. M. Davis and V. Dwarakanath (2002). "Single-well "push-pull" partitioning tracer test for NAPL detection in the subsurface." Environmental Science & Technology. **36**: 2708-2716.

Interstate Technology and Regulatory Councol [ITRC]. (2008). "Technical/Regulatory Guidance: In Situ Bioremediation of Chlorinated Ethene DNAPL Source Zones. BioDNAPL-2." Retrieved June, 2014, from www.itrcweb.org.

Kavanaugh, M. C. and S. C. Rao (2003) "The DNAPL Remediation Challenge: Is There a Case for Source Depletion?" EPA/600/R-03/143. U.S. Environmental Protection Agency, Washington, DC, USA.

Kube, M, A. Beck, S. H. Zinder, H. Kuhl, R. Reinhardt and L. Adrain (2005) "Genome sequence of the chlorinated compound respiring bacterium *Dehalococcoides* species strain CBDB1." Natural Biotechnology **23**:1269-1273.

Löffler, F.E., Q. Sun, J. Li, and J.M. Tiedje (2000). "16S rRNA gene-based detection of tetrachloroethene-dechlorinating desulfuromonas and *Dehalococcoides* species." Applied Enivironmental Microbiology **66**: 1369-1374.

Löffler, F. E., R. A. Sanford and K. M. Ritalahti (2005). "Enrichment, cultivation, and detection of reductively dechlorinating bacteria." Environmental Microbiology **397**: 77-111.

Löffler, F. E., K. M. Ritalahti and S. H. Zinder (2013a). Chapter 2: *Dehalococcoides* and Reductive Dechlorination of Chlorinated Solvents. Bioaugmentation for Groundwater Remediation. H. F. Stroo and C. H. Ward, Springer New York.

Löffler, F. E., J. Yan, K. M. Ritalahti, L. Adrian, E. A. Edwards, K. T. Konstantinidis, J. A. Muller, H. Fullerton, S. H. Zinder and A. M. Spormann (2013b). "*Dehalococcoides mccartyi* gen. nov., sp. nov., obligately organohalide-respiring anaerobic bacteria relevant to halogen cycling and bioremediation, belong to a novel bacterial class, *Dehalococcoidia classis* nov., order *Dehalococcoidales* ord. nov. and family *Dehalococcoidaceae* fam. nov., within the phylum Chloroflexi." International Journal of Systematic and Evolutionary Microbiology **63**(Pt 2): 625-635.

Lyon, D. Y. and T. M. Vogel (2013). Chapter 1: Bioaugmentation For Groundwater Remediation: An Overview. Bioaugmentation for Groundwater Remediation. H. F. Stroo, A. Leeson and C. H. Ward, Springer New York: 1-37.

Marcet, T. (2014). Secondary Impacts of In Situ Chlorinated Solvent Remediation Due to Metal Sulfide Precipiation and Thermal Treatment. Master Thesis, Tufts University, Medford, MA.

McCarty, P. L. (2010). Groundwater Contamination by Chlorinated Solvents: History, Remediation Technologies and Strategies. In Situ Remediation of Chlorinated Solvent Plumes. H. F. Stroo and C. H. Ward, Springer New York**:** 1-28.

McDade, J. M., T. M. McGuire and C. J. Newell (2005). "Analysis of DNAPL source-depletion costs at 36 field sites." Remediation Journal **15**(2): 9-18.

McGuire, T. M., C. J. Newell, B. B. Looney, K. M. Vangelas and C. H. Sink (2004). "Historical analysis of monitored natural attenuation: A survey of 191 chlorinated solvent sites and 45 solvent plumes." Remediation Journal **15**(1): 99-112.

Meylan, W. M., P. H. Howard and R. S. Boethling (1996). "Improved method for estimating water solubility from octanol/water partitioning coefficient." Environmental Toxicity and Chemistry **15**(2): 100-106.

NRC (1994). Alternatives for Groundwater Cleanup. Washington, D.C., National Academy Press.

NRC (2013). Alternatives for Manageing the Nation's Complex Contaminated Groundwater Sites**:** Washington, D.C., National Academy Press.

Park, S.K. and A.R. Bielefeldt (2003). Equilibrium partitioning of a non-ionic surfactant and pentachlorophenol between water and a non-aqueous phase liquid.” Water Resource. **37**: 3412-3420.

Pubchem. (2014). "Compound Summary.” Retrieved June, 2014, from http://pubchem.ncbi.nlm.nih.gov/

Ramsburg, C. A., L. M. Abriola, K. D. Pennell, F. E. Loffler, M. Gamache, B. K. Amos and E. A. Petrovskis (2004). "Stimulated microbial reductive dechlorination following surfactant treatment at the Bachman Road site." Environmental Science & Technology **38**(22): 5902-5914.

Ritalahti, K. M., B. K. Amos, Y. Sung, Q. Wu, S. S. Koenigsberg and F. E. Löffler (2006). "Quantitative PCR targeting 16S rRNA and reductive dehalogenase genes simultaneously monitors multiple *Dehlococcoides* strains." Applied and Environmental Microbiology **72**(4):2765-2774.

Ritalahti, K. M., F. E. Löffler, E. E. Rasch and S. S. Koenigsberg (2005). "Bioaugmentation for chlorinated ethene detoxication: bioaugmentation and molecular diagnostics in the bioremediation of chlorinated ethene-contaminated sites." Industrial Biotechnology **1**(2): 114-118.

Roberts, J. D. (2008). Bench Scale Performance of Partitioning Electron Donors for TCE DNAPL Bioremediation. Master Thesis, University of Waterloo, Waterloo, ON.

Russell, H. H., J. E. Matthews and G. W. Sewell (1992). "TCE removal from contaminated soil and groundwater." EPA Ground Water Issue **540**(002).

Schink, B. (2002). "Synergistic interactions in the microbial world." Antonie van Leeuwenhoek **81**:257-261.

Schwarzenbach, R. P., Gshwend, P. M. and Imboden, D. M. (2003). Environmental Organic Chemisty; 2nd ed; Wiley & Sons.

Sechadri, R., L. Adrian, D. E. Fouts, J. A. Eisen, A. M. Phillippy, B. A. Methe, N. L. Ward, W. C. Nelson, R. T. Deboy, H. M. Khouri, J. F. Kolonay, R. J. Dodson, S. C. Daugherty, L. M. Brinkac, S. A. Sullivan, R. Madupu, K. T. Nelson, K. H. Kang, M. Impraim, K. Tran, J. M. Robinson, H. A. Forberger, C. M. Fraser, S. H. Zinder and J. F. Heidelberg (2005). "Genome sequence of the PCE dechlorinating bacterium *Dehalococcoides ethenogenes*." Science **307**: (105-108).

Simmonds, A. C. (2007). Dechlorination Rates in KB-1, a Commercial Trichloroethylene-Degrading Bacterial Culture. Master of Science, University of Toronto, Toronto, ON.

Sleep, B. E., D. J. Sepersad, K. Mo, C. M. Heidorn, L. Hrapovic, P. L. Morrill, M. L. McMaster, E. D. Hood, C. Lebron, B. Sherwood-Lollar, D. W. Major, E. A. Edwards (2006). "Biological enhancement of tetrachloroethene dissolution and associated microbial community changes." Environmental Science & Technology **40**: 3623-3633.

State Coalition for the Remediation of Drycleaners [SCRD]. (2010). "State coalition for the remediation of dry cleaners december 2010 newletter." Retrieved September, 2014, from https://drycleancoalition.org/download/news1210.pdf

Stroo, H. F., A. Leeson, J. A. Marqusee, P. C. Johnson, C. H. Ward, M. C. Kavanaugh, T. C. Sale, C. J. Newell, K. D. Pennell, C. A. Lebron and M. Unger (2012). "Chlorinated ethene source remediation: lessons learned." Environmental Science & Technology **46**(12): 6438-6447.

Suchomel, E. J., C. A. Ramsburg and K. D. Pennell (2007). "Evaluation of trichloroethene recovery processes in heterogeneous aquifer cells flushed with biodegradable surfactants." Journal of Contaminant Hydrology **94**(3–4): 195-214.

Sung, Y., K. M. Ritalahti, R. A. Sanford, J. W. Urbance, S. J. Flynn, J. M. Tiedje and F. E. Löffer (2003). "Characterization of two tetrachloroethene-reducing, acetate-oxidizing anaerobic bacteria and their description as Desulfuromonas michiganensis sp. nov." Applied and Environmental Microbiology **69**(5): 2964-2974.

Texas A&M University [TAMU]. (2008). "Groundwater Remediation." Retrieved July, 2014, from http://oceanworld.tamu.edu/resources/environment-book/groundwaterremediation.html.

United States Envronmental Protection Agency [USEPA]. (1993). "Guidance for Evaluating the Techical Impracticability of Ground-Water Restoration." Retrieved June, 2014, from http://www.epa.gov/superfund/health/conmedia/gwdocs/techimp.htm.

van Genuchten, M. T. (1981). Non-equilibrium transport parameters from miscible displacement experiments. USDA Science and Education Administration. U. S. S. Labatory. Riverside, CA.

van Genuchten, M. T. and R. J. Wagenet (1989). "Two-site/two-region models for pesticide transport and degradation: theoretical development and analytical solutions." Soil Science Society of America Journal **53**(5): 1303-1310.

Wang, Y., Y. Li, H. Kim, S. L. Walker, L. M. Abriola and K. D. Pennell (2010). "Transport and retention of fullerene nanoparticles in natural soils." Journal of Environmental Quality **39**(6): 1925-1933.

Williamson, K. L. (1994). *Macroscale and Microscale Organic Experiments*. Boston, Houghton Mifflin.

Wilson, J. L., S. H. Conrad, W. R. Mason, W. Peplinski and E. Hagan (1990). Labatory Investigations of Residual Liquid Organics from Spills, Leaks, and the Disposal of Hazardous Wastes in Groundwater. Socorro, New Mexico.

Yang, Y. and P. L. McCarty (1998). "Competition for hydrogen within a chlorinated solvent dehalogenating anaerobic mixed culture." Environmental Science & Technology **32**(22): 3591-3597.

Yang, Y. and P. L. McCarty (2000). "Biologically enhanced dissolution of tetrachloroethene DNAPL." Environmental Science & Technology **34**(14): 2979-2984.

Yang, Y. and P. L. McCarty (2002). "Comparison between donor substrates for biologically enhanced tetrachloroethene DNAPL dissolution." Environmental Science & Technology **36**(15): 3400-3404.

Yu, S. and L. Semprini (2004). "Kinetics and modeling of reductive dechlorination at high PCE and TCE concentrations." Biotechnology and Bioengineering **88**(4): 451-464.

Yu, S., M. E. Dolan and L. Semprini (2005). "Kinetics and inhibition of reductive dechlorination of chlorinated ethylenes by two different mixed cultures." Environmental Science & Technology **39**(1): 195-205.

Zytner, R.G. (1991). "Adsorption-desorption of trichloroethylene in granular media." Water, Air, and Soil Pollution **65**:245-255.